# ANEXOS

**A. LEGISLACIÓN ACTUAL DE COMBUSTIBLES PARA TRANSPORTE POR CARRETERA. ¿BIOCOMBUSTIBLES SI? 3**

**B. PRUEBAS DE VARIACIÓN DE TEMPERATURA DE LOS MÓDULOS FOTOVOLTAICOS. 9**

**C. CAPTURAS DE PANTALLA DE LAS SIMULACIONES MEDIANTE ADVISOR. 13**

**D. DIVULGACIÓN DEL PROYECTO DESPERTAFERRO II. 47**

D.1. ISOFOTON: Artículo publicado en el "Twenty-first European Photovoltaic Solar Energy Conference (Dresden 4-8 Sep 2006)" 47

D.1.1. Abstracto 47

D.1.2. Artículo publicado 48

D.1.3. Poster divulgativo 52

D.2. Ciencia en Acción. 53

D.2.1. Premio Categoría Sostenibilidad 53

D.3. Science on Stage 2 54

D.3.1. Exposición permanente 54

D.3.2. Press Kit 55

D.3.3. Training Workshop: THE SOLAR FUEL CELL CAR From theory to practice . 56

**E. TRABAJOS ADICIONALES EN EL DISEÑO Y CONSTRUCCIÓN DEL DESPERTAFERRO II. 119**

E.1. Maleta de telemetría. Calibración de sensores Ibat y Vbat 119

E.2. CAD Despertaferro II. Diseño cúpula. 121

E.3. Prueba de carga del sistema de captación. 122

E.3.1. Carga grupos de menor tensión 122

E.3.2. Ecualización de baterías. 123

E.3.3. Descarga controlada. 123

E.3.4. • Carga sistema captación fotovoltaica 124

**F. DATOS TÉCNICOS. 127**

F.1. Datos de los módulos fotovoltaicos proporcionados por ISOFOTON. 127

F.2. Curvas características del Motor MA-55 129

ETSEIB

**G. ADVISOR. BLOQUES PRINCIPALES. 131**

G.1. Bloque Subsistema Fotovoltaico ..... 131

G.2. Bloque optimización velocidades ..... 131

G.2.1. Tabla de potencias eléctricas en función de la velocidad del vehículo y la pendiente del tramo. ..... 132

G.2.2. Tabla de interpolación de tres dimensiones. ..... 132

G.3. Caracterísitcas modeladas del motor MA-55 + Driver SMT-BD1/a ..... 134

**H. PRESUPUESTO DETALLADO. 135**

H.1. Materiales de fabricación ..... 135

H.2. Herramientas y accesorios ..... 138

H.3. Recursos Humanos ..... 139

H.4. Logística ..... 140

# A. Legislación actual de combustibles para transporte por carretera. ¿Biocombustibles si?

El futuro presenta nuevos retos, y uno de ellos se centra en la innovación tecnológica en busca de un futuro sostenible. Un sector importante a desarrollar se encuentra en las fuentes de energía renovables, cuya misión es desplazar al petróleo como una de las principales fuentes de energía a través de aumentar la eficiencia energética en sus aplicaciones.

El gran caballo de batalla se encuentra actualmente en la reducción de los gases de efecto invernadero con el objetivo de decelerar el cambio climático, y establecer un equilibrio entre la técnica, el progreso, la economía y la sostenibilidad.

Los motores alternativos de combustión interna son unos de los principales responsables de esta situación tan preocupante debido en primer lugar a su escaso rendimiento respecto a las escasas reservas de combustibles fósiles y de las altas emisiones de CO2 que incrementan el efecto invernadero.

En los gráficos Figura A.1 y Figura A.2 se observa el importante papel de la demanda de energía del sector transporte respecto al consumo final tanto en la UE-27 (Unión Europea de los 27 miembros) como en España. La hegemonía del petróleo en el sector del transporte provoca una fuerte dependencia energética hacia los escasos combustibles fósiles, con una fracción mayor del 94% frente a otras fuentes energéticas. Los datos que nos ofrece EUROSTAT [1] nos indican que el 22,4% en UE-27 y el 31,3% en España del consumo de energía final se destina únicamente al **transporte por carretera** utilizando combustibles fósiles.

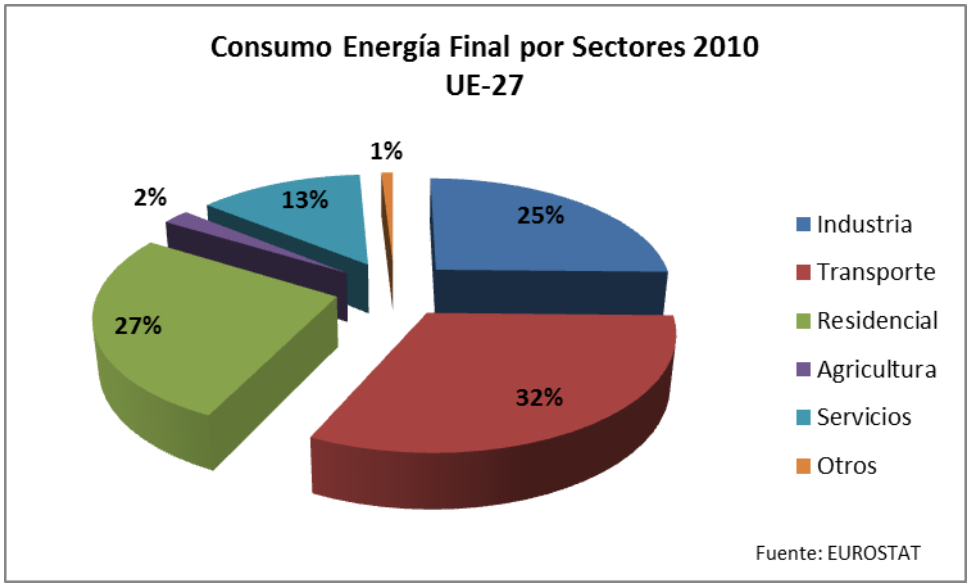


**Figura A.1.- Consumo de Energía Final por Sectores en el año 2010 en la UE-27**

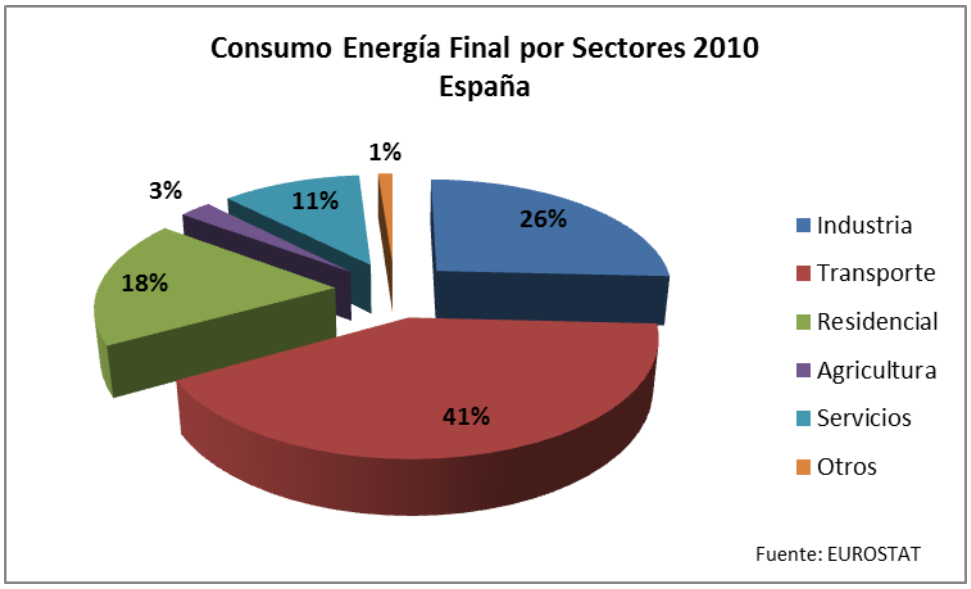


**Figura A.2.- Consumo de Energía Final por Sectores en el año 2010 en España**

Según el Resumen del Plan de Energías Renovables 2011-2020 ([2], p.3), la Directiva 2009/28/CE ([4], p.28 y p.46) establece como objetivo conseguir una cuota mínima del 20% de energía procedente de fuentes renovables en el consumo final bruto de energía de la Unión Europea, el mismo objetivo establecido para España, y una cuota mínima del 10% de energía procedente de fuentes renovables en el consumo de energía en el sector del transporte en cada Estado miembro para el año 2020.

La fracción de energías renovables dentro del consumo de energía final del transporte fue de un 4,2% para la UE-27 y de un 3,5% para España durante el 2009 según EUROSTAT[1]. El método para el cálculo queda definido en el Artículo 2 de la Directiva 2009/28/CE ([4], p.28). No obstante en esta proporción se incluye la contribución del uso de los biocombustibles como "energías renovables" siempre que cumplan con ciertos criterios de sostenibilidad.

En la tabla Tabla A.1 extraída del Resumen del Plan de Energías Renovables 2011-2020 ([2], p.28) se muestra los objetivos parciales para dar cumplimiento a los requisitos establecidos en la a directiva 2009/28/CE en el año 2020.

**Tabla A.1.- Objetivos del Plan de energías renovables 2011-2020 en el sector del transporte**

| ktep | 2005 | 2010 | 2011 | 2012 | 2013 | 2014 | 2015 | 2016 | 2017 | 2018 | 2019 | 2020 |
|---|---|---|---|---|---|---|---|---|---|---|---|---|
| Bioetanol/bio-ETBE | 113 | 226 | 232 | 281 | 281 | 290 | 301 | 300 | 325 | 350 | 375 | 400 |
| *De los cuales biocarburantes del artículo 21.2 (*)* | *0* | *0* | *0* | *0* | *0* | *0* | *7* | *7* | *7* | *19* | *19* | *52* |
| Biodiesel | 24 | 1.217 | 1.816 | 1.878 | 1.900 | 1.930 | 1.970 | 2.020 | 2.070 | 2.120 | 2.170 | 2.313 |
| *De los cuales biocarburantes del artículo 21.2 (*)* | *0* | *5* | *15* | *45* | *75* | *105* | *135* | *160* | *186* | *158* | *180* | *200* |
| Electricidad procedente de fuentes renovables | 107 | 96 | 126 | 172 | 182 | 198 | 229 | 266 | 307 | 356 | 420 | 503 |
| *De la cual transporte por carretera* | *0* | *0* | *0* | *0* | *5* | *11* | *21* | *34* | *49* | *67* | *90* | *122* |
| *De la cual transporte no por carretera* | *107* | *96* | *126* | *172* | *176* | *187* | *207* | *232* | *258* | *289* | *330* | *381* |
| *Total biocarburantes* | *137* | *1.442* | *2.048* | *2.159* | *2.181* | *2.220* | *2.271* | *2.320* | *2.395* | *2.470* | *2.545* | *2.713* |
| **Total EERR en el transp.** | **245** | **1.538** | **2.174** | **2.331** | **2.363** | **2.418** | **2.500** | **2.586** | **2.702** | **2.826** | **2.965** | **3.216** |

(*) Artículo 21, Apartado 2 de la Directiva 2009/28/CE: biocarburantes obtenidos a partir de desechos, residuos, materias celulósicas no alimentarias y material lignocelulósico.

Existe un fuerte debate social acerca del uso de los biocombustibles, dado que por un lado permite potenciar el desarrollo de zonas rurales y reducir efectos de desertización, pero a su vez provoca que los denominados cultivos energéticos sean más competitivos que los cultivos destinados a la alimentación debido a los altos precios del petróleo. Por tanto políticas de subvención del uso de biocombustibles en los países desarrollados pueden provocar desequilibrios en el abastecimiento alimentario de los países en vías de desarrollo que son los centros de producción de dichos cultivos.

El uso de los biocombustibles disminuye la emisión de gases de efecto invernadero en comparación con productos derivados del petróleo, pero muchas políticas no están teniendo en cuenta las emisiones producidas en la producción y la transformación de los cultivos a los biocombustibles correspondiente. Prueba de ellos se puede encontrar en el reportaje “El biocombustible se quema” [5] donde se cita al premio Nobel de la Química Harmut Michel “Con los biocombustibles no se ahorran emisiones de CO2” o en el artículo publicado en Science [6] donde se fomenta que no se están estimando las emisiones de las plantaciones de bioenergía para el cómputo final de los requisitos del protocolo de Kyoto.

Queda entre dicho también el balance energético positivo si no se analizan convenientemente factores determinantes como la tipología del suelo, disponibilidad de para el regadío, etc.

**Figura A.3.-Viñeta representativa del debate social del uso de los biocombustibles.**

La evolución del sector del transporte tiene que encaminarse hacia una reducción drástica del consumo de combustibles fósiles, para reducir las emisiones de gases de efecto invernadero y alcanzar los niveles de sostenibilidad para un futuro a medio-largo plazo establecidos en los acuerdos internacionales y legislaciones internas.

El uso de los biocombustibles parece una alternativa al uso de los derivados del petróleo únicamente a medio plazo, por lo que se debe potenciar el uso de vehículos de emisiones locales 0, que permitan reducir también a largo plazo las emisiones de $CO_2$ y trasladen el conflicto de la sostenibilidad al proceso de generación de energía en su origen.

Bibliografía

**[1]** EUROSTAT. OFICINA ESTADÍSTICA DE LA COMUNIDAD EUROPEA. *Energy. Data. Main tables* [en línea]. Luxembourg, fecha de actualización 6 de marzo de 2012 [Consulta: 6 de abril de 2012]. Disponible en: http://epp.eurostat.ec.europa.eu/portal/page/portal/statistics/search_database.

**[2]** ESPAÑA. MINISTERIO DE INDUSTRIA, ENERGÍA Y TURISMO. IDAE. *Resumen del Plan de Energías Renovables 2011-2020* [en línea]. Creado el 11 de noviembre de 2011 [Consultado el 17 de febrero de 2012]. Disponible en: http://www.idae.es/index.php/mod.documentos/mem.descarga?file=/documentos_Resumen_PER_2011-2020_15f3dad6.pdf

**[3]** ESPAÑA. MINISTERIO DE INDUSTRIA, ENERGÍA Y TURISMO. IDAE. *Plan de Energías Renovables 2011-2020* [en línea]. Creado el 13 de diciembre de 2011 [Consultado el 17 de febrero de 2012]. Disponible en: http://www.idae.es/index.php/mod.documentos/mem.descarga?file=/documentos_11227_PER_2011-2020_def_93c624ab.pdf

**[4]** PARLAMENTO EUROPEO; CONSEJO DE LA UNIÓN EUROPEA. Directiva 2009/28/CE del parlamento europeo y del consejo de 23 de abril de 2009, relativa al fomento del uso de energía procedente de fuentes renovables y por la que se modifican y se derogan las Directivas 2001/77/CE y 2003/30/CE. *Diario Oficial de la Unión Europea*. Estrasburgo, 5 de junio de 2009 , núm.L 140 , p. 16-62.

**[5]** PÉREZ, C.; DELGADO C. *El biocombustible se quema* [en línea]. El País, 11 de mayo de 2008, sec. Negocios, p.4. [Consultado el 17 de febrero de 2012] Disponible en: http://elpais.com/diario/2008/05/11/negocio/1210511665_850215.html

**[6]** SEARCHINGER, D. T. et al. Fixing a Critical Climate Accounting Error. *Science* [en línea]. Vol. 326 no. 5952 pp. 527-528 [Consultado el 17 de febrero de 2012] http://www.sciencemag.org/content/326/5952/527.short

Bibliografía complementaria

**[7]** MILIARIUM.COM. *Cultivos Energéticos* [en línea]. Madrid 2008 [Consulta 15 de abril de 2012] http://www.miliarium.com/Bibliografia/Monografias/Biocombustibles/CultivosEnergeticos.asp

**[8]** PÉREZ, C.; DELGADO C. *El biocombustible se quema*[en línea]. El País, 11 de mayo de 2008, sec. Negocios, p.4. [Consultado el 17 de febrero de 2012] Disponible en: http://elpais.com/diario/2008/05/11/negocio/1210511665_850215.html

# B. Pruebas de variación de temperatura de los módulos fotovoltaicos.

**Objetivo**

Las pruebas de variación de temperatura servirán para determinar el coeficiente de temperatura de la tensión de circuito abierto de los módulos fotovoltaicos, i poderlo contrastar con el valor típico de los módulos fotovoltaicos comerciales.

Se verificará si el sustrato (policarbonato alveolar) de los módulos fotovoltaicos del Despertaferro II ayudan a la refrigeración de las células, de manera que el coeficiente de temperatura para la tensión de circuito abierto sea menor que el de los módulos comerciales.

Para las células fotovoltaicas de Si monocristalino, el coeficiente de temperatura suelen ser de 2,2mV/K. Por tanto por cada grado centígrado por encima de la temperatura STC (standard test conditions), la tensión de circuito abierto se reduce 2,2mV. El rendimiento del módulo fotovoltaico se reduce al incrementar su temperatura, manteniendo el resto de los parámetros constantes. Un valor típico de la reducción de rendimiento es del 0,5%/ºC.

**Procedimiento**

Se introducirán en un horno dos segmentos, de 6 células solares cada uno, de un módulo fotovoltaico, con una lámpara halógena para cada módulo para generar tensión directa en las células fotovoltaicas.

Los segmentos se introducen del horno a una distancia de 5cm de las bandejas de soporte. Los conductos del sustrato de policarbonato se dejan libres, de forma que la disipación de calor se realiza por convección natural a través de los conductos y la parte inferior.

Se incrementará gradualmente la temperatura del horno hasta alcanzar los 70ºC, y se registrará la temperatura ambiente a la que está cada módulo y su tensión de circuito abierto.

El objetivo es trazar la recta que relaciona la tensión de circuito abierto en función de la temperatura, la pendiente obtenida será el coeficiente de temperatura.

**Figura B.1 - Pruebas de variación de temperatura de los módulos fotovoltaicos.**

## Alcance

Las medidas en laboratorio para las células solares se efectúan con equipamiento muy sofisticado. A continuación se detallarán simplificaciones aplicadas para dar como válido el resultado obtenido.

La fuente luminosa utilizada en los laboratorios debe ser lo más parecido posible al espectro de radiación del sol, una alternativa a los costosos simuladores solares son las lámparas halógenas dicroicas, usadas para la verificación de los módulos a la salida de la cadena de producción.

Se ha escogido una lámpara halógena para iluminar los segmentos del módulo. La distribución de radiación en la superficie del módulo debe ser la misma para que todas las células trabajen en el mismo punto y tengan la misma temperatura. Al buscar la variación de tensión en función de la temperatura, no es necesario estimar la radiación incidente en cada célula.

Entre las células de cada módulo existirá una diferencia de temperatura, al no haber equidistribución de radiación. No obstante la variación de tensión respecto la temperatura es lineal, por lo que se tomará como referencia para trazar la regla lineal la temperatura ambiente.

No se tiene en cuenta posibles variaciones en la radiación de la fuente luminosa en función de la temperatura, ya que no afectan significativamente a la tensión de circuito abierto de las células fotovoltaicas, en todo caso repercutiría en la intensidad de cortocircuito si fuera la finalidad de las pruebas.

**Resultados**

En el siguiente gráfico se muestra los registros de las pruebas.

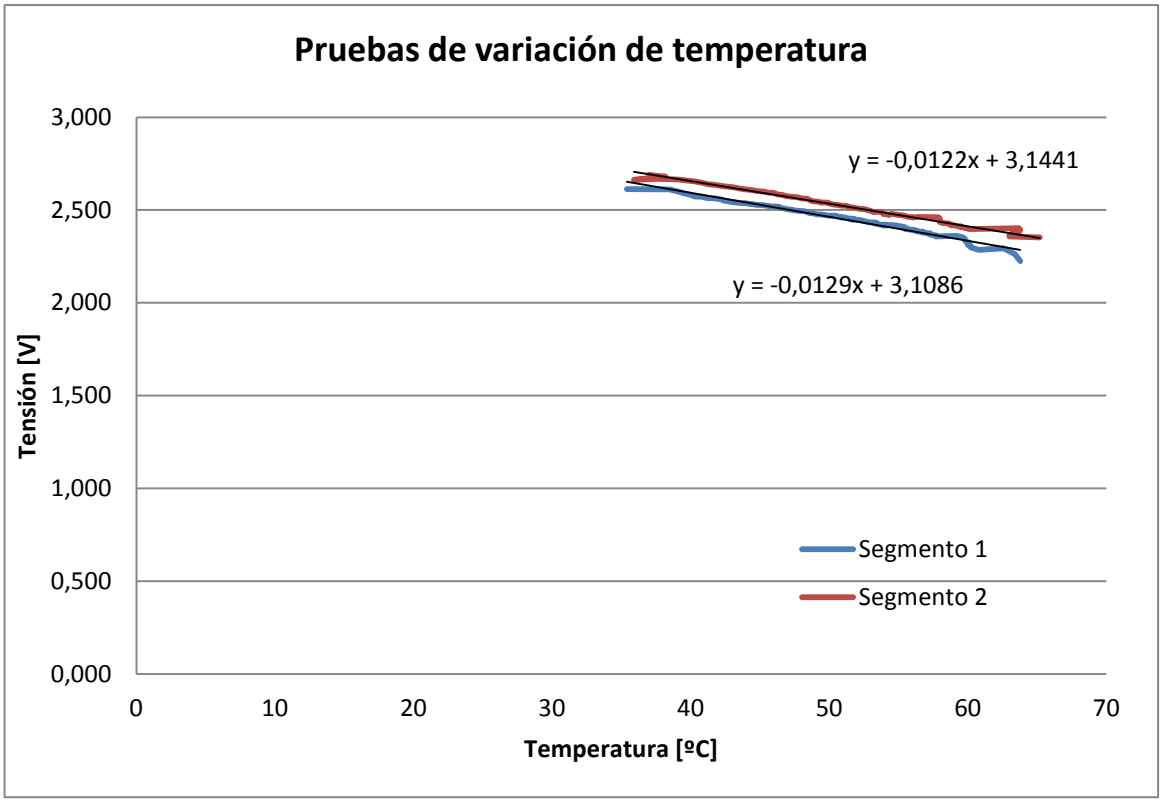


Se obtienen los siguientes coeficientes de temperatura para los segmentos:

Segmento 1= 0,0129V/ºC (6 células)

Segmento 2= 0,0122V/ºC (6 células)

Y la media para las células fotovoltaicas ensayadas es de 2,09mV/ºC.

El valor obtenido es ligeramente inferior al de los módulos comerciales que es de 2,2mV/ºC, pero son del mismo orden. A pesar que no se han tenido en cuenta que el módulo real es cuatro veces más grande.

Hacer circular un fluido refrigerante por los conductos del sustrato debería mejorar el rendimiento de los módulos de manera significativa.

# C. Capturas de pantalla de las simulaciones mediante ADVISOR.

En el siguiente anexo se mostrarán las capturas de pantallas resultantes de la simulación mediante ADVISOR para cada uno de los condicionantes expuestos en el capítulo 5 y 6.

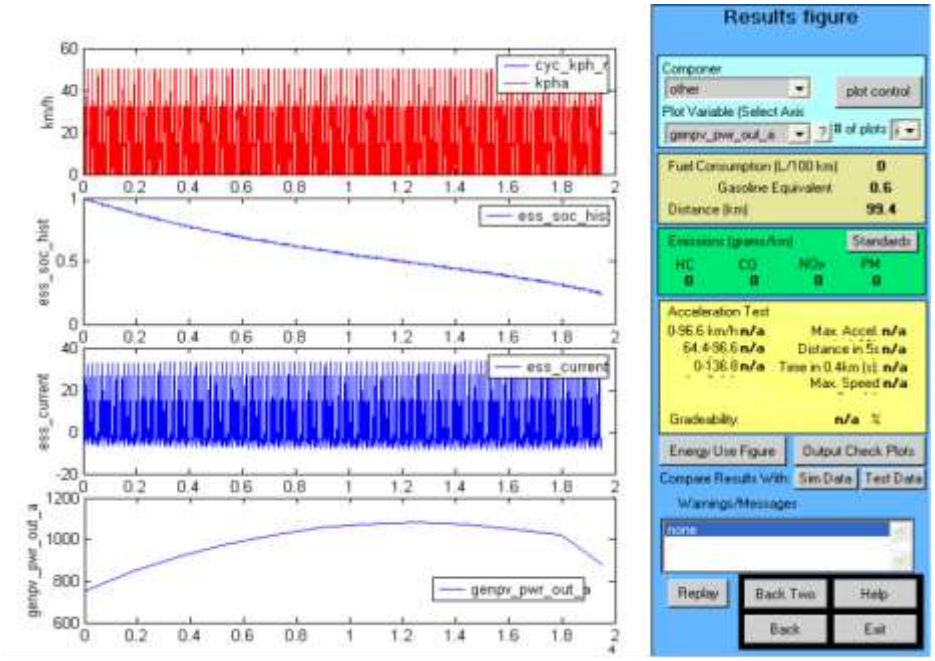


**Figura C.1 - Simulación 100·ECE día soleado. 7Ah. Captura pantalla ADVISOR.**

La Figura C.1 muestra la ventana accesible al usuario que ofrece ADVISOR con los resultados obtenidos de la simulación.

En el primer gráfico se representa en color rojo el ciclo de conducción que debe seguir el vehículo y en azul se representa el ciclo resultado de la simulación. En el eje de abscisas se representa el tiempo y en $s \cdot 10^3$ y en el de ordenadas la velocidad en km/h.

En el segundo gráfico se traza el SOC, estado de carga de las baterías, en función del tiempo en $s \cdot 10^3$.

En el siguiente gráfico se representa la corriente que proporcionan la bancada de baterías en Amperios, en función del tiempo en $s \cdot 10^3$. El signo es positivo para potencia entregada y en negativo para la corriente de carga.

Finalmente en el gráfico inferior se grafica la potencia generada por los módulos fotovoltaicos en Watios en función del tiempo en $s \cdot 10^3$. Alternativamente se representa también la elevación en metros, para dar una orientación de la altimetría del recorrido.

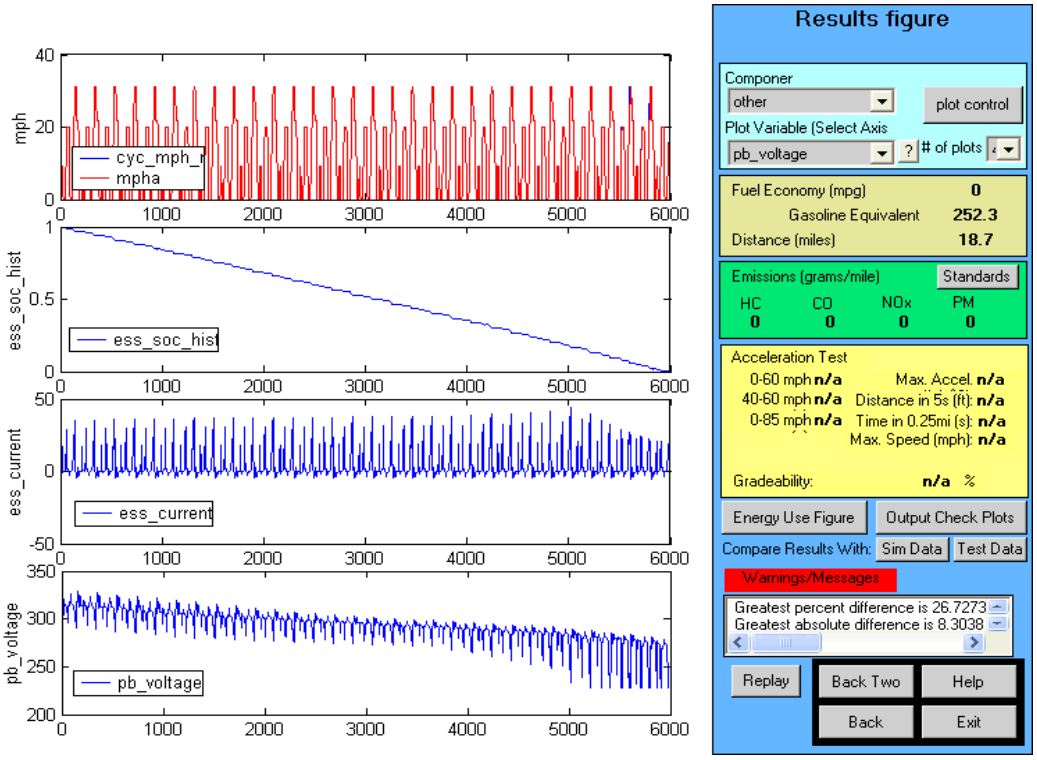


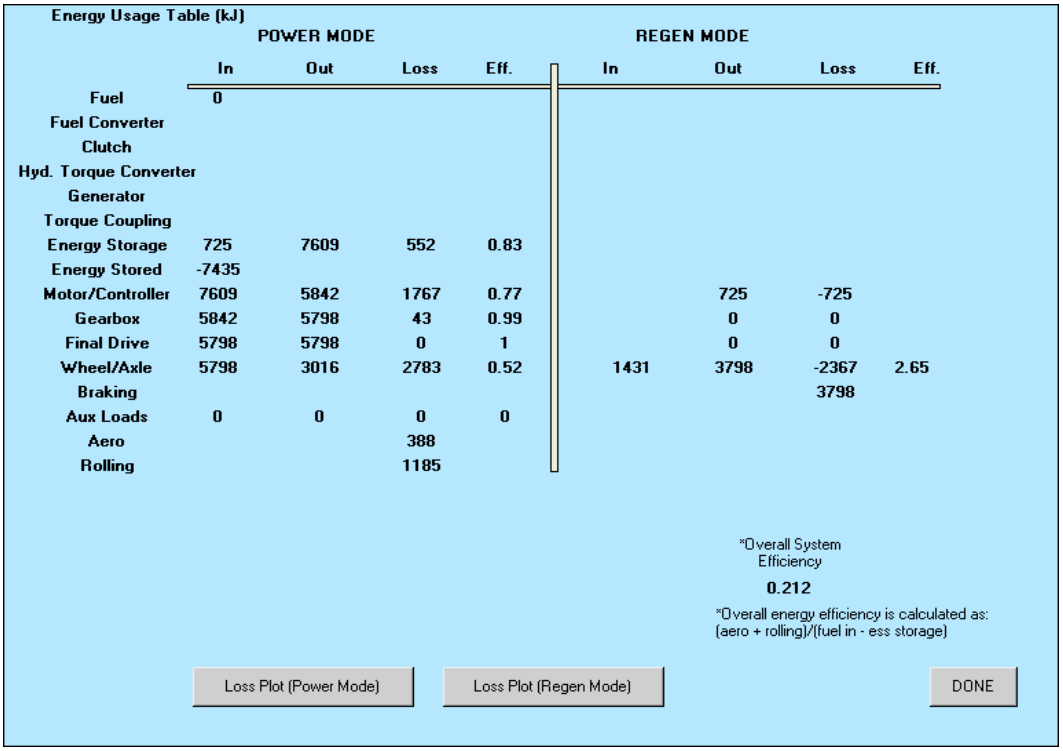


5.1.2.- Sin Radiación. Baterías 7Ah

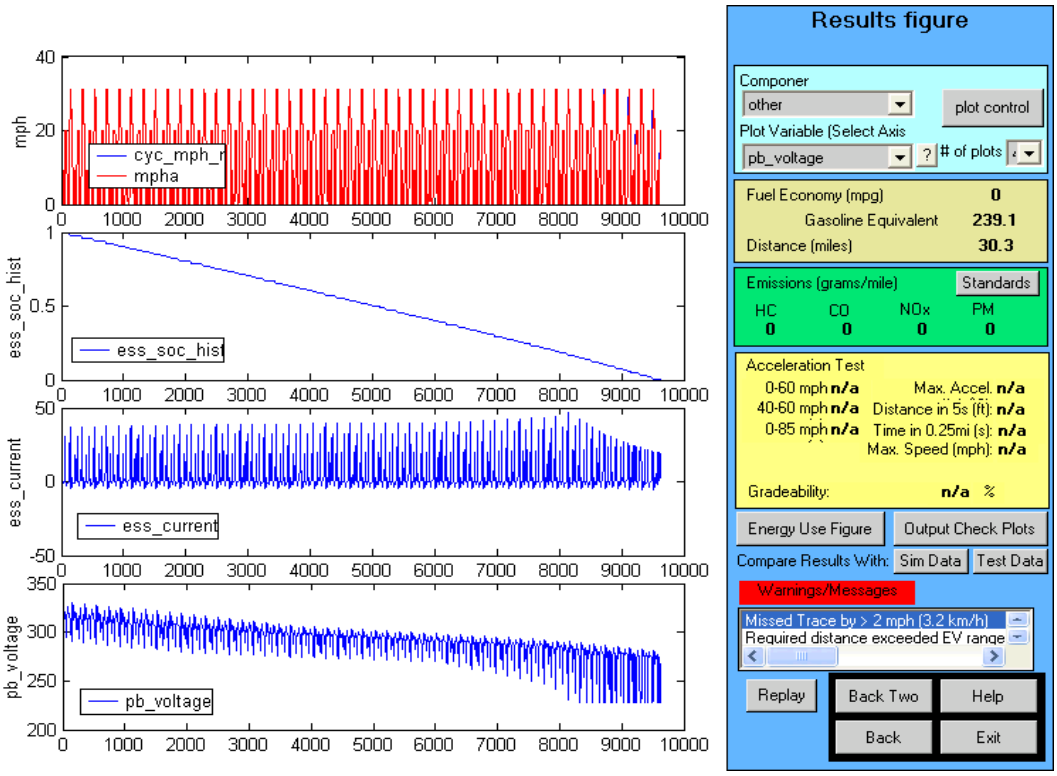


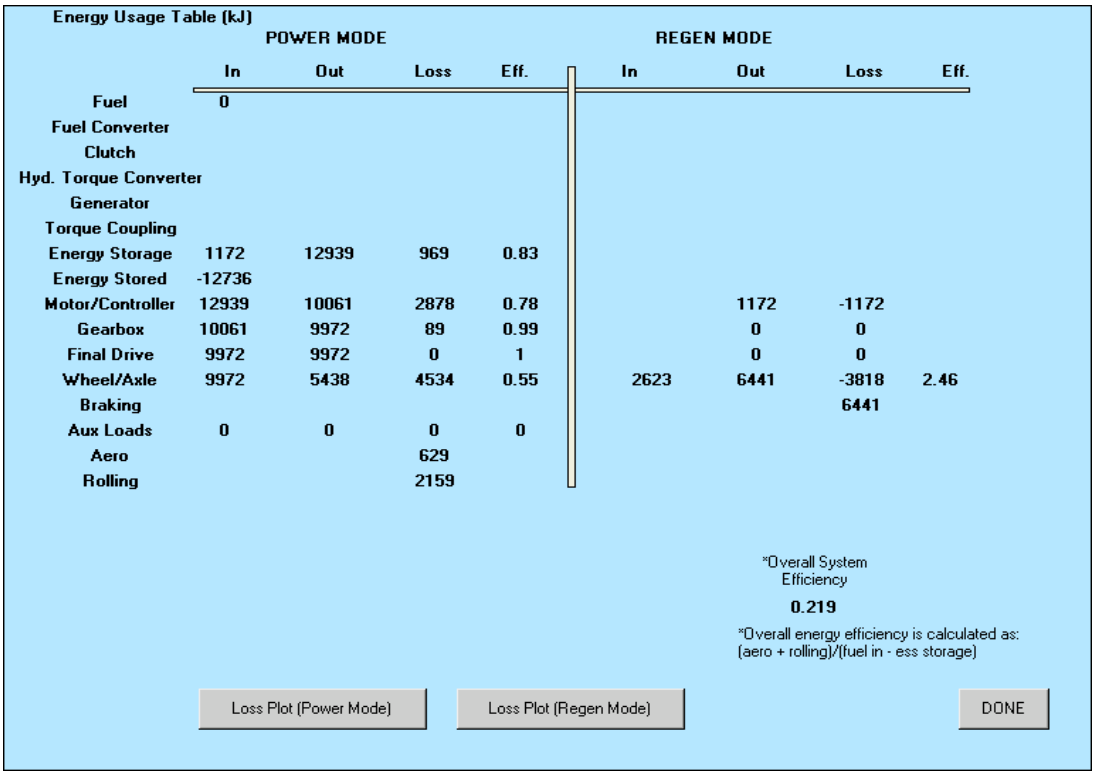


5.1.2.- Sin Radiación. Baterías 12Ah

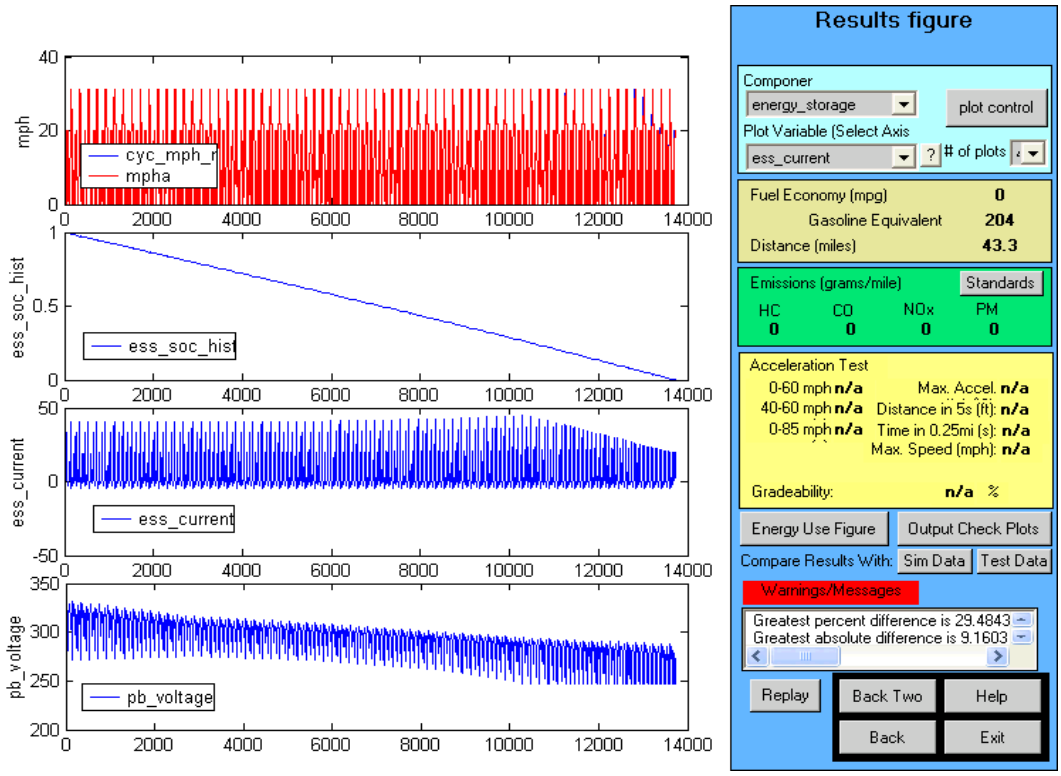


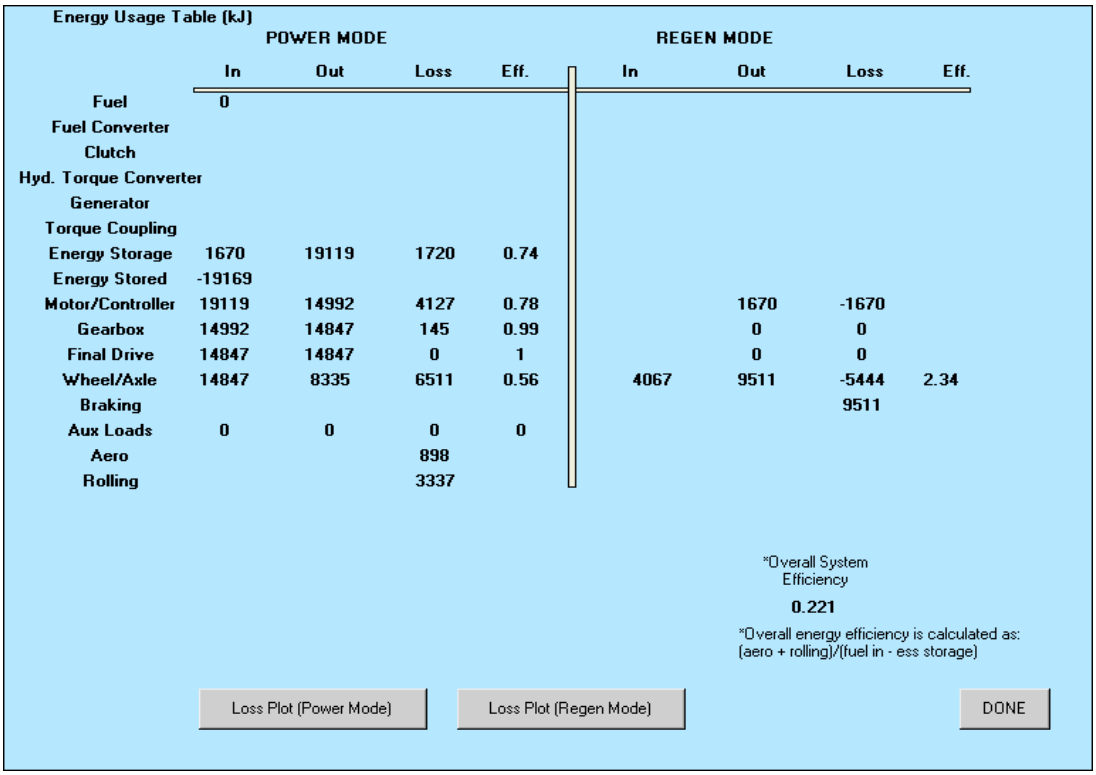


5.1.2.- Sin Radiación. Baterías 16Ah

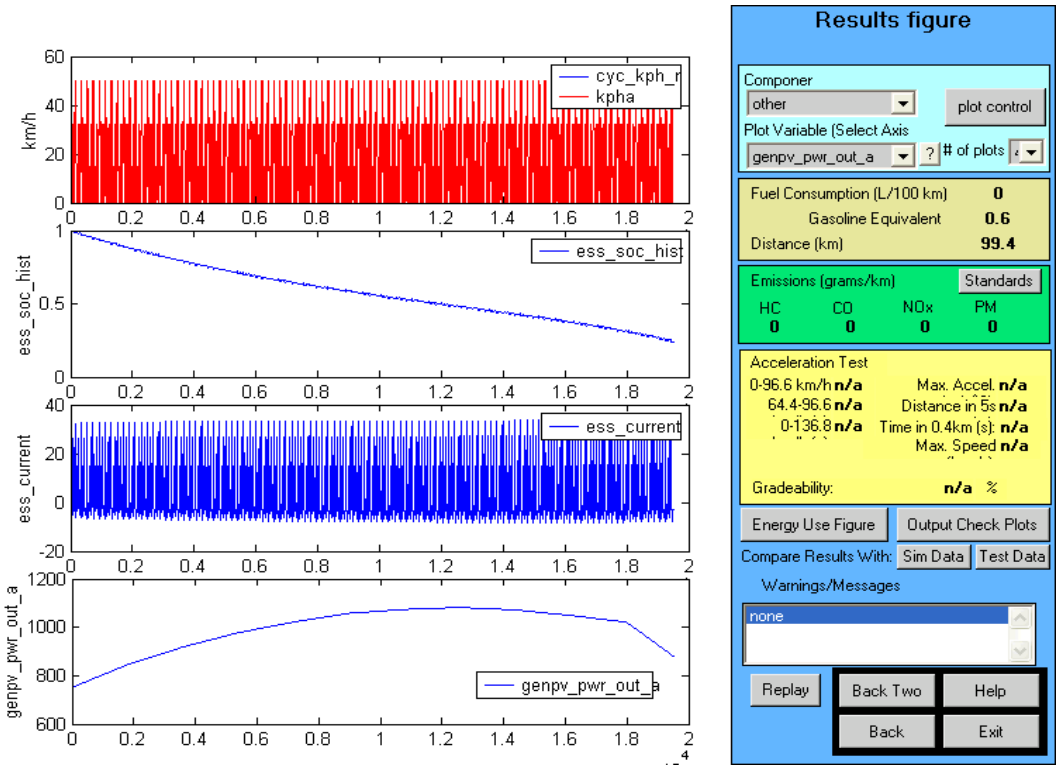


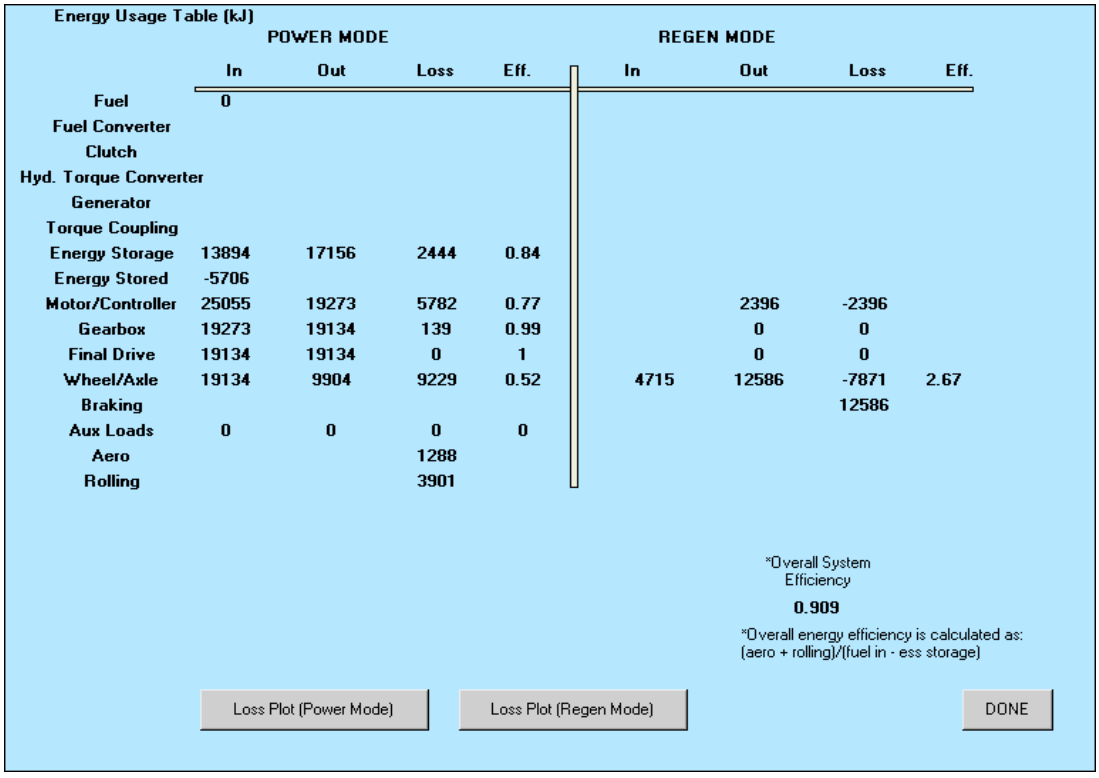


5.1.3.- Día soleado. Baterías 7Ah

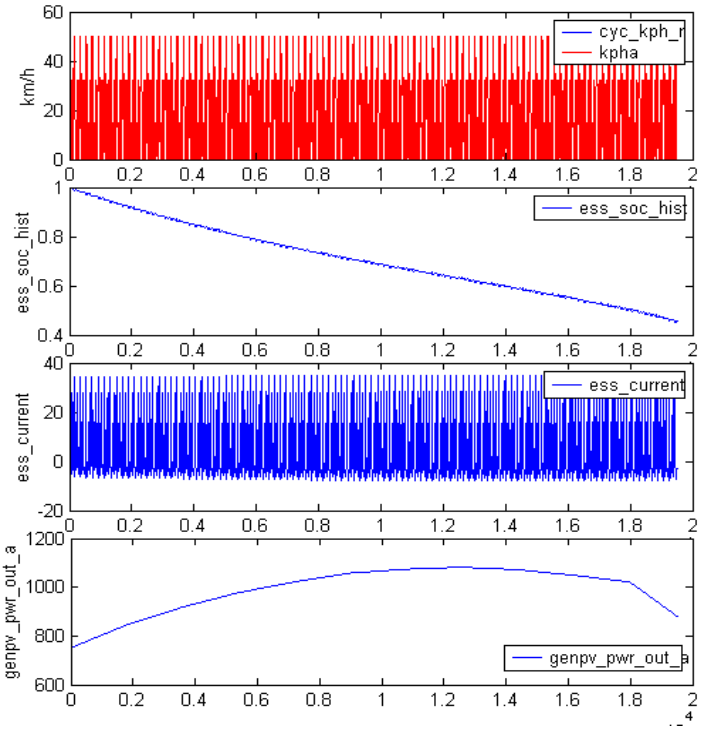


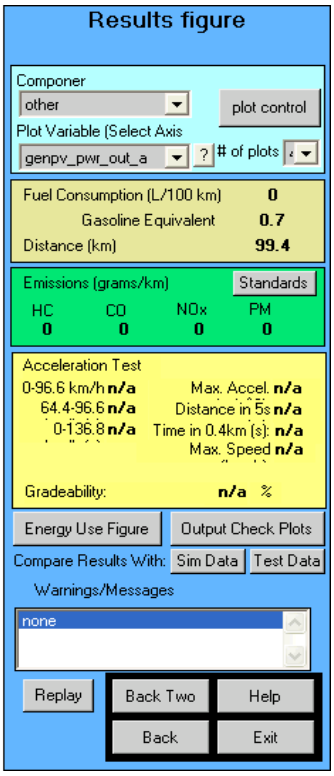


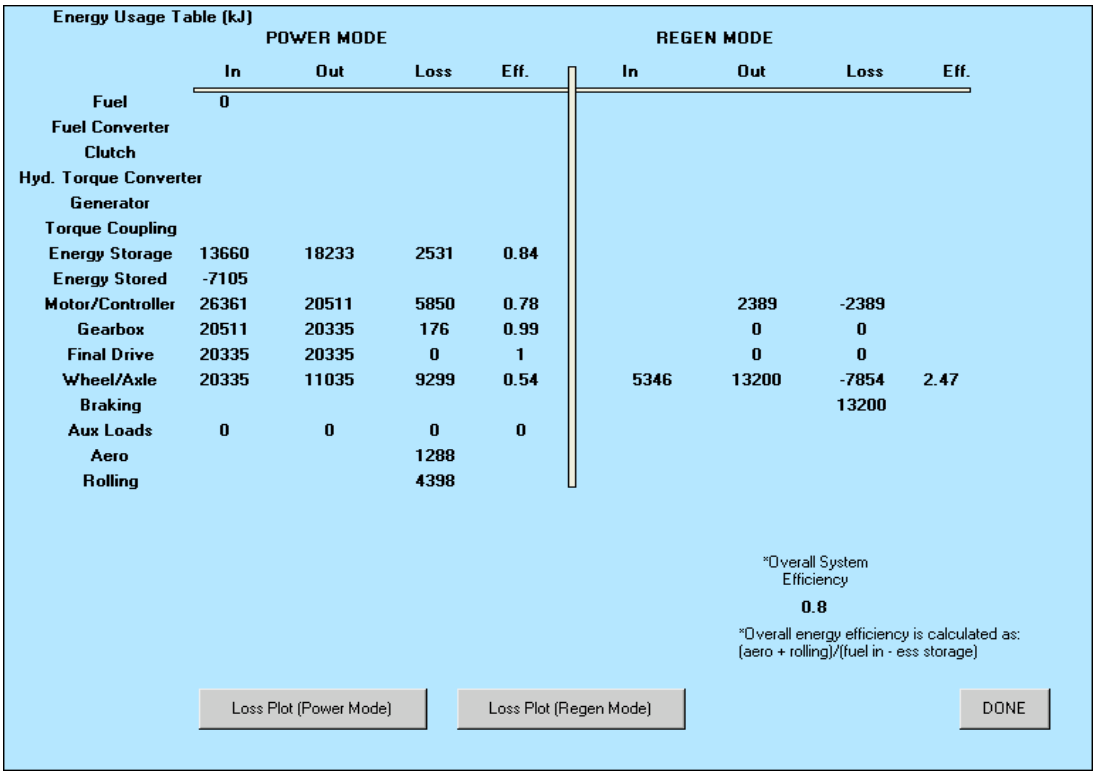


5.1.3.- Día soleado. Baterías 12Ah

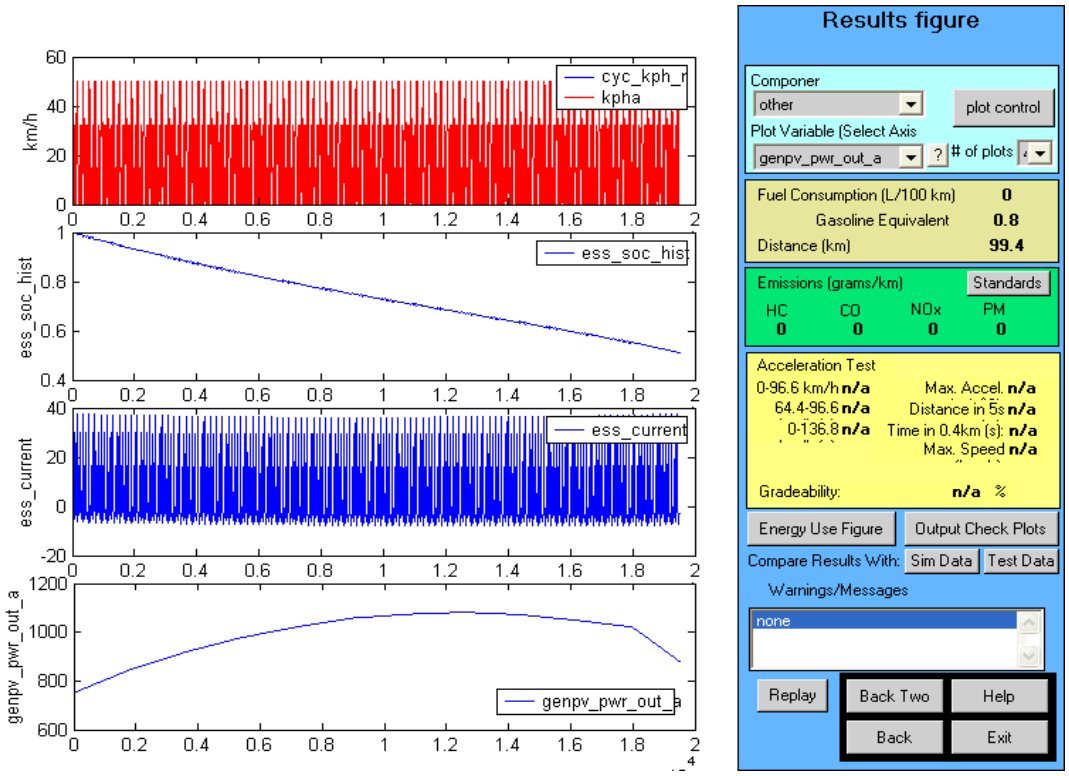


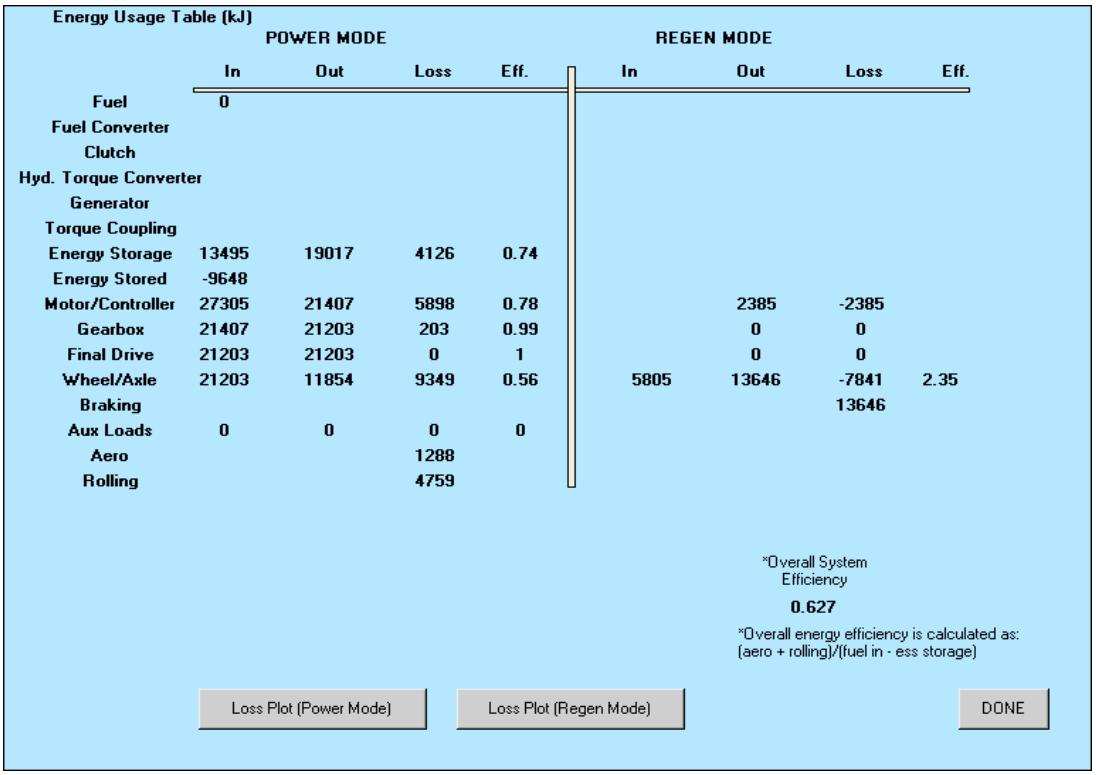


5.1.3.- Día soleado. Baterías 16Ah

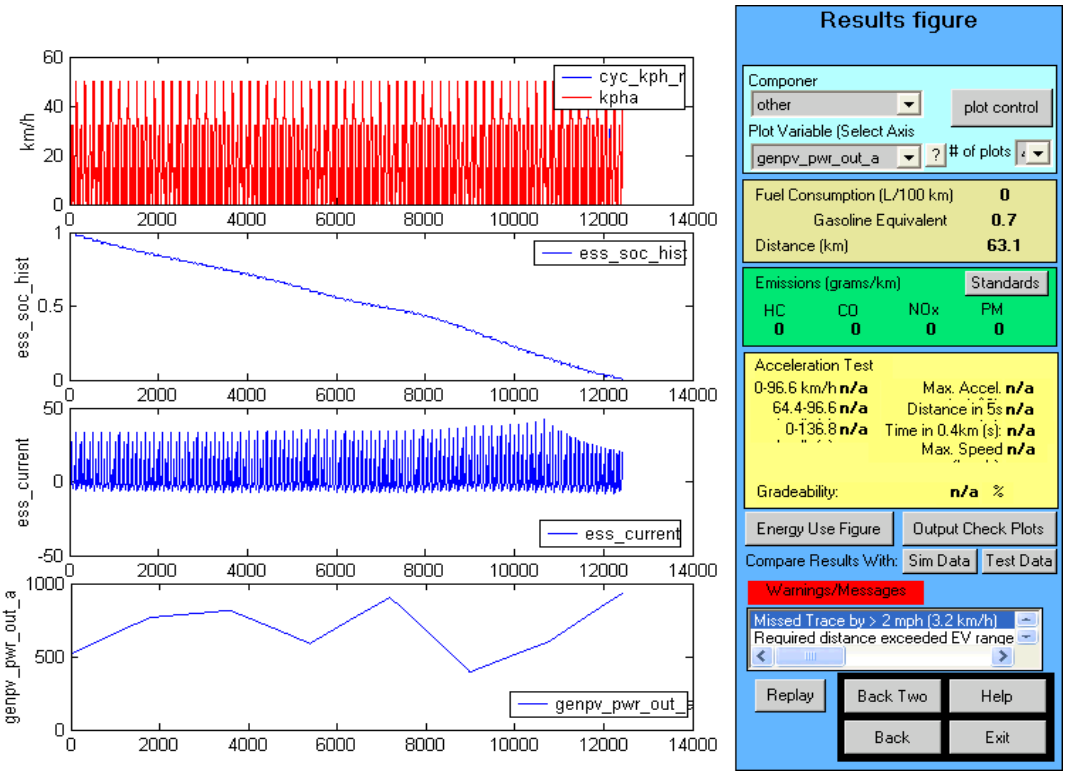


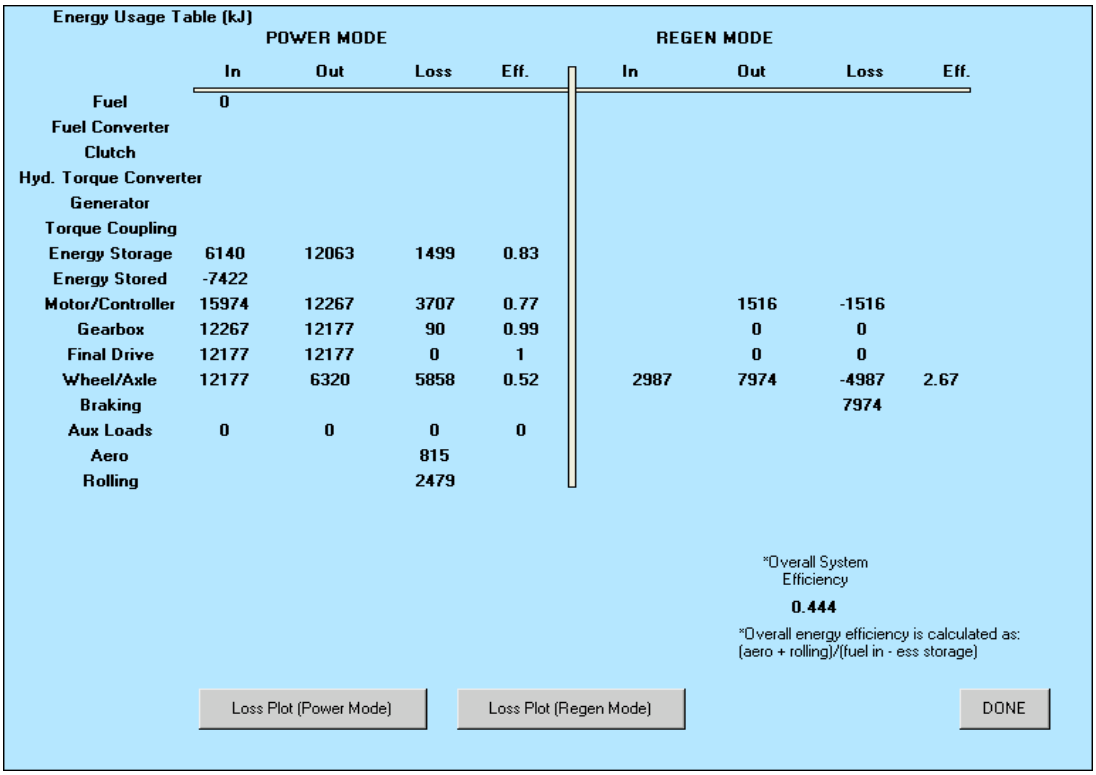


5.1.4.- Nubosidad intermitente. Baterías 7Ah

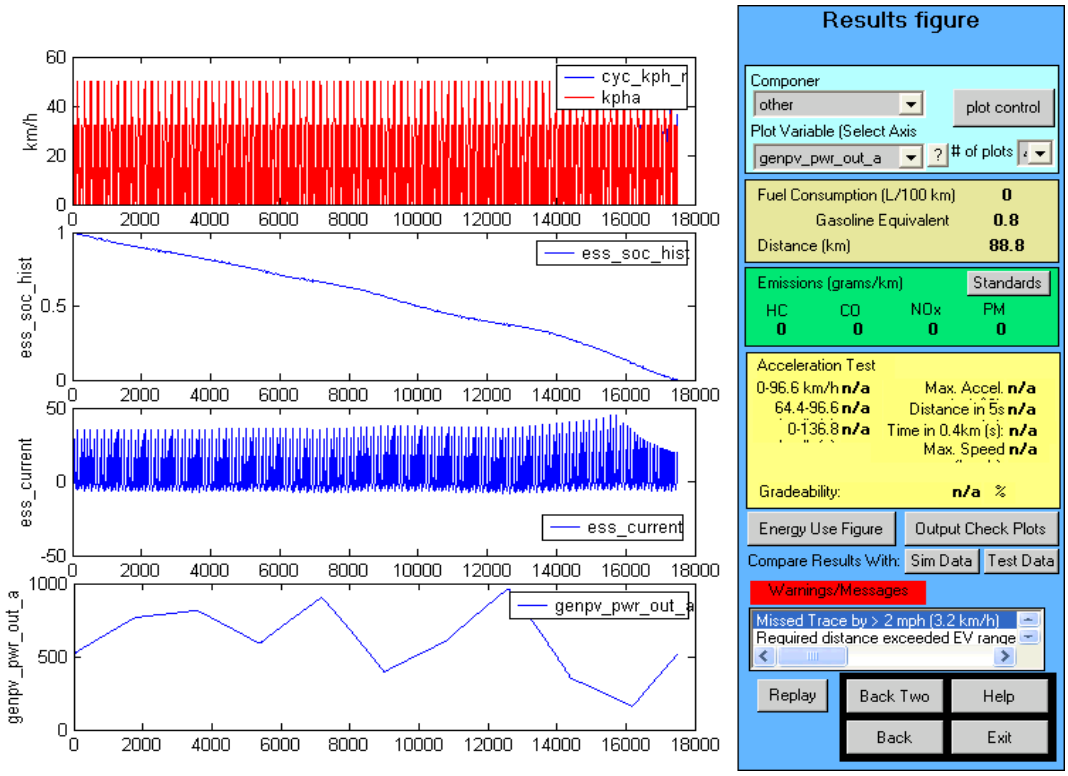


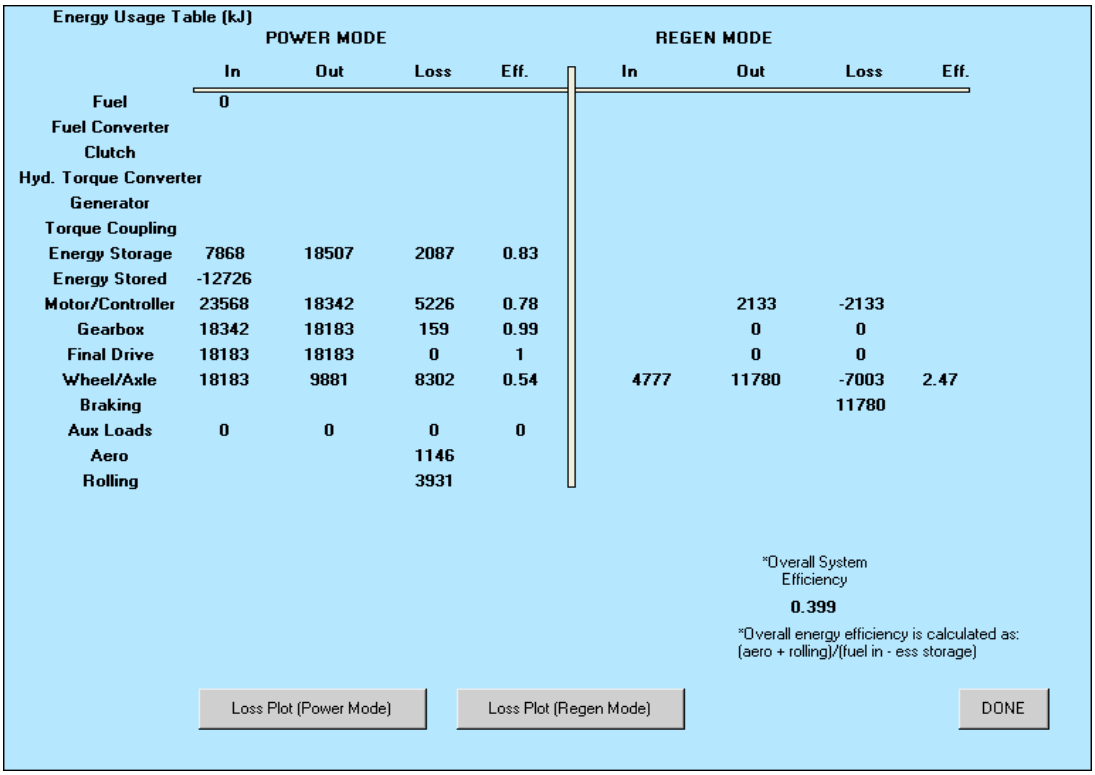


5.1.4.- Nubosidad intermitente. Baterías 12Ah

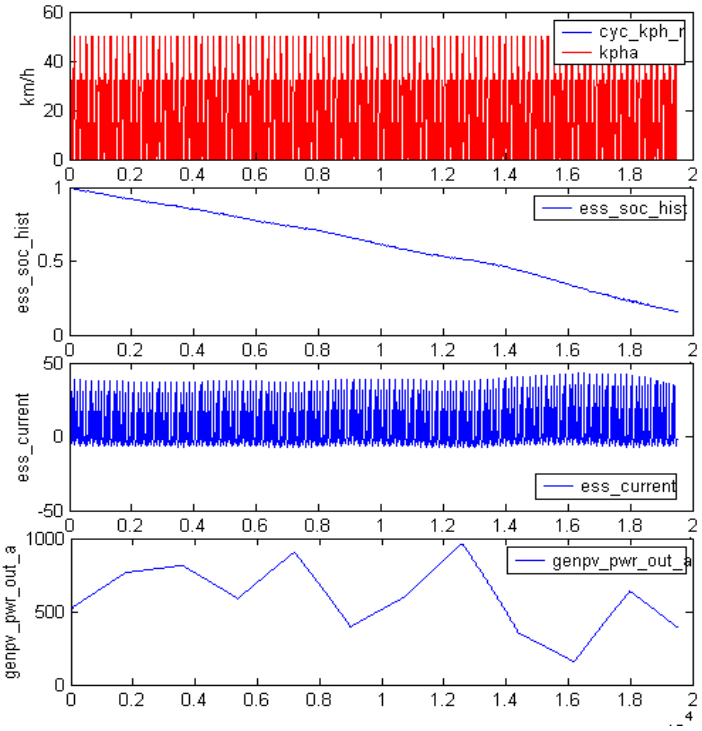


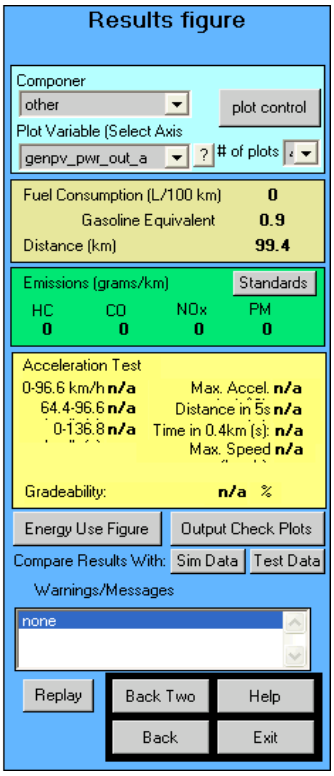


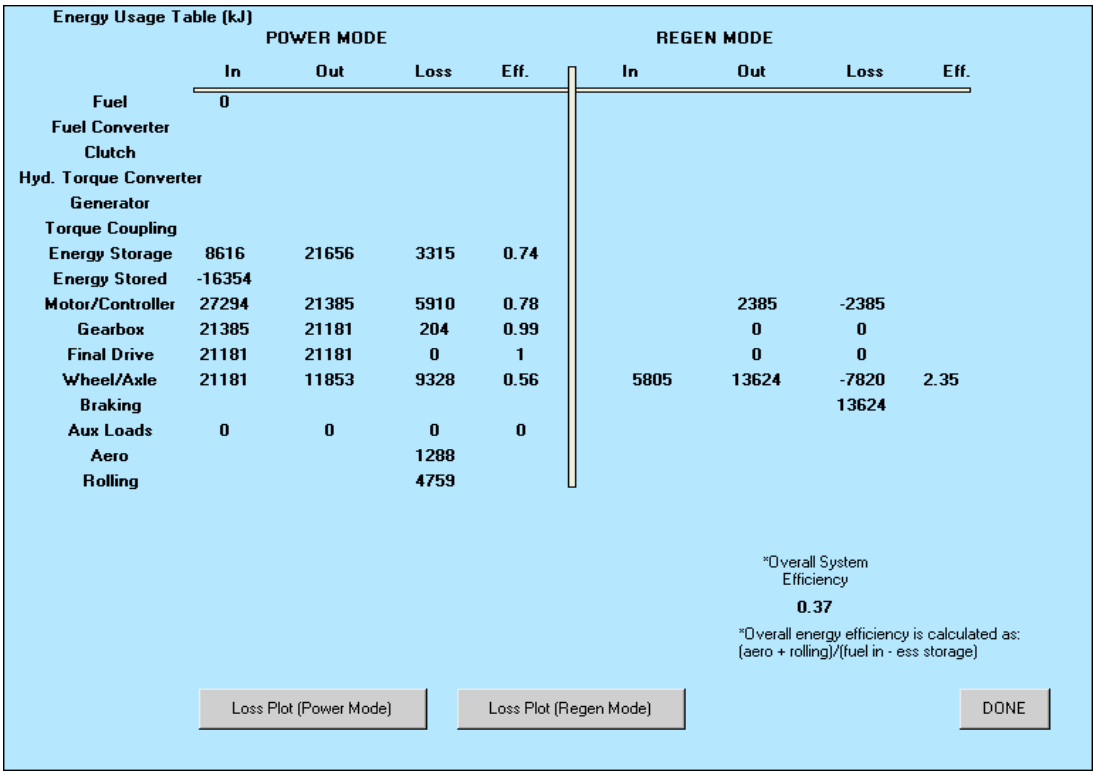


5.1.4.- Nubosidad intermitente. Baterías 16Ah

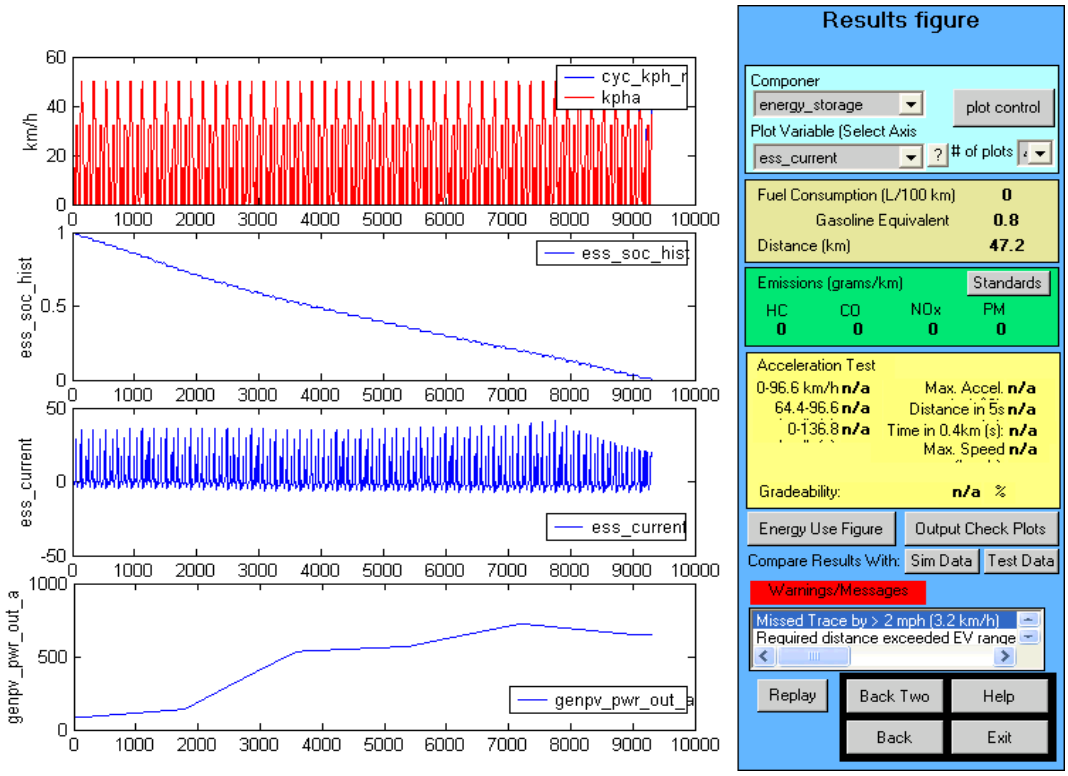


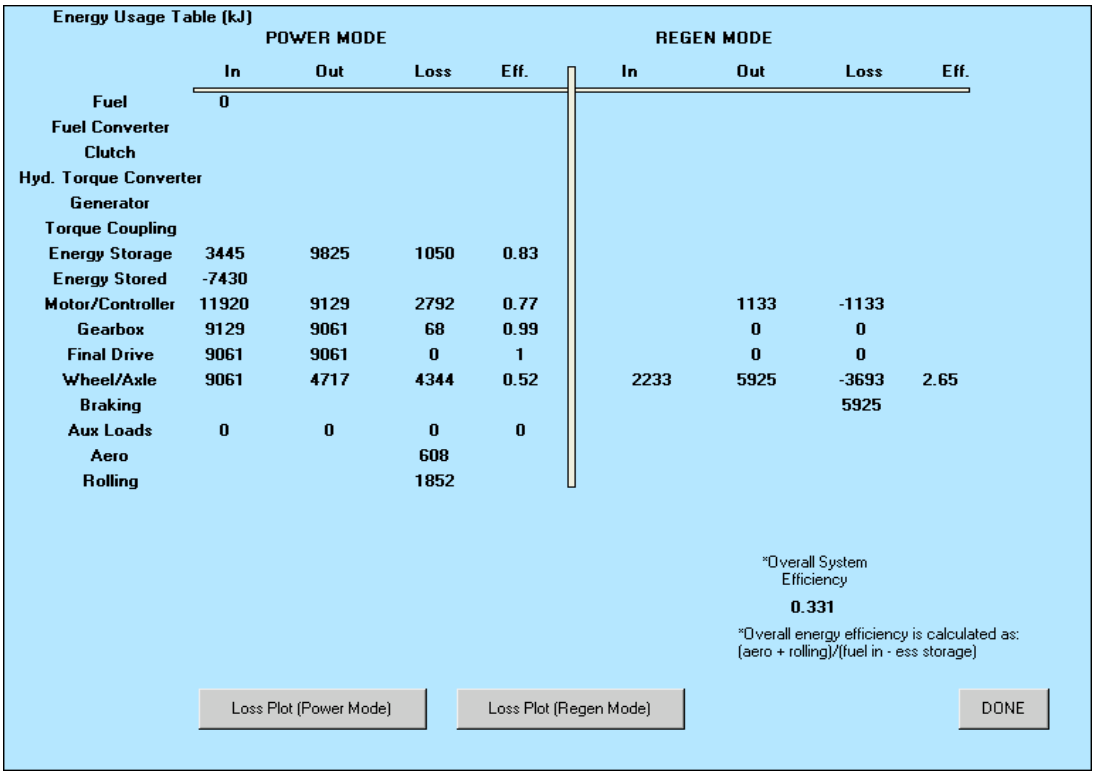


5.1.5.- Nubosidad abundante. Baterías 7Ah

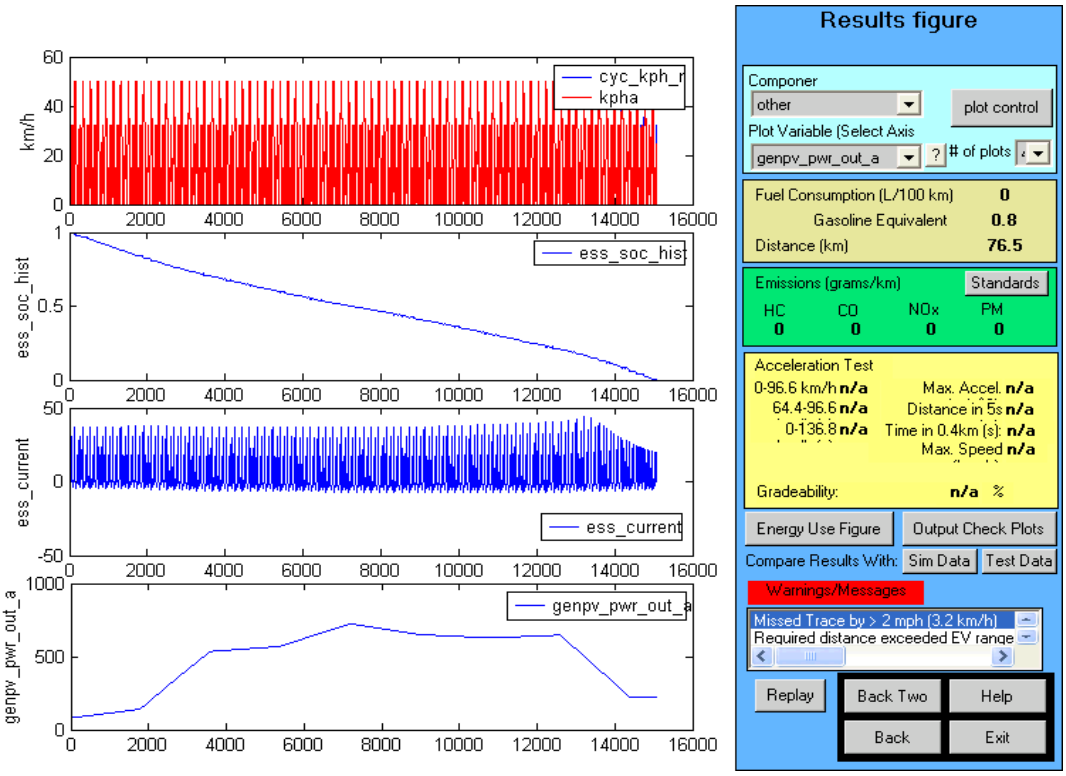


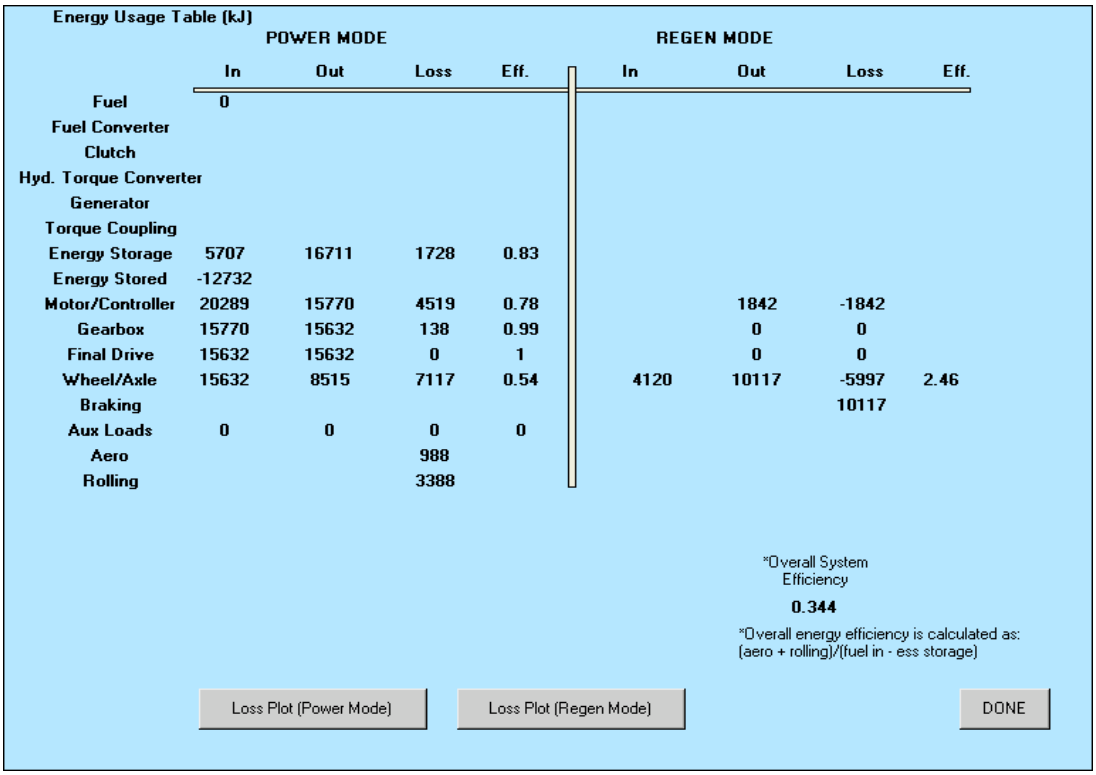


5.1.5.- Nubosidad abundante. Baterías 12Ah

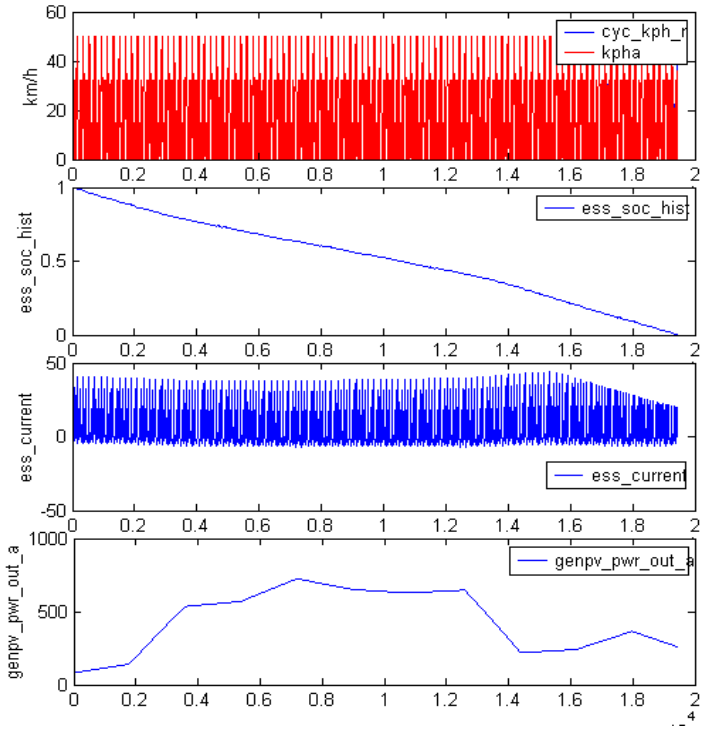


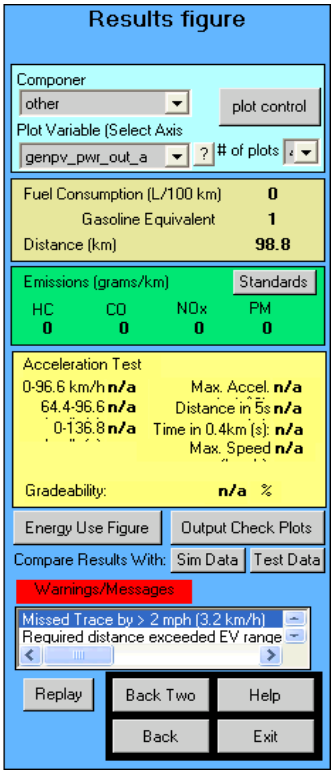


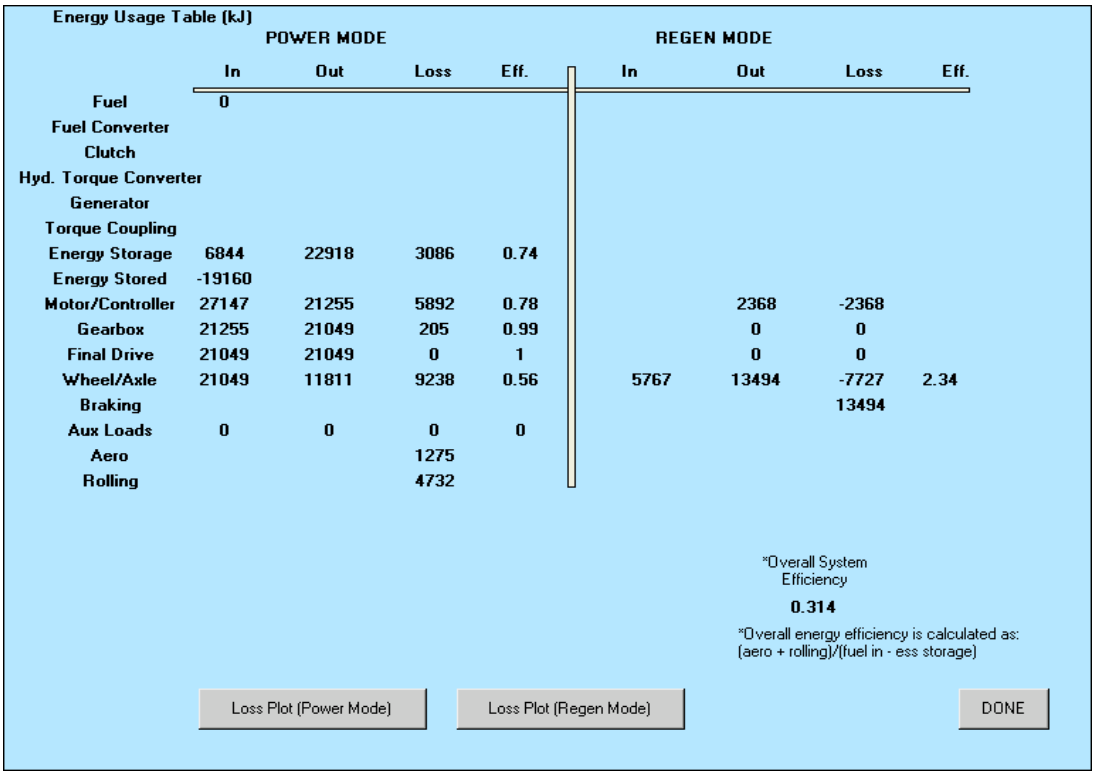


5.1.5.- Nubosidad abundante. Baterías 16Ah

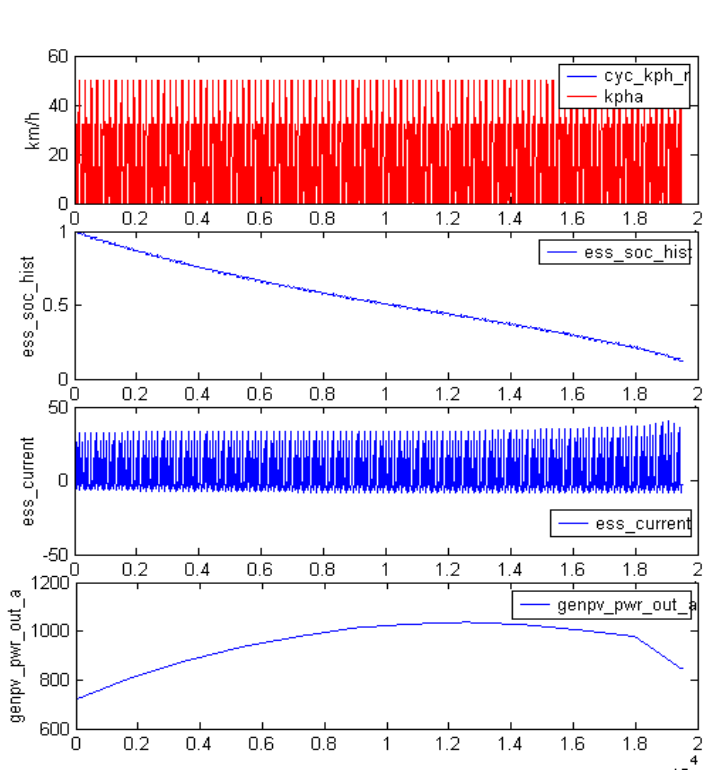


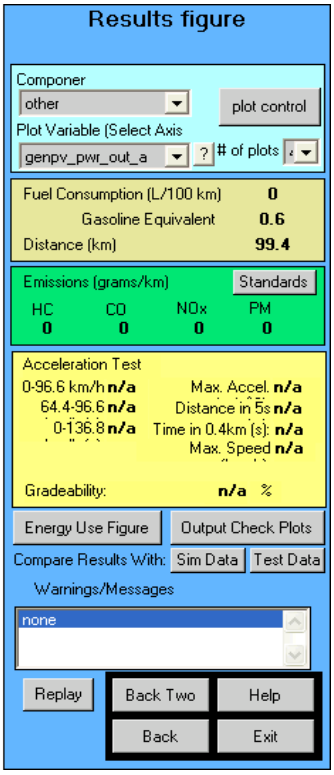


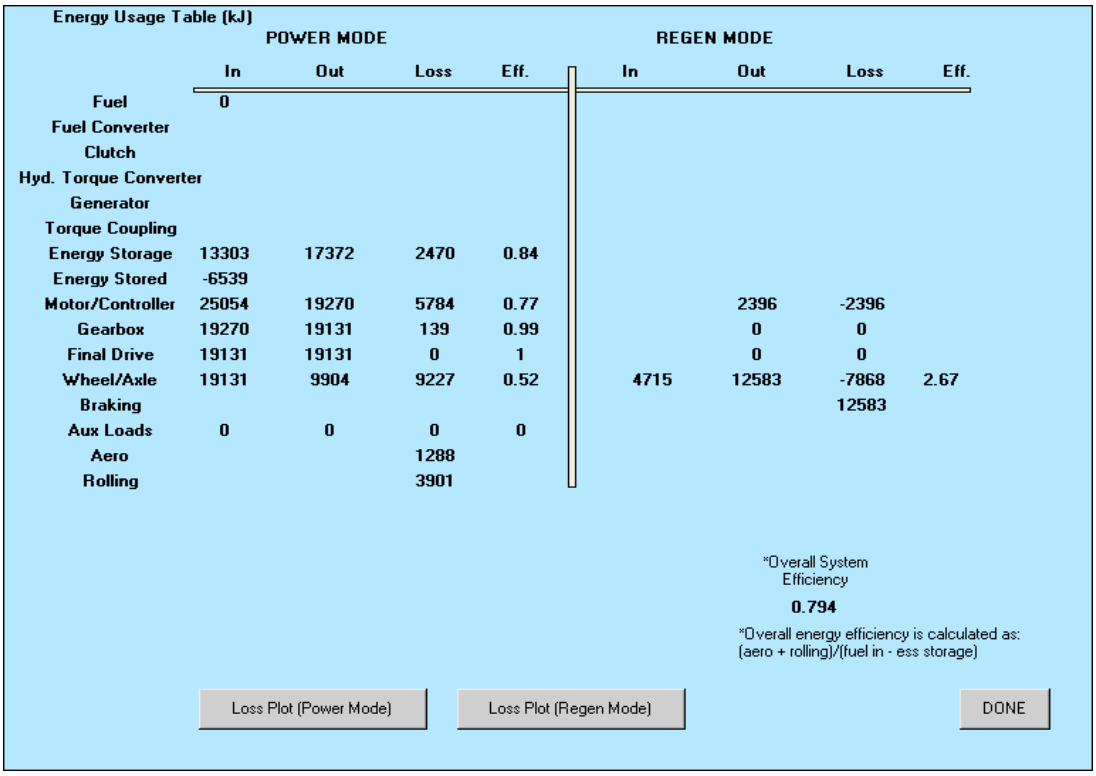


5.1.6.- Avería módulo fotovoltaico. Baterías 7Ah

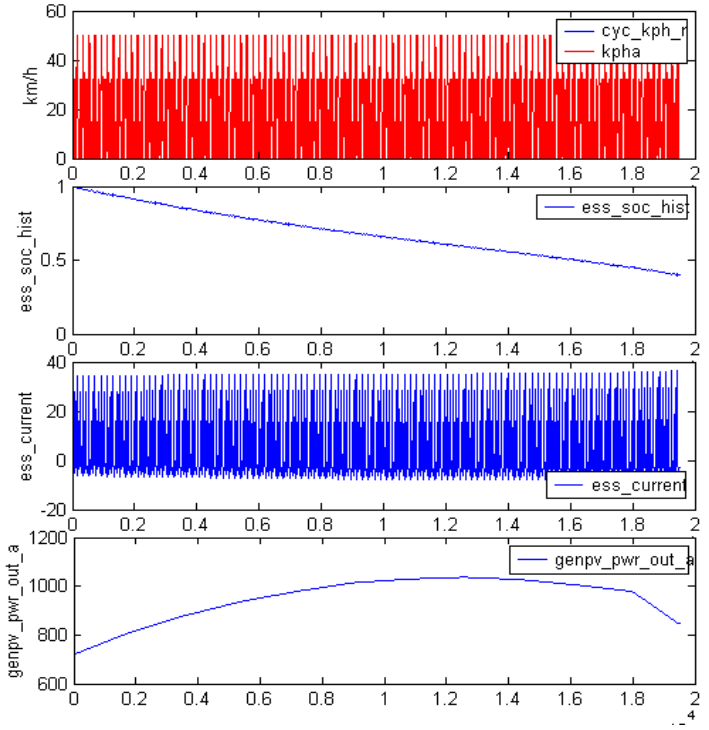


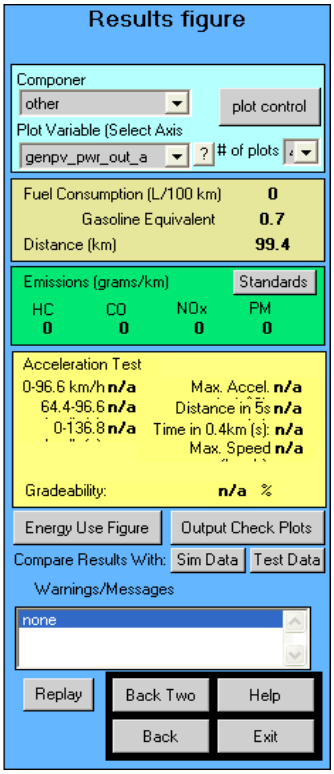


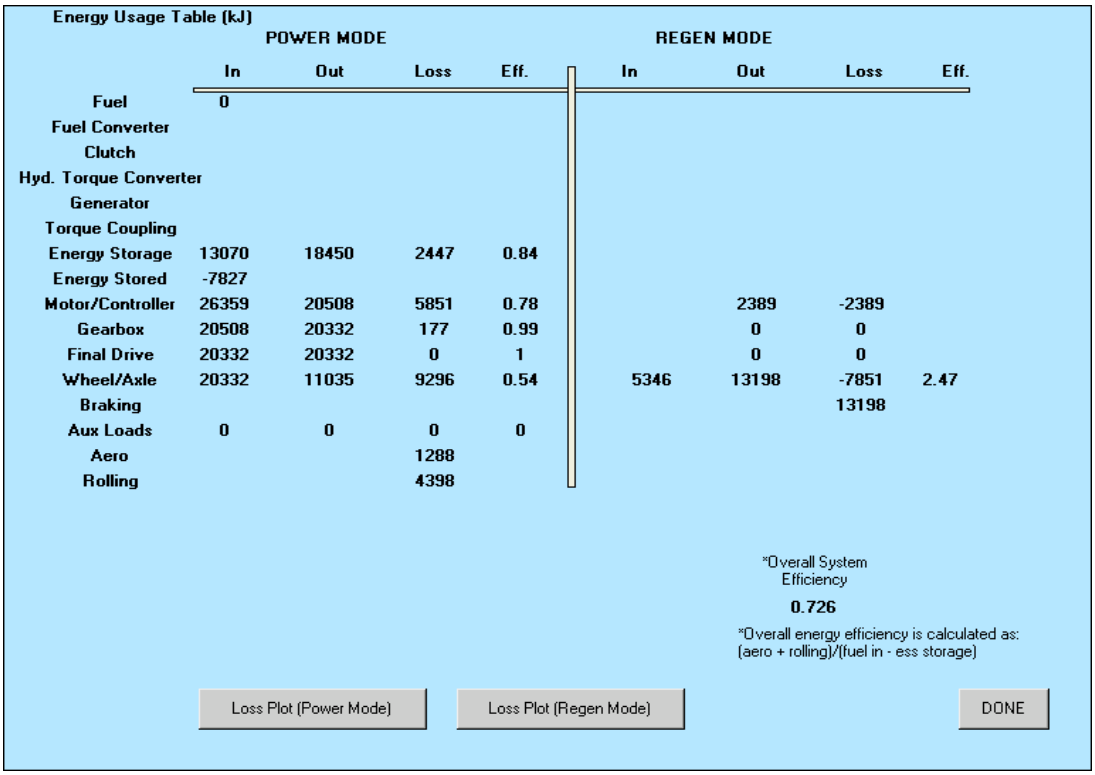


5.1.6.- Avería módulo fotovoltaico. Baterías 12Ah

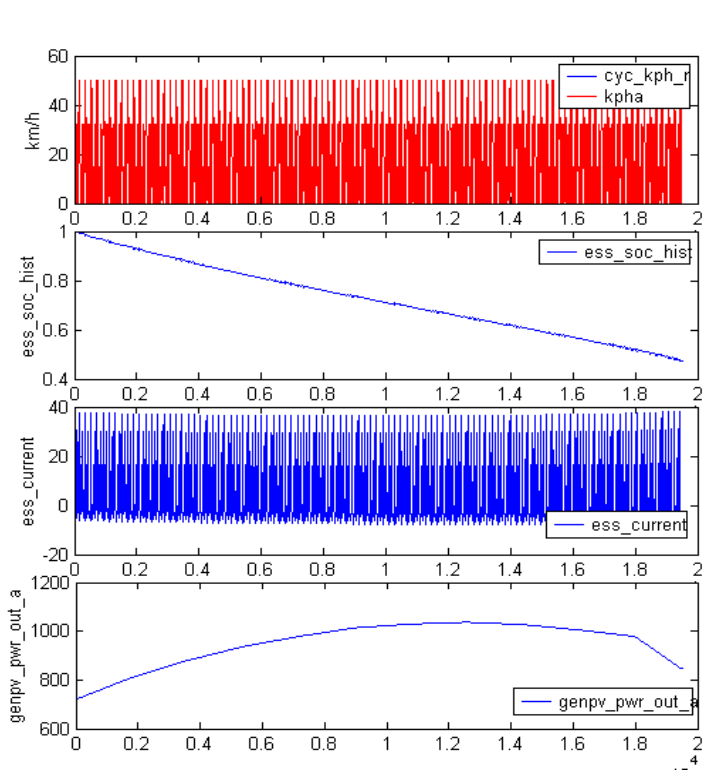


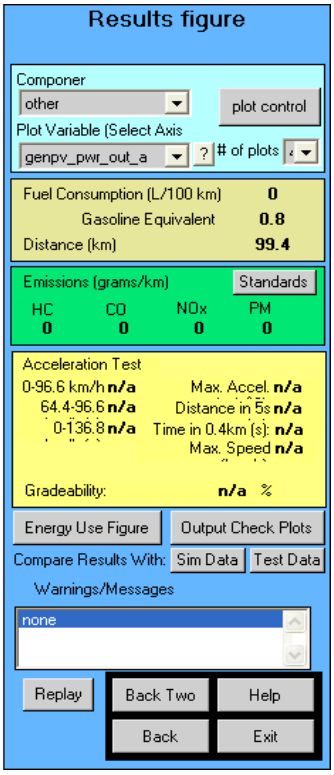


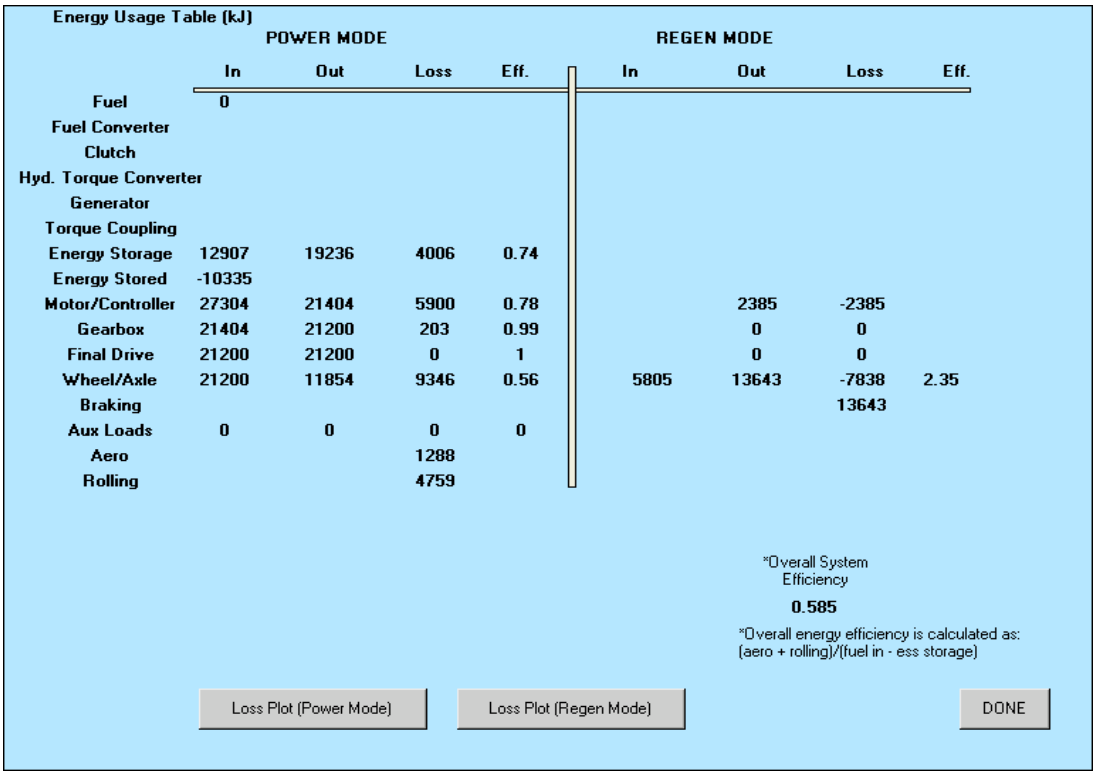


5.1.6.- Avería módulo fotovoltaico. Baterías 16Ah

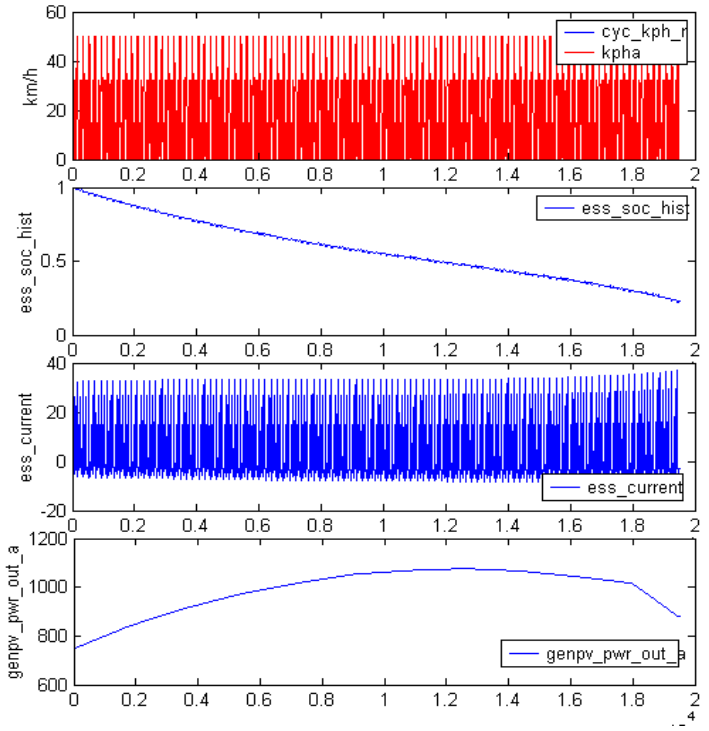


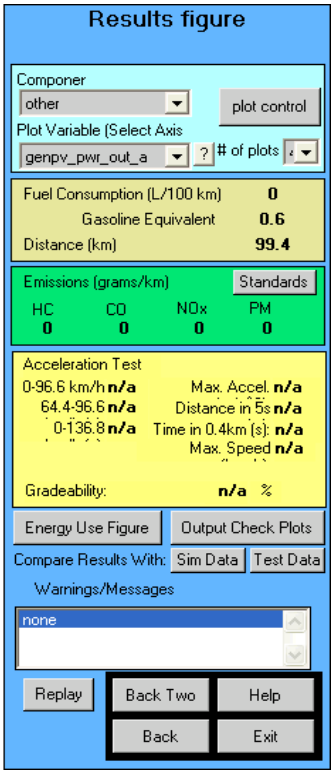


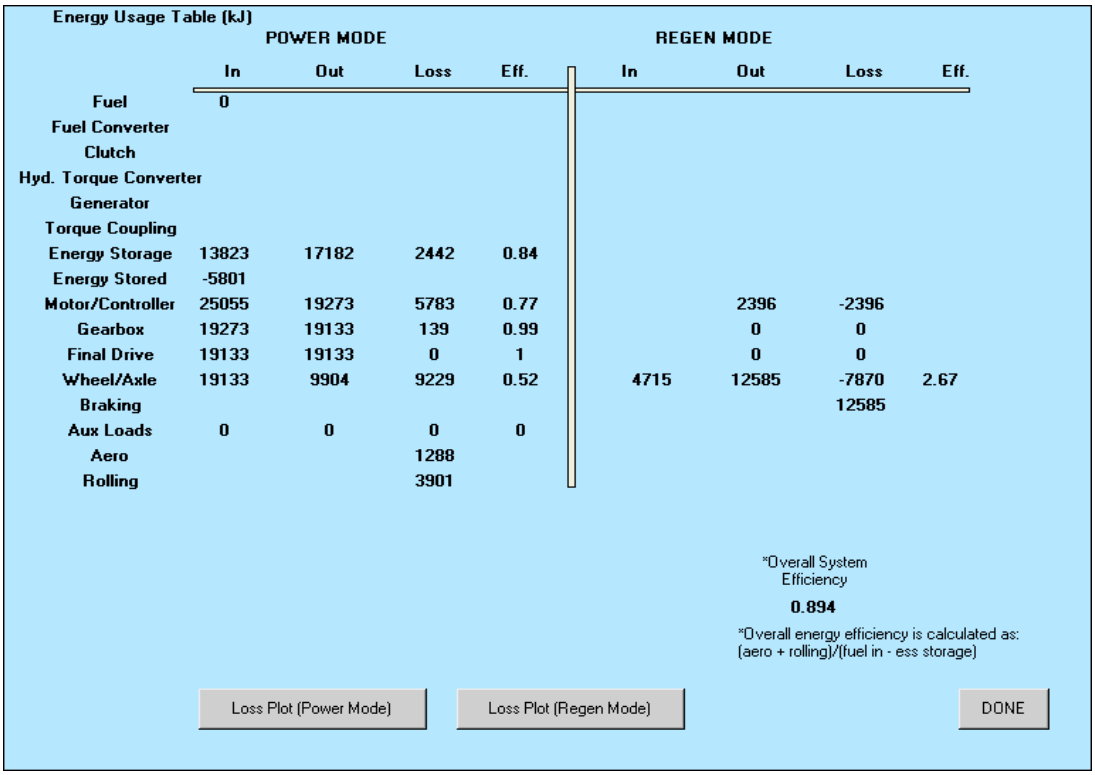


5.1.7.- Temperatura ambiente 30ºC. Baterías 7Ah

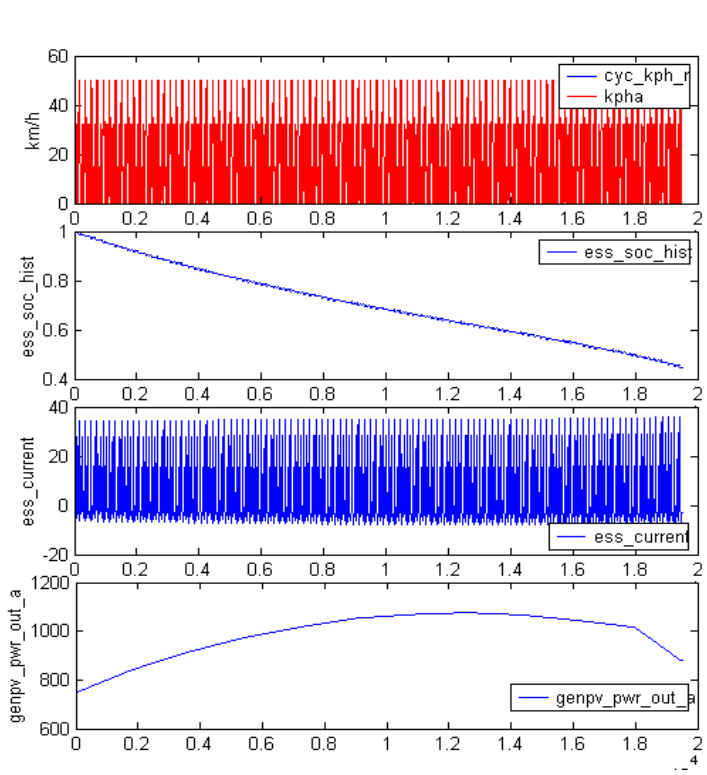


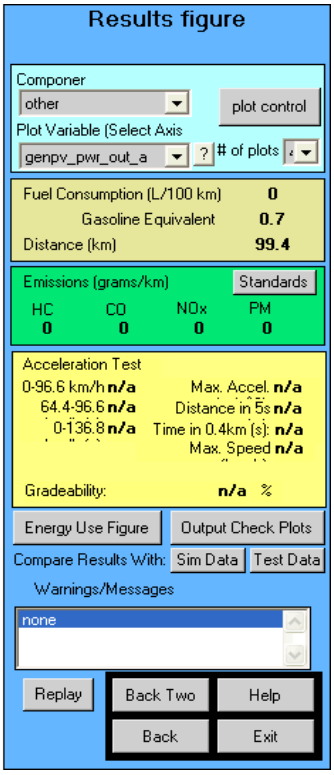


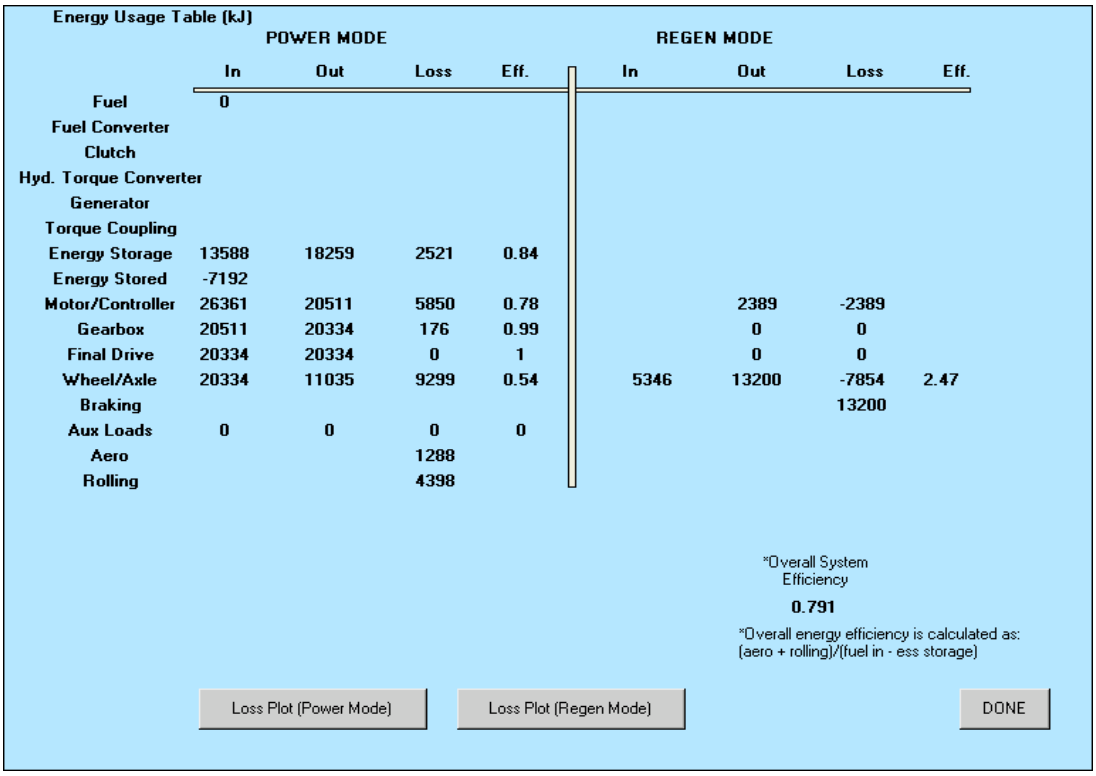


5.1.7.- Temperatura ambiente 30ºC. Baterías 12Ah

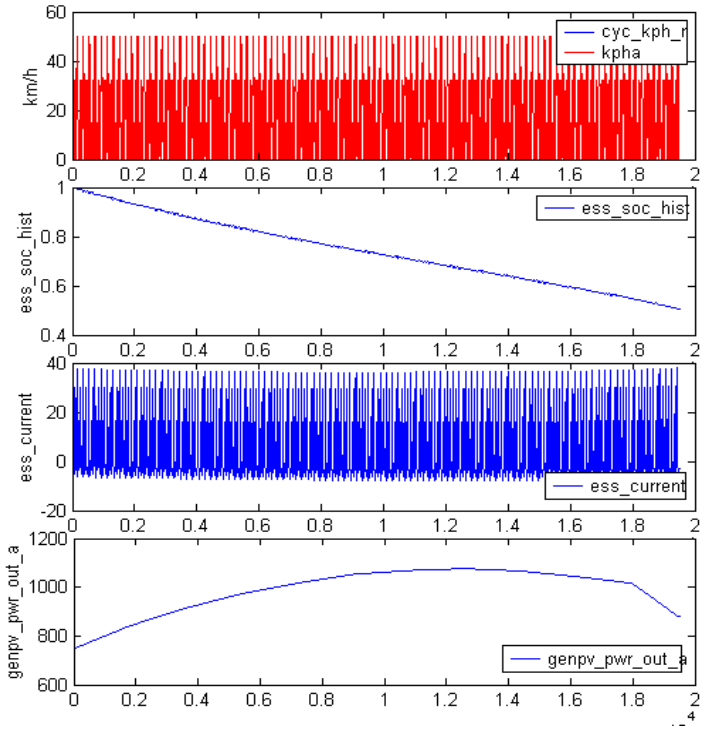


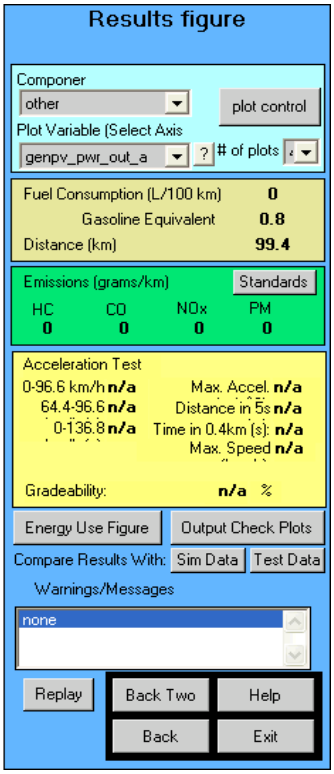


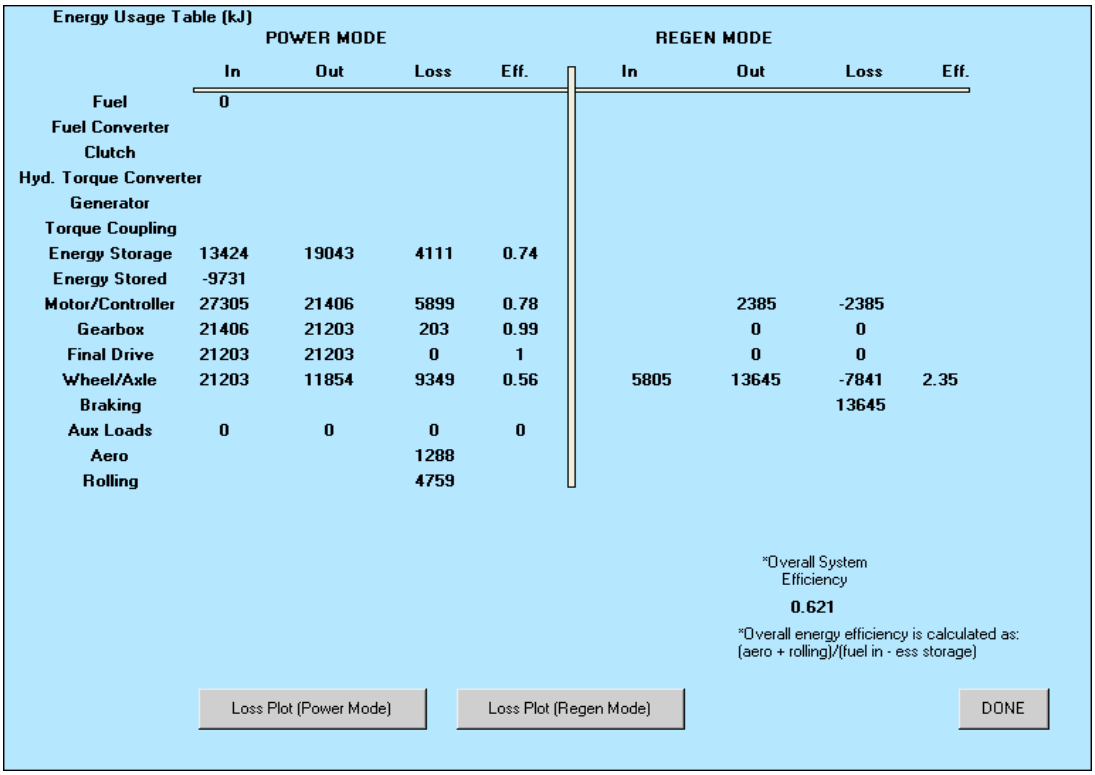

Energy Usage Table (kJ)

| | POWER MODE In | Out | Loss | Eff. | REGEN MODE In | Out | Loss | Eff. |
|---|---|---|---|---|---|---|---|---|
| Fuel | 0 | | | | | | | |
| Fuel Converter | | | | | | | | |
| Clutch | | | | | | | | |
| Hyd. Torque Converter | | | | | | | | |
| Generator | | | | | | | | |
| Torque Coupling | | | | | | | | |
| Energy Storage | 13424 | 19043 | 4111 | 0.74 | | | | |
| Energy Stored | -9731 | | | | | | | |
| Motor/Controller | 27305 | 21406 | 5899 | 0.78 | | 2385 | -2385 | |
| Gearbox | 21406 | 21203 | 203 | 0.99 | | 0 | 0 | |
| Final Drive | 21203 | 21203 | 0 | 1 | | 0 | 0 | |
| Wheel/Axle | 21203 | 11854 | 9349 | 0.56 | 5805 | 13645 | -7841 | 2.35 |
| Braking | | | | | | | 13645 | |
| Aux Loads | 0 | 0 | 0 | 0 | | | | |
| Aero | | | 1288 | | | | | |
| Rolling | | | 4759 | | | | | |



5.1.7.- Temperatura ambiente 30ºC. Baterías 16Ah

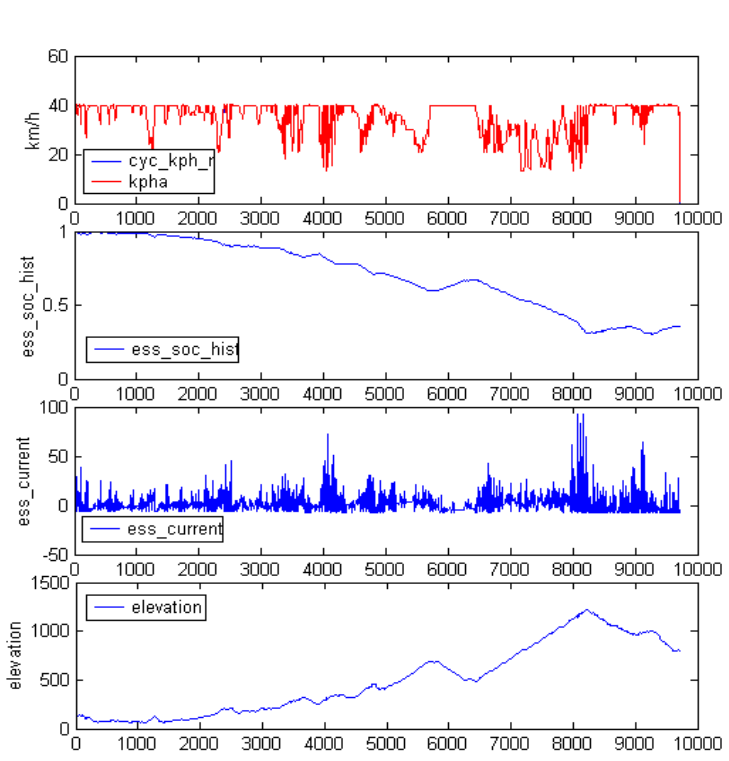


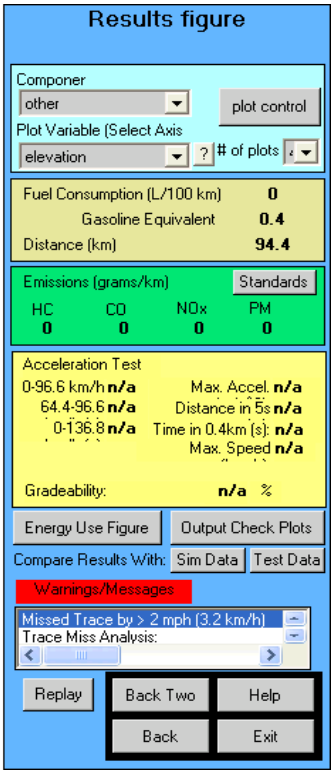


**Energy Usage Table (kJ)**

| | POWER MODE | | | | REGEN MODE | | | |
|---|---|---|---|---|---|---|---|---|
| | In | Out | Loss | Eff. | In | Out | Loss | Eff. |
| Fuel | 0 | | | | | | | |
| Fuel Converter | | | | | | | | |
| Clutch | | | | | | | | |
| Hyd. Torque Converter | | | | | | | | |
| Generator | | | | | | | | |
| Torque Coupling | | | | | | | | |
| Energy Storage | 5635 | 9483 | 1064 | 0.84 | | | | |
| Energy Stored | -4912 | | | | | | | |
| Motor/Controller | 15733 | 14352 | 1381 | 0.91 | 1723 | 1868 | -145 | 1.08 |
| Gearbox | 14352 | 13940 | 412 | 0.97 | 1776 | 1723 | 53 | 0.97 |
| Final Drive | 13940 | 13940 | 0 | 1 | 1776 | 1776 | 0 | 1 |
| Wheel/Axle | 13940 | 12664 | 1276 | 0.91 | 5102 | 5042 | 60 | 0.99 |
| Braking | | | | | | | 3266 | |
| Aux Loads | 0 | 0 | 0 | 0 | | | | |
| Aero | | | 1272 | | | | | |
| Rolling | | | 3699 | | | | | |

*Overall System Efficiency

1.012

*Overall energy efficiency is calculated as: (aero + rolling)/(fuel in - ess storage)

Loss Plot (Power Mode) Loss Plot (Regen Mode) DONE

5.2.1.- Día soleado. Baterías 7Ah

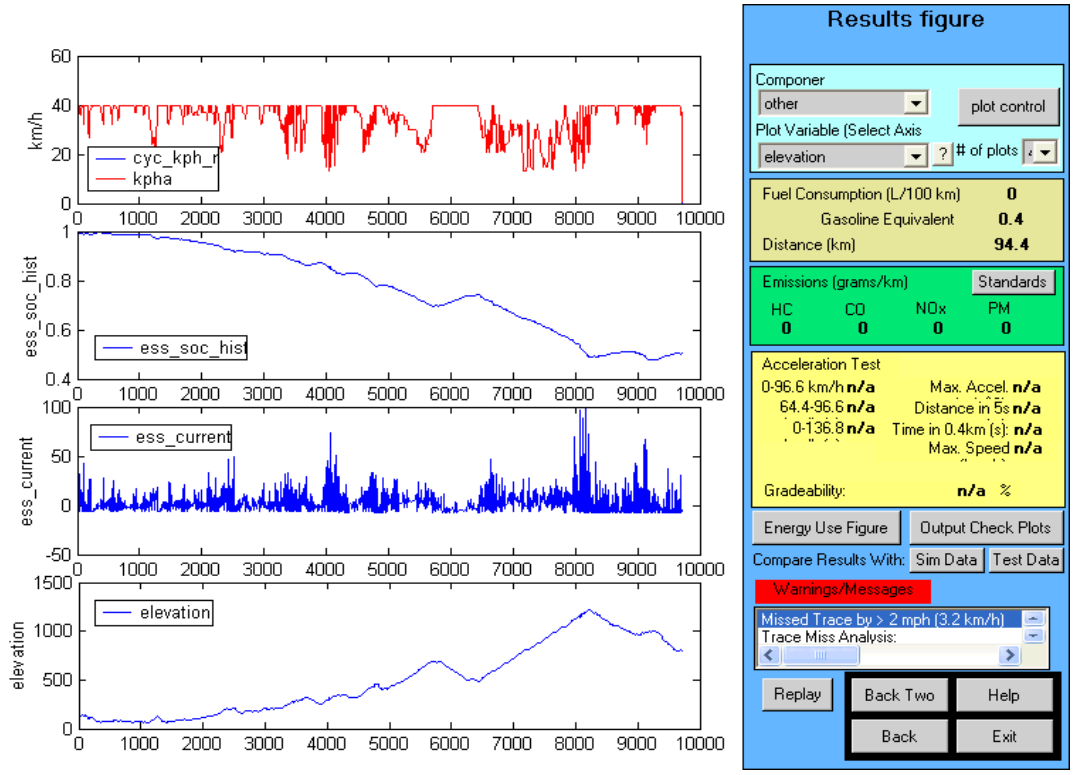


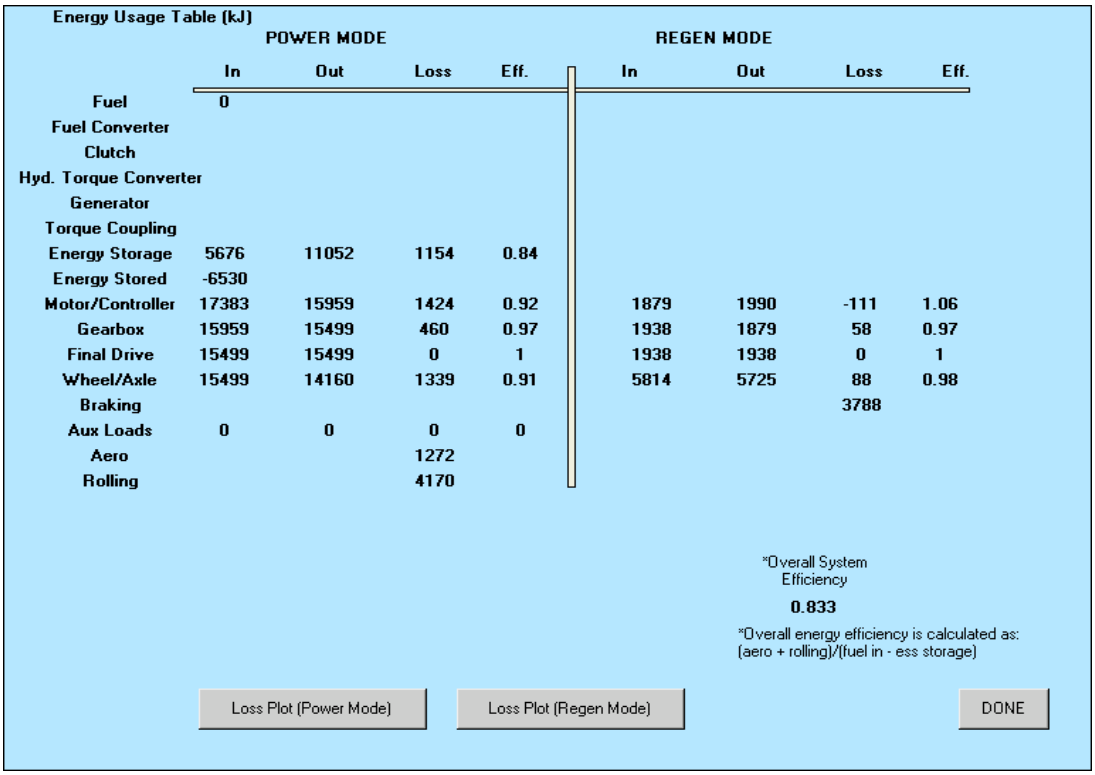


5.2.1.- Día soleado. Baterías 12Ah

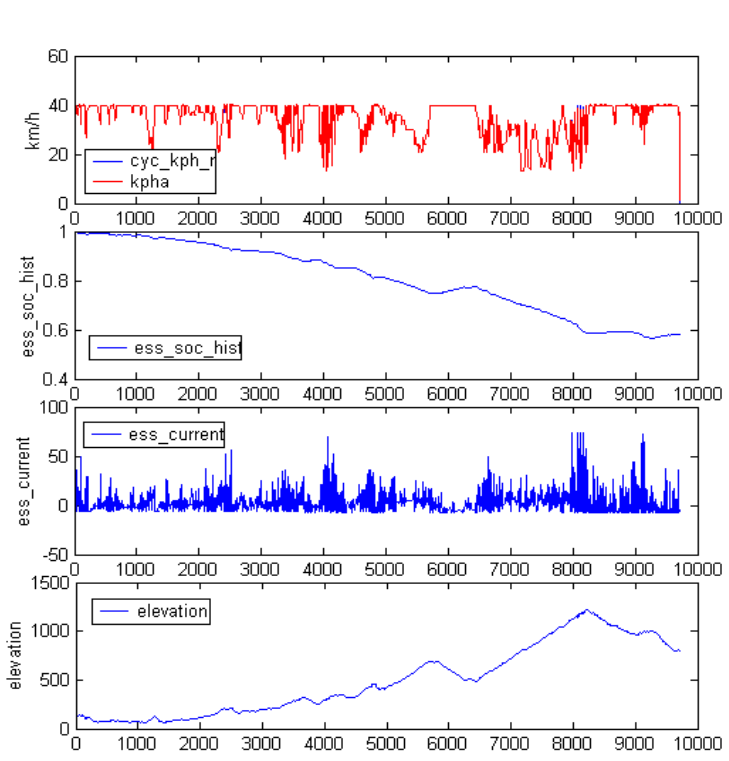


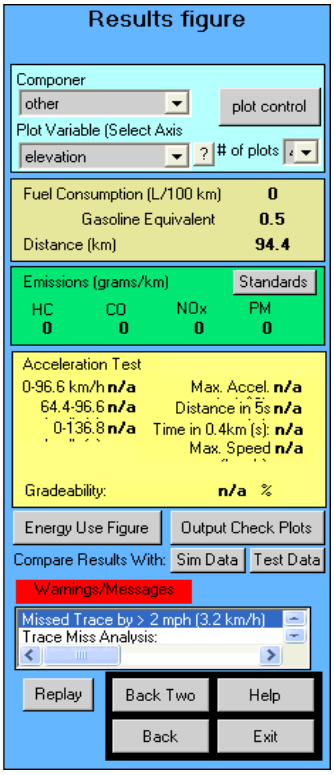


**Energy Usage Table (kJ)**

| | POWER MODE | | | | REGEN MODE | | | |
|---|---|---|---|---|---|---|---|---|
| | In | Out | Loss | Eff. | In | Out | Loss | Eff. |
| Fuel | 0 | | | | | | | |
| Fuel Converter | | | | | | | | |
| Clutch | | | | | | | | |
| Hyd. Torque Converter | | | | | | | | |
| Generator | | | | | | | | |
| Torque Coupling | | | | | | | | |
| Energy Storage | 5711 | 12159 | 1876 | 0.74 | | | | |
| Energy Stored | -8324 | | | | | | | |
| Motor/Controller | 18532 | 17103 | 1429 | 0.92 | 1992 | 2067 | -75 | 1.04 |
| Gearbox | 17103 | 16608 | 495 | 0.97 | 2054 | 1992 | 62 | 0.97 |
| Final Drive | 16608 | 16608 | 0 | 1 | 2054 | 2054 | 0 | 1 |
| Wheel/Axle | 16608 | 15233 | 1375 | 0.92 | 6314 | 6191 | 122 | 0.98 |
| Braking | | | | | | | 4137 | |
| Aux Loads | 0 | 0 | 0 | 0 | | | | |
| Aero | | | 1271 | | | | | |
| Rolling | | | 4512 | | | | | |

*Overall System Efficiency

0.695

*Overall energy efficiency is calculated as: (aero + rolling)/(fuel in - ess storage)

Loss Plot (Power Mode) Loss Plot (Regen Mode) DONE

5.2.1.- Día soleado. Baterías 16Ah

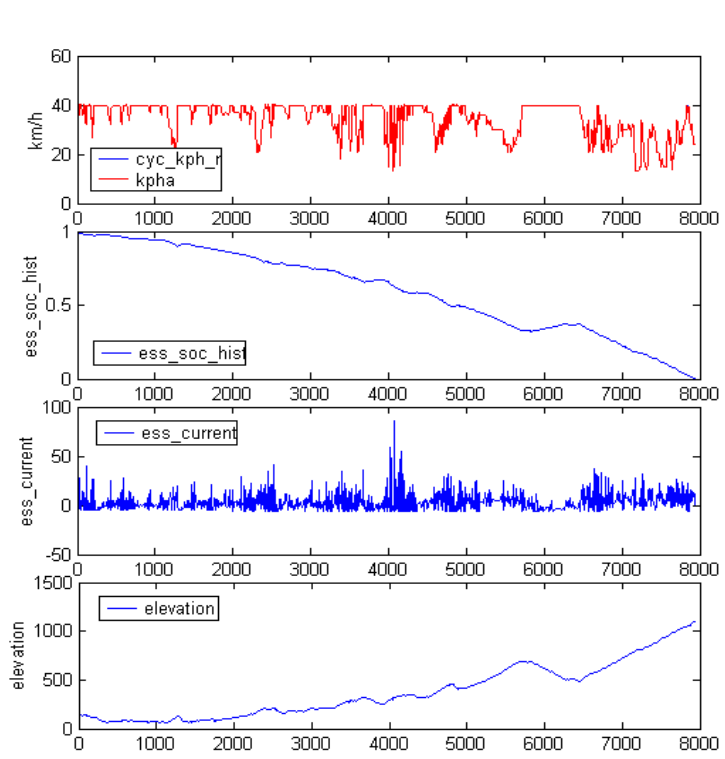


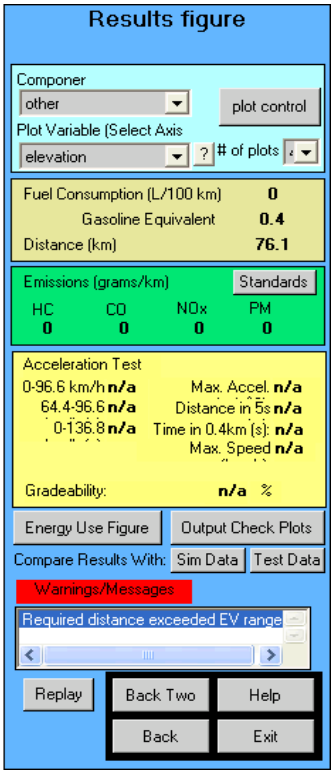


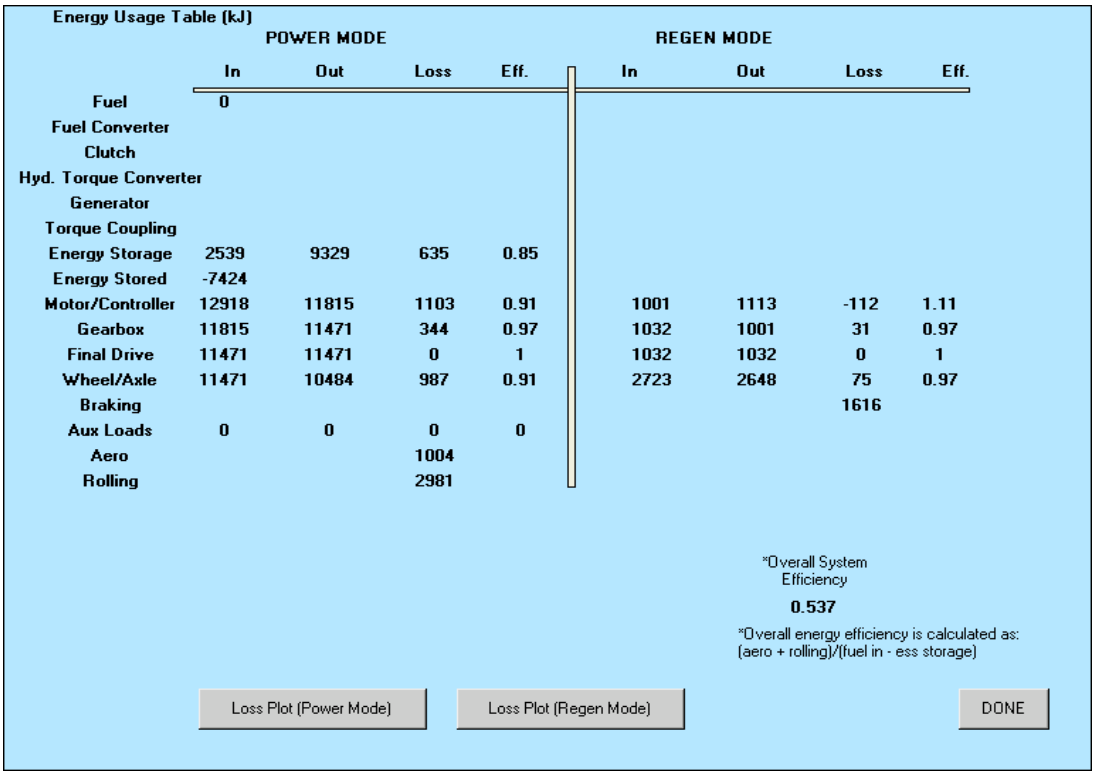


5.2.2.- Nubosidad abundante. Baterías 7Ah

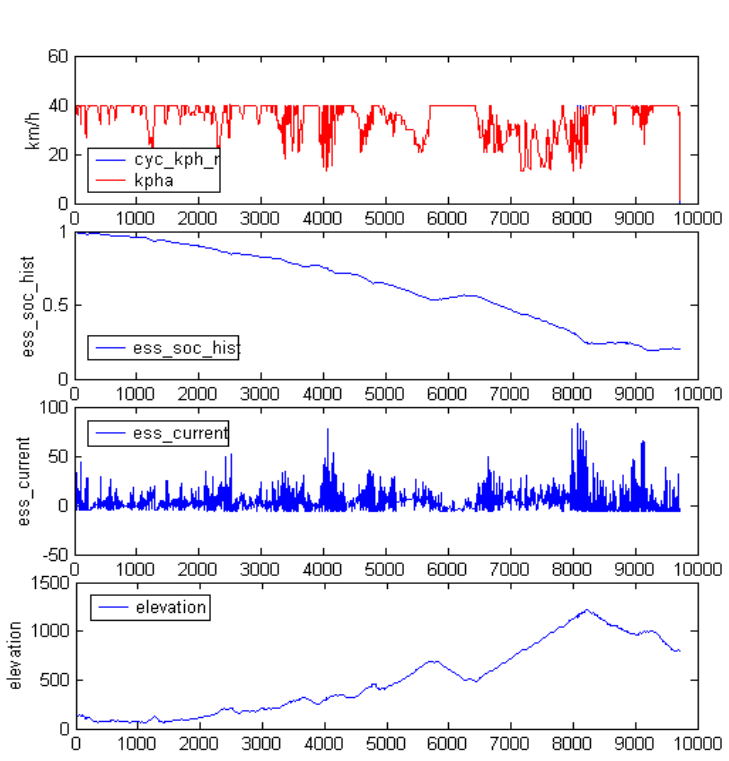


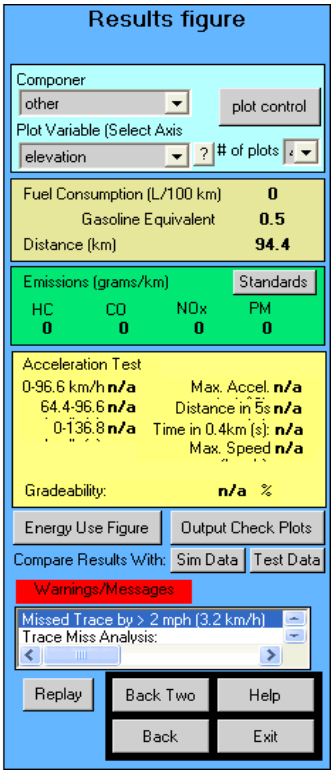


**Energy Usage Table (kJ)**

| | POWER MODE | | | | REGEN MODE | | | |
|---|---|---|---|---|---|---|---|---|
| | In | Out | Loss | Eff. | In | Out | Loss | Eff. |
| Fuel | 0 | | | | | | | |
| Fuel Converter | | | | | | | | |
| Clutch | | | | | | | | |
| Hyd. Torque Converter | | | | | | | | |
| Generator | | | | | | | | |
| Torque Coupling | | | | | | | | |
| Energy Storage | 3995 | 13250 | 1043 | 0.84 | | | | |
| Energy Stored | -10298 | | | | | | | |
| Motor/Controller | 17345 | 15947 | 1398 | 0.92 | 1890 | 1987 | -97 | 1.05 |
| Gearbox | 15947 | 15487 | 460 | 0.97 | 1948 | 1890 | 58 | 0.97 |
| Final Drive | 15487 | 15487 | 0 | 1 | 1948 | 1948 | 0 | 1 |
| Wheel/Axle | 15487 | 14154 | 1333 | 0.91 | 5802 | 5705 | 98 | 0.98 |
| Braking | | | | | | | 3757 | |
| Aux Loads | 0 | 0 | 0 | 0 | | | | |
| Aero | | | 1271 | | | | | |
| Rolling | | | 4170 | | | | | |

*Overall System Efficiency

**0.528**

*Overall energy efficiency is calculated as: (aero + rolling)/(fuel in - ess storage)

Loss Plot (Power Mode) Loss Plot (Regen Mode) DONE

5.2.2.- Nubosidad abundante. Baterías 12Ah

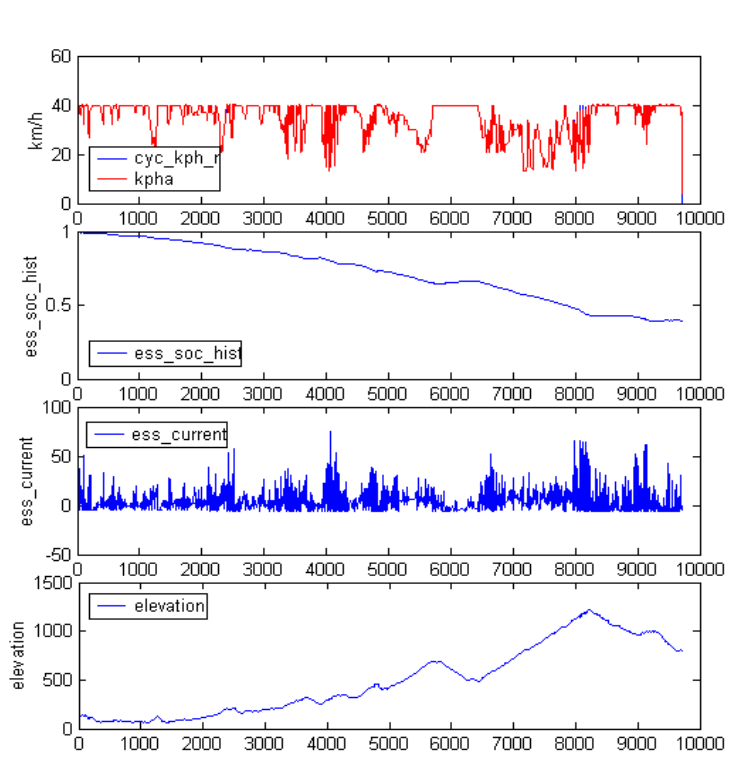


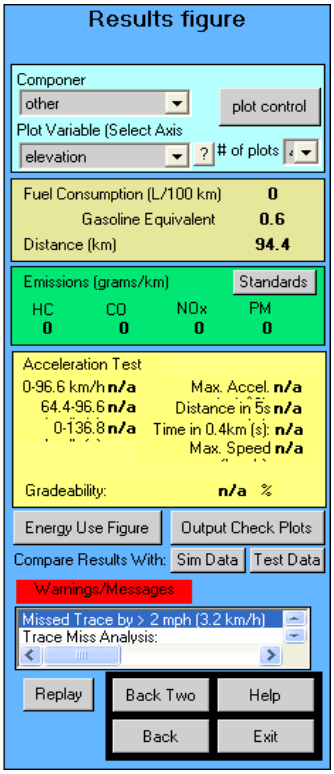


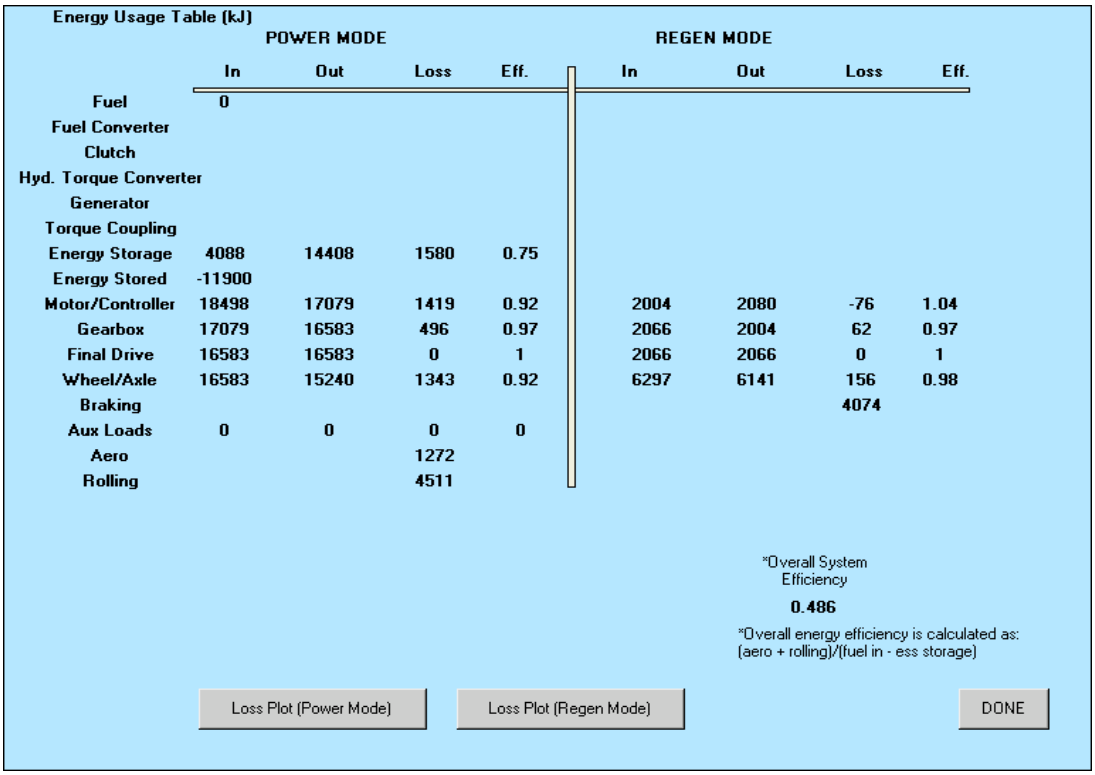


5.2.2.- Nubosidad abundante. Baterías 16Ah

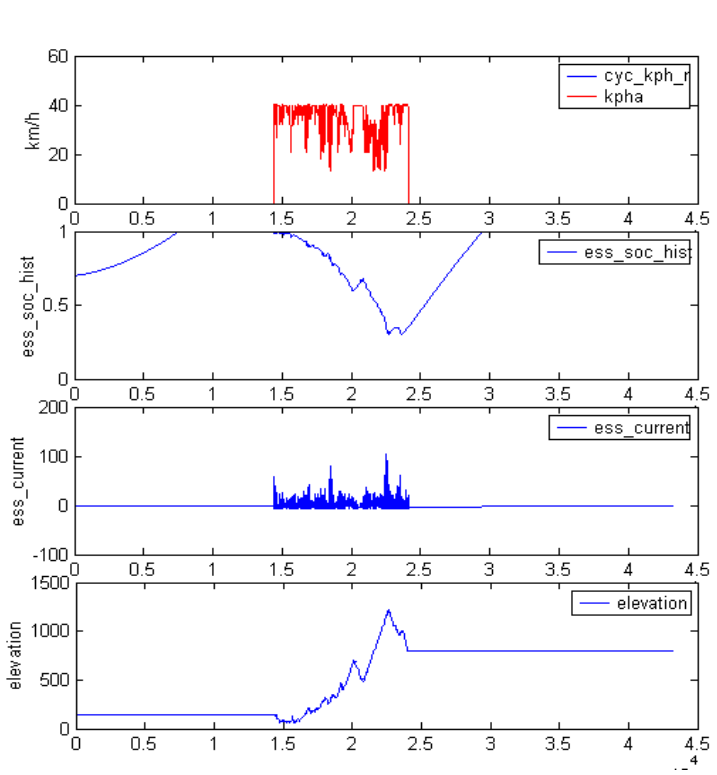


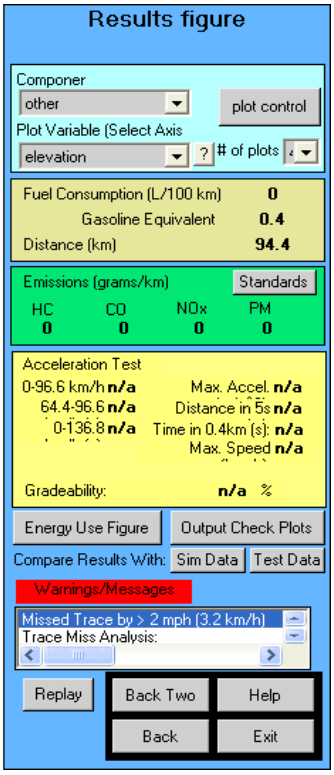


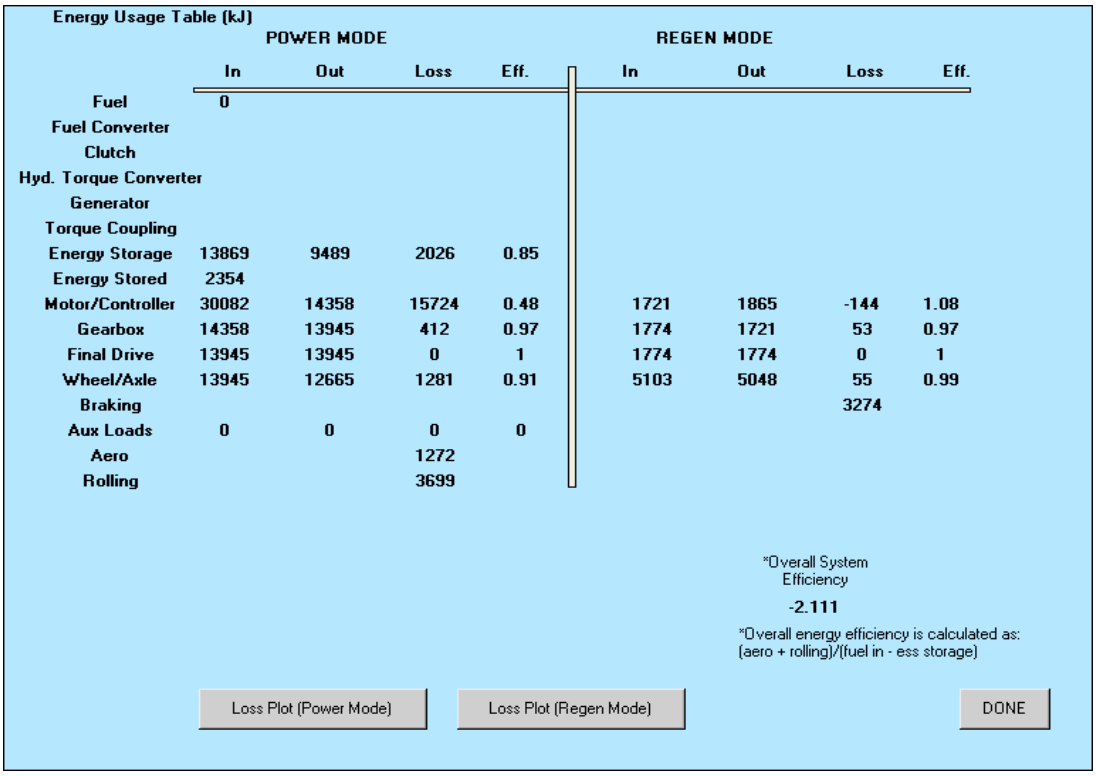


6.1.1- Día Soleado. Baterías 7Ah

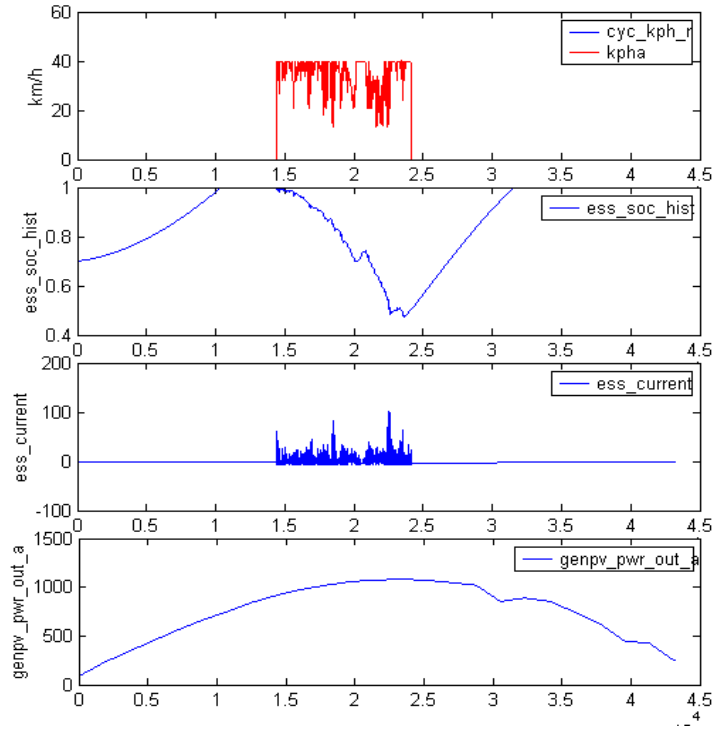


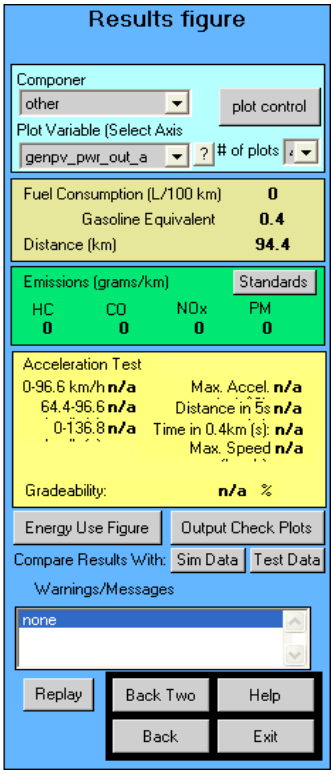


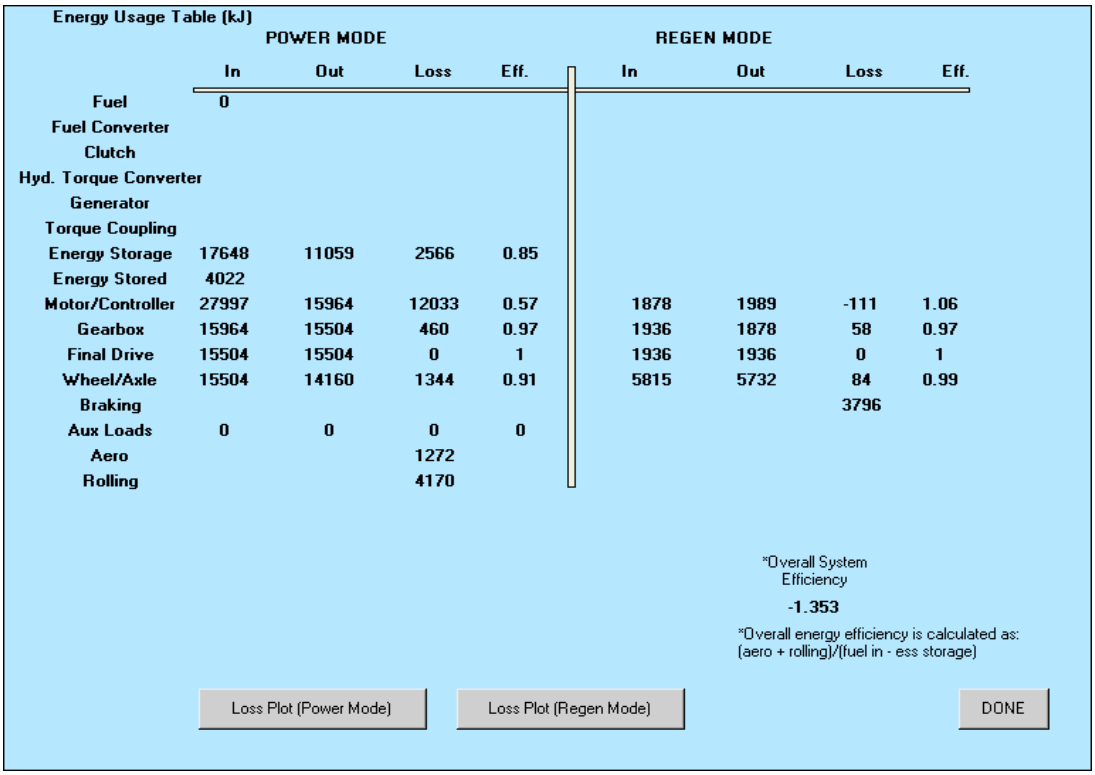


6.1.2.- Día Soleado. Baterías 12Ah

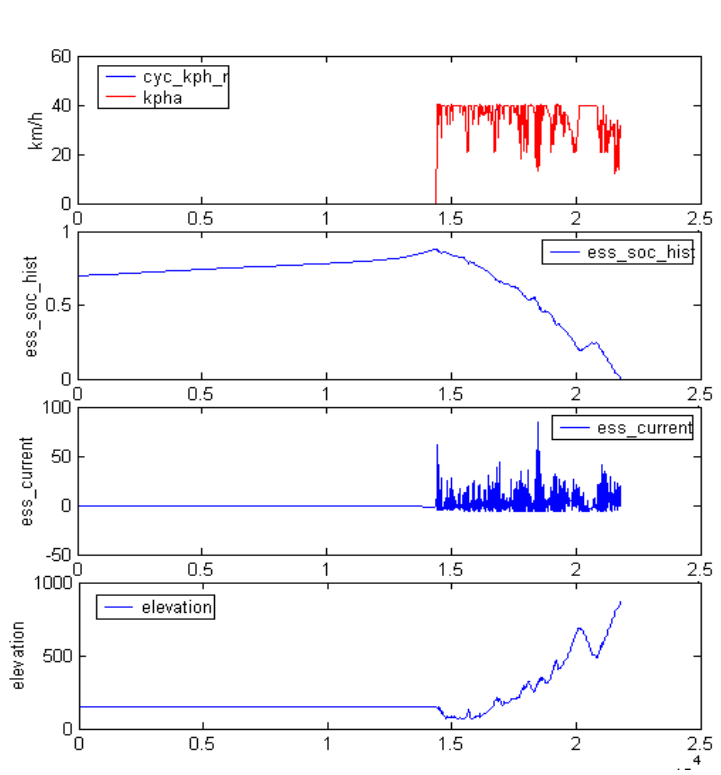


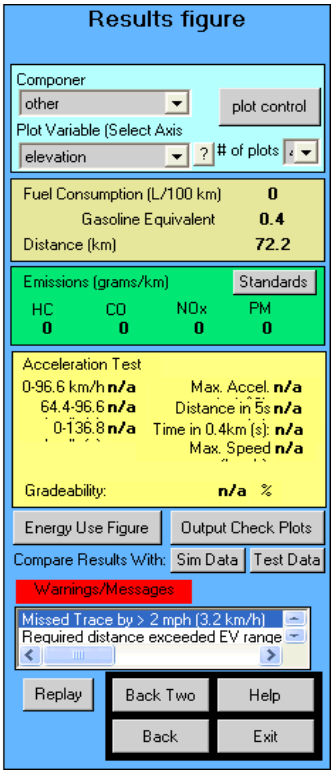


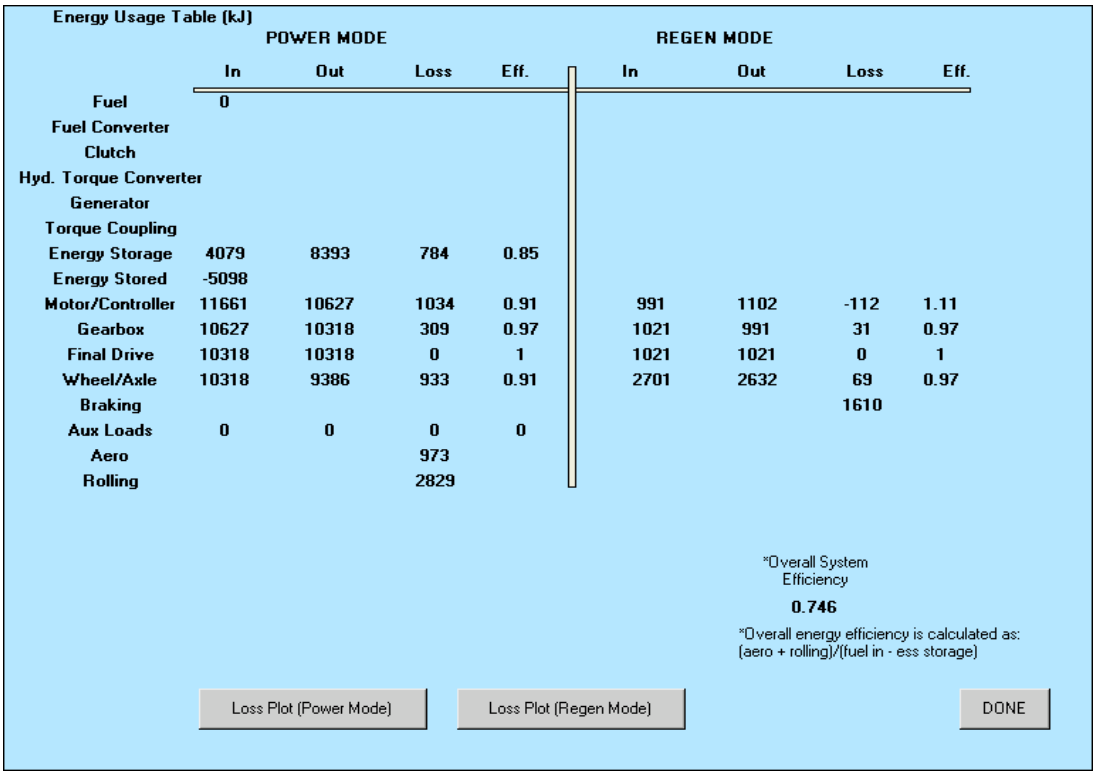


6.1.3.- Nubosidad Abundante. Baterías 7Ah

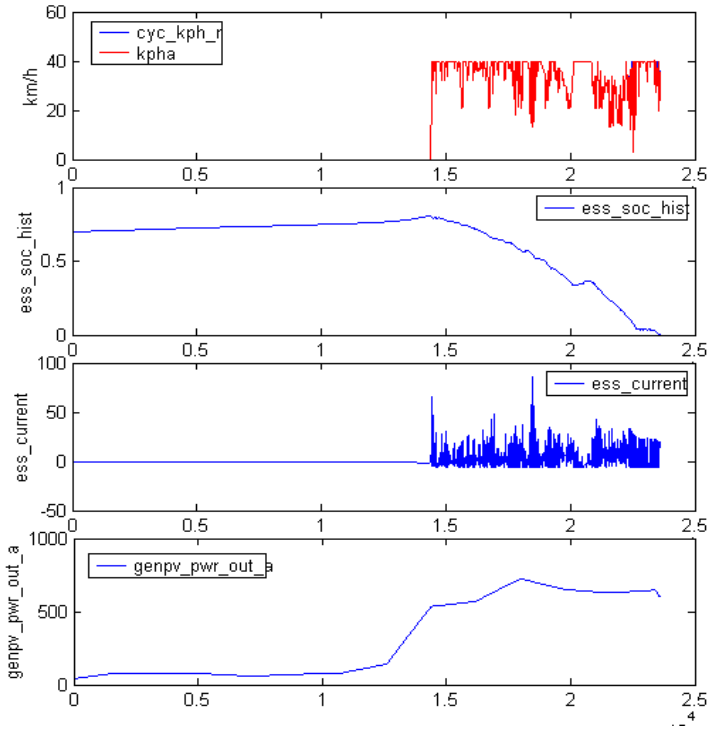


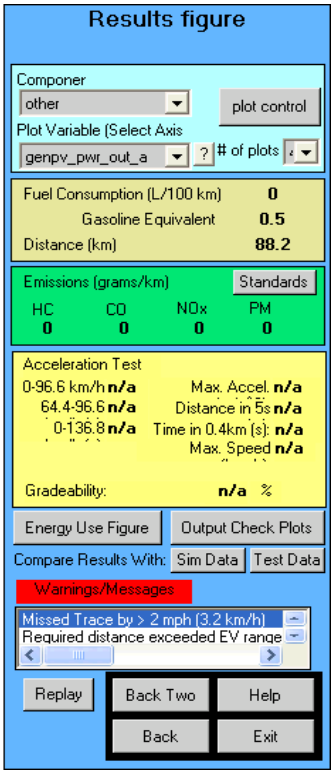


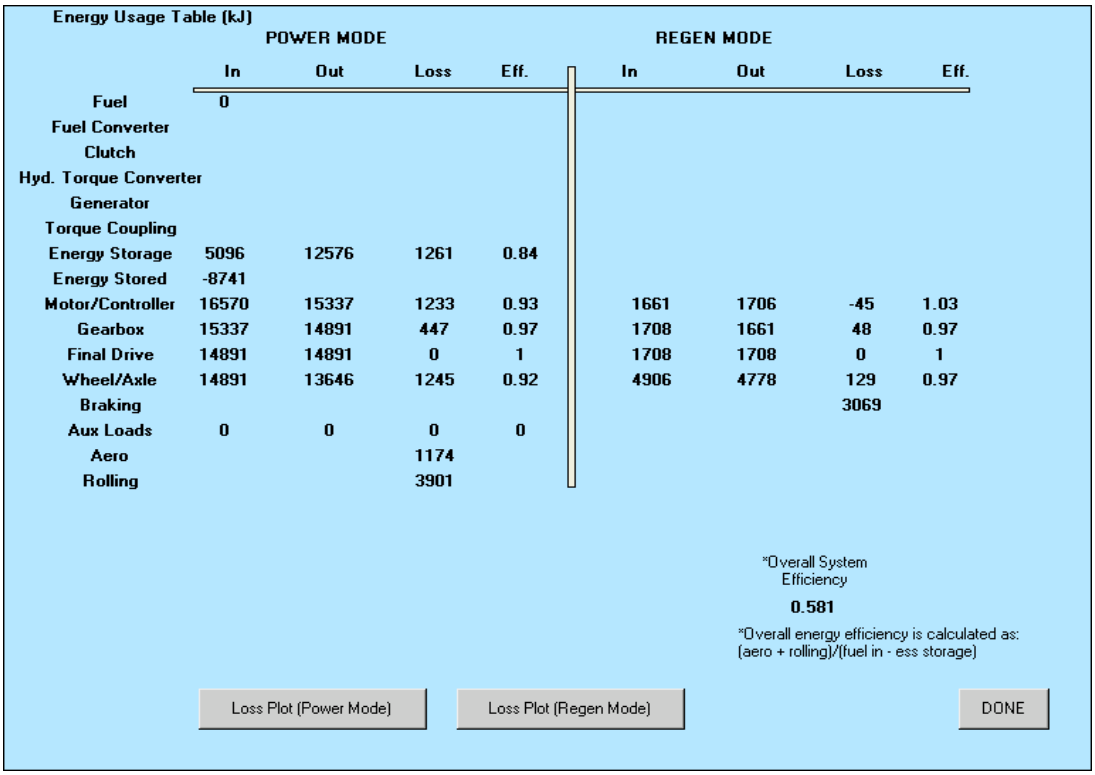

Energy Usage Table (kJ)

| | POWER MODE In | Out | Loss | Eff. | REGEN MODE In | Out | Loss | Eff. |
|---|---|---|---|---|---|---|---|---|
| Fuel | 0 | | | | | | | |
| Fuel Converter | | | | | | | | |
| Clutch | | | | | | | | |
| Hyd. Torque Converter | | | | | | | | |
| Generator | | | | | | | | |
| Torque Coupling | | | | | | | | |
| Energy Storage | 5096 | 12576 | 1261 | 0.84 | | | | |
| Energy Stored | -8741 | | | | | | | |
| Motor/Controller | 16570 | 15337 | 1233 | 0.93 | 1661 | 1706 | -45 | 1.03 |
| Gearbox | 15337 | 14891 | 447 | 0.97 | 1708 | 1661 | 48 | 0.97 |
| Final Drive | 14891 | 14891 | 0 | 1 | 1708 | 1708 | 0 | 1 |
| Wheel/Axle | 14891 | 13646 | 1245 | 0.92 | 4906 | 4778 | 129 | 0.97 |
| Braking | | | | | | | 3069 | |
| Aux Loads | 0 | 0 | 0 | 0 | | | | |
| Aero | | | 1174 | | | | | |
| Rolling | | | 3901 | | | | | |

*Overall System Efficiency

0.581

*Overall energy efficiency is calculated as: (aero + rolling)/(fuel in - ess storage)

Loss Plot (Power Mode) Loss Plot (Regen Mode) DONE

6.1.4.- Nubosidad Abundante. Baterías 12Ah

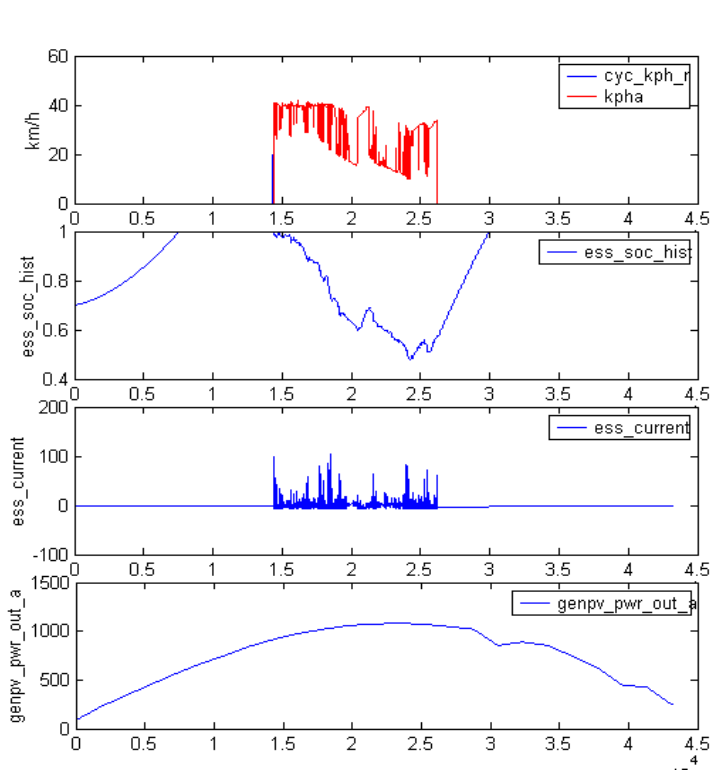


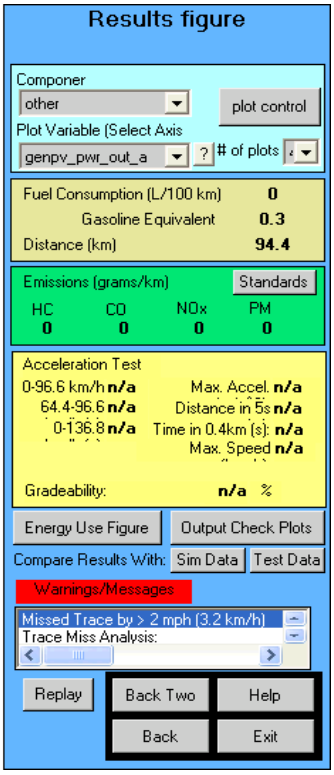


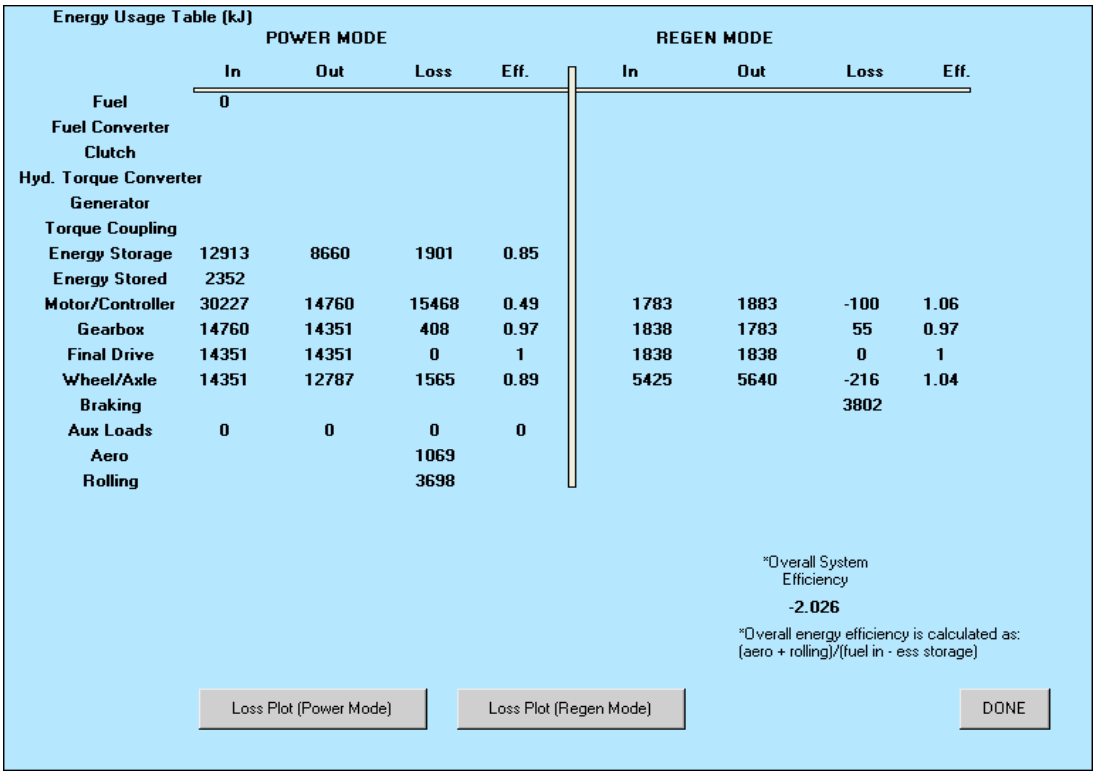


6.3.1.- Día Soleado. Baterías 7Ah

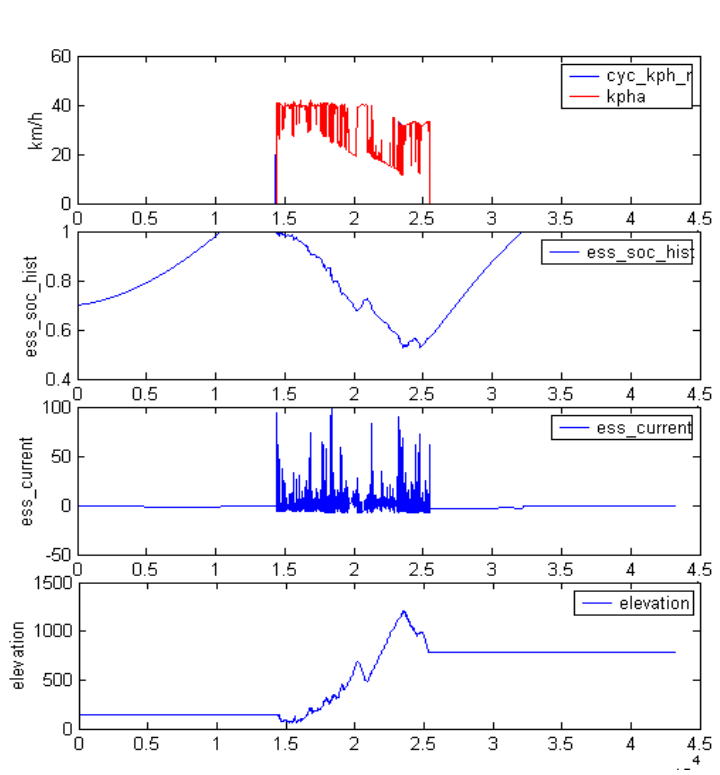


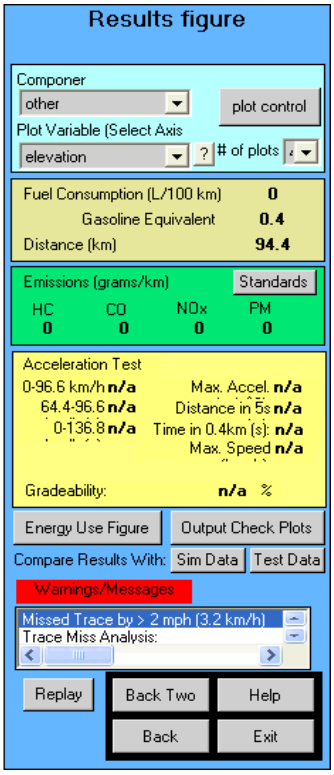


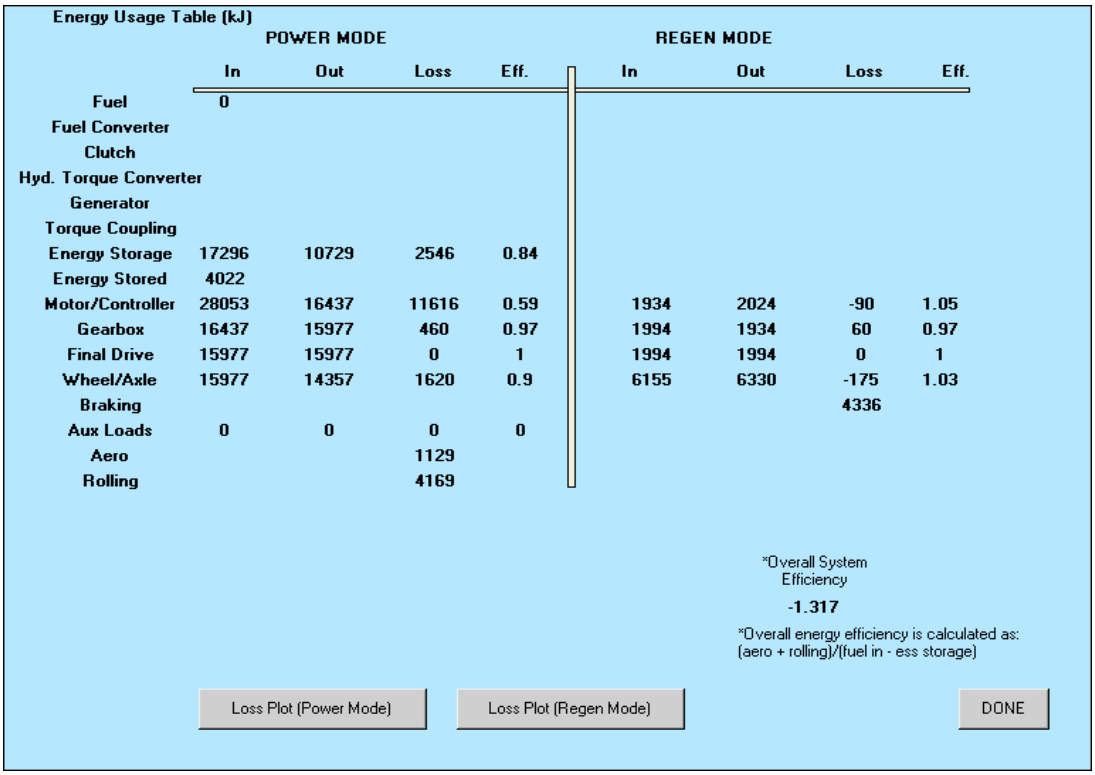


6.3.2.- Día Soleado. Baterías 12Ah

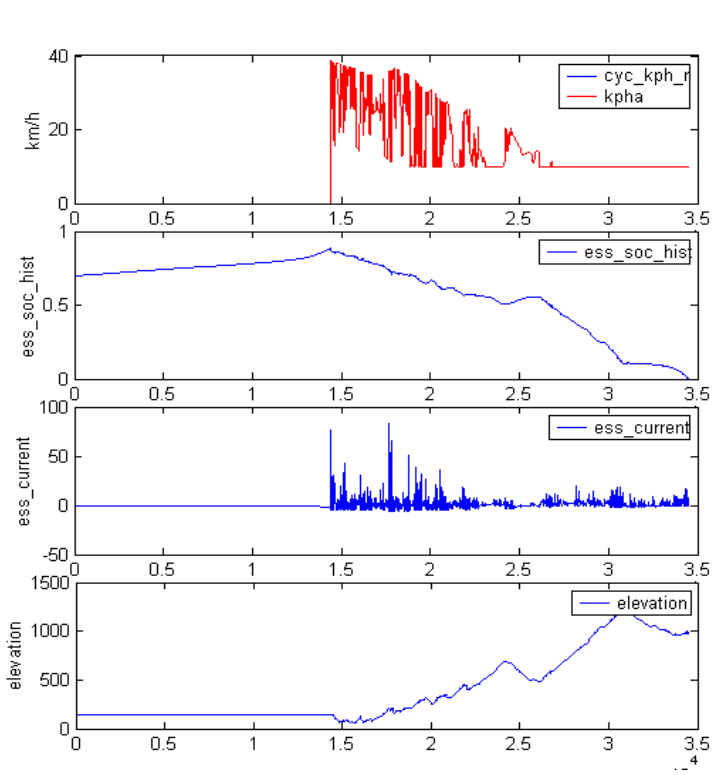


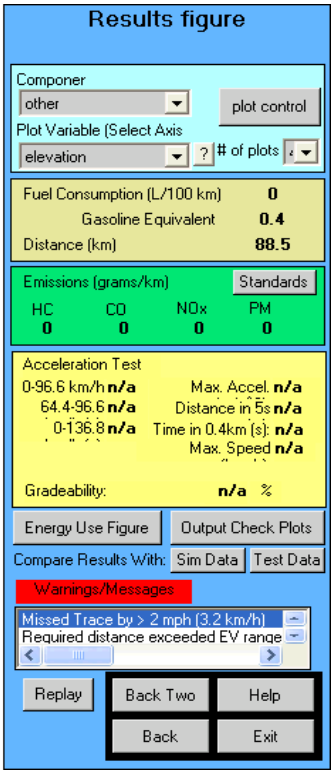


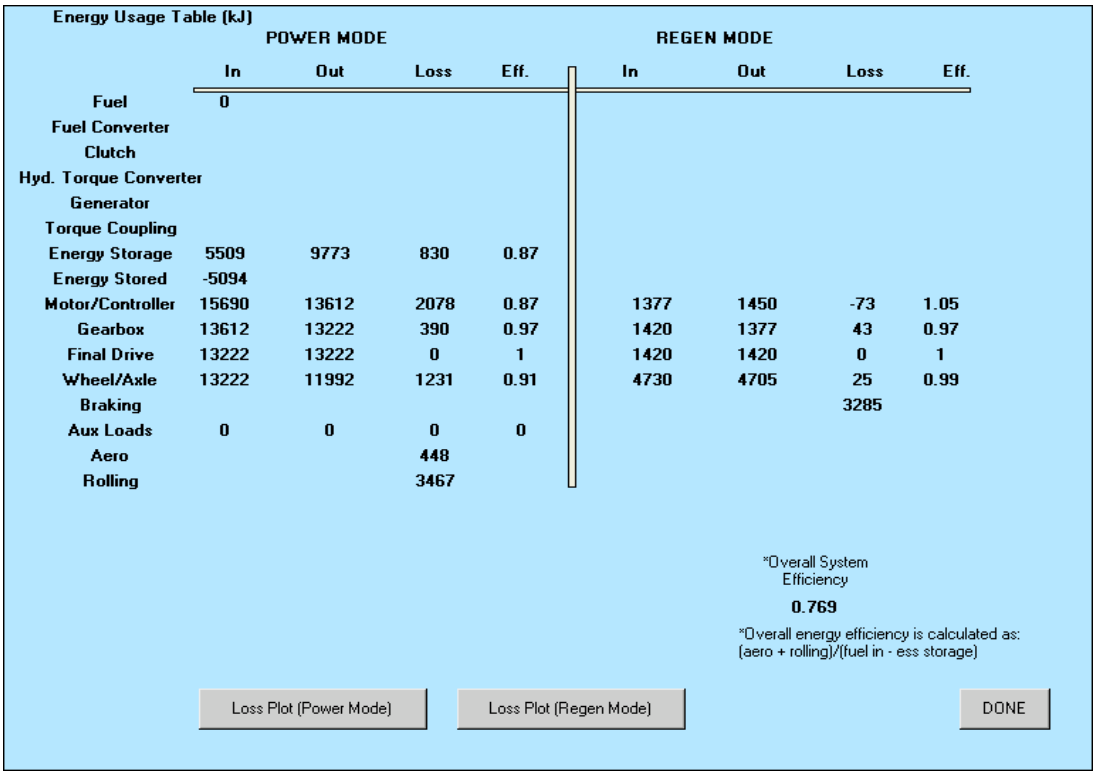


6.3.3.- Nubosidad Abundante. Baterías 7Ah

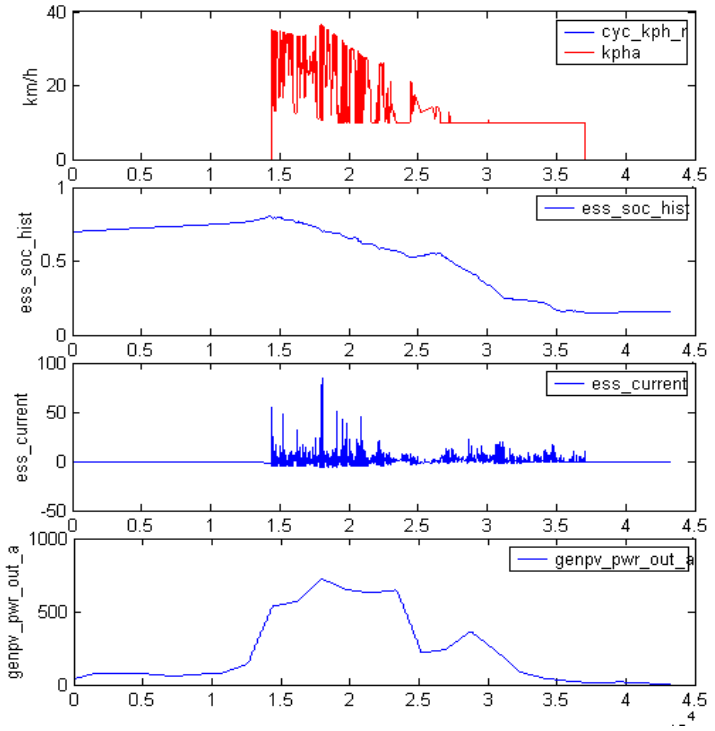


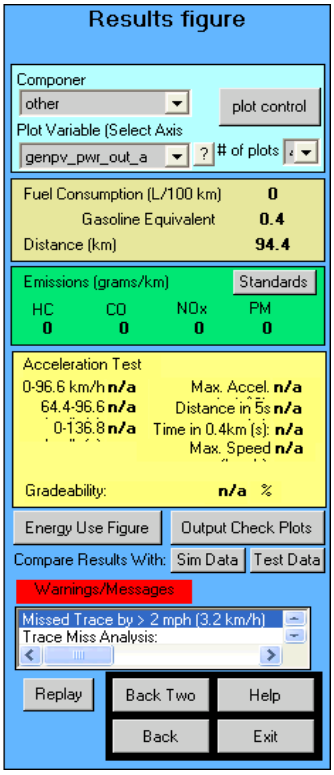


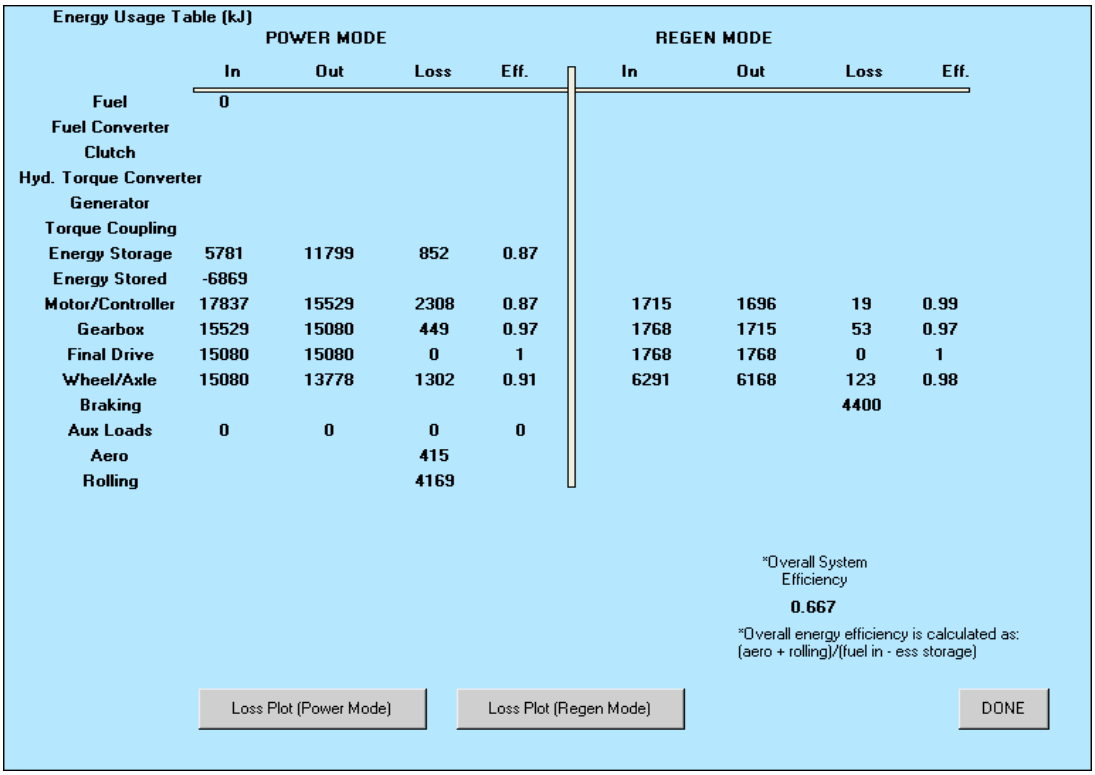


6.3.4.- Nubosidad Abundante. Baterías 12Ah

# D. Divulgación del proyecto Despertaferro II.

## D.1. ISOFOTON: Artículo publicado en el "Twenty-first European Photovoltaic Solar Energy Conference (Dresden 4-8 Sep 2006)"

### D.1.1. Abstracto

Anexo: Abstract de artículo aceptado para publicación en 21st EPVSEC Dresden 2006.

21st European Photovoltaic Solar Energy Conference and Exhibition

**Photovoltaic module design for a solar race car: a technological challenge**

Paula Sánchez-Friera[1], Jesús Alonso[1], Roberto López[2], David Casas[2], Kiko Salguero[2], Marta Almazán[2], Ferran Farré[2], Jordi Tarrega[2], Ricard Bosch[2]

[1]Isofotón SA, R&D department, Parque Tecnológico de Andalucía, Severo Ochoa 50, Málaga 29590, Spain
[2]ETSEIB. Escola Tècnica Superior d'Enginyeria Industrial de Barcelona, Universitat Politècnica de Catalunya. Avda. Diagonal 647, 08028 Barcelona, Spain

Author for correspondance : Paula Sánchez-Friera, tel: +34 951233500, fax: +34 951233212, email: paula.sanchez@isofoton.com

The growth of the photovoltaic market in the past decades has been spectacular, with average growth rates of over 30%. Nevertheless, its contribution to the global energy market nowadays is still minimal, and its use as a major source of energy is still far from reality. Many efforts are being devoted to promote a wider spread of this environmentally friendly technology, focussed mainly on cost reductions and efficiency increase, and also on promoting public awareness and favourable legislation.

In order to demonstrate the applicability of photovoltaic energy in an exciting and challenging field such as race cars, a prototype has been designed and constructed to participate in the European race Phebus, taking place in June 2006 crossing the Pyrenees from Girona (Spain) to Toulousse (France).

A special module design has been carried out in order to provide the solar car with an autonomous high efficient PV system, of light weight and minimum space consumption. The modules have been designed of small size to be able to adapt to the aerodynamic shape of the race car. Several alternative encapsulating materials have been evaluated in order to produce light-weight, rigid, high-efficiency modules.

In particular, glass is substituted by a high-transmittance polymeric sheet such as ETFE. High transmittance silicones and resins have been studied to be used as an alternative to the standard material EVA. For the back layer, a light-weight fiber will be used to give rigidity to the modules.

With a regenerative braking system, a telemetric control system and a specifically designed carbon fiber structure, a very competitive car is being constructed, whose capabilities will be demonstrated in real life during the solar race in June 2006.

*Fig. 1 Simulated model of the race car Despertaferro2 designed by the Politechnical University of Cataluña with the participation of Isofotón.*

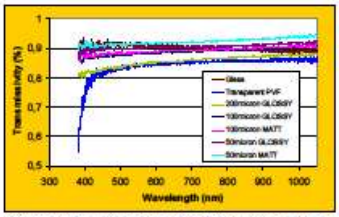


*Fig. 2: Transmissivity of different front-sheet materials to be used as a light-weight substitute to glass*

ETSEIB

## D.1.2. Artículo publicado

# PHOTOVOLTAIC MODULE DESIGN FOR A SOLAR RACE CAR

P. Sánchez-Friera[1], F. Farré[2], B. Lalaguna[1], C. Vázquez[1], J. Alonso[1], M. Fernández[1], M.A. Vázquez[1], J.A. Montañez[1], R. Bosch[2], R. López[2], D. Casas[2], K. Salguero[2], M. Almazán[2], J. Tárrega[2]
[1]Isofotón SA, Parque Tecnológico de Andalucía, Severo Ochoa 50, Málaga 29590, Spain.
Tel: +34 951233500, Fax: +34 951233212, E-mail: paula.sanchez@isofoton.com
[2]ETSEIB. Escola Tècnica Superior d'Enginyeria Industrial de Barcelona, Universitat Politècnica de Catalunya, Spain

ABSTRACT: A system of photovoltaic modules has been designed to be used in a competition solar car. Some of the features of the innovative design of these PV modules are: extremely light weight, high efficiency with minimal area loss, and an elongated shape to enhance the aerodynamics of the race car and minimize mismatch losses due to shadows along the circuit. In addition, the modules incorporate a multi-wall polycarbonate backsheet which promotes ventilation and helps to reduce the nominal operation cell temperature of the modules. The modules have been subject to an outdoor exposure test and to accelerated degradadation tests showing no power degradation. The solar cells were processed over 103x103 mm 200 µm Si wafers with TiOx AR coating and Al back-surface field technology, reaching efficiencies up to 17%. A system of 24 modules was constructed supplying the car with 1.2 kWp peak power, optimized with the use of maximum power point trackers (MPPT) for each individual module. The first trials on the car have been performed and in the next few months it will compete in a high-mountain solar car race across the Pyrinees.
Keywords: Module manufacturing, encapsulation, stand-alone systems.

## 1 INTRODUCTION

The growth of the photovoltaic market in the past decades has been spectacular, with average growth rates of over 30%. Nevertheless, its contribution to the global energy market nowadays is still minimal, and its use as a major source of energy is still far from reality. Many efforts are being devoted to promote a wider spread of this environmentally friendly technology, focused mainly on cost reductions and device efficiencies increase, and on promoting public awareness and favorable legislation.

In order to demonstrate the applicability of photovoltaic energy in an exciting and challenging field such as race cars, a prototype has been constructed to participate in the European race Phebus, crossing the Pyrenees from Girona (Spain) to Toulousse (France). This high mountain circuit involves very steep slopes, a large number of tunnels and likely adverse meteorological conditions, all which makes the competition a true challenge for solar vehicles. The car constructed, named Despertaferro 2, has been based on a previous project [1] by the Polytechnical University of Catalonia with the collaboration of Isofotón and other companies, which participated in the Australian solar race SunRace 2000 with excellent results.

## 2 PV SYSTEM SPECIFICATIONS

In order to optimise the previous version of the car, designed for long plains in Australia, to compete in a high mountain circuit such as the Pyrinees, three aspects of the car required re-design: the energy system (PV modules, regulators, and batteries) the transmission and the data management system.

From the previous experience gained in the original Despertaferro project, and also following the guidelines from the solar race organizing committee, a set of specifications for the new PV system was defined:

- The total weight must be minimized.
- The total area used should be around 8 m$^2$.
- The total power should be at least 1 kWp.
- The modules will be connected independently to maximum power point trackers (MPPT) charge regulators and batteries, in order to maximize the output power of the PV system. As only one module is connected to each MPPT there is no need for by-pass diodes.
- The modules should have the shape of elongated rectangles, which will be fixed to the car housing along the longitudinal direction. In this way mismatch losses due to partial shadowing on the road would be avoided. Also, this module shape would facilitate the modelled aerodynamical shape of the car, as shown in Figure 1, which provides an aerodynamical coefficient of 0.16.
- The modules would be easily replaceable in case of damage.

**Figure 1:** Simulated model of the solar race car Desperfaferro2.

With the above specifications the PV system was defined consisting of 24 PV modules. Each module contains two strings of 16 solar cells, all connected in series to maximise the voltage.

The total area per module is set to 0.37 m$^2$, with a total peak power of 1.2 kWp.

## 3 PV MODULE DESIGN AND CONSTRUCTION

### 3.1 Front cover selection

Standard PV modules are fabricated with extra clear tempered glass as front cover. This gives rigidity to the module and acts as an excellent barrier against moisture, UV and other aging factors. This type of glass, however, can weigh more than 7 kg/m$^2$, which turns impractical for the application of PV to vehicles. To minimize the weight of the modules it was decided to use a plastic back cover to give mechanical stability to the module. With this substrate configuration the front cover does no longer need to provide rigidity to the module, and there is more freedom to choose a polymeric film of high transparency and good endurance properties.

Several films were tested for adhesion, durability and light transmittance. In particular, the polymer ethylene-tetra-fluoroethilene (ETFE) presents several advantages as excellent weatherability, high transparency and good adhesion to EVA. Figure 2 shows the transmittance curves of several films compared to glass. For ETFE the absorption dependence on the film thickness is indicated.

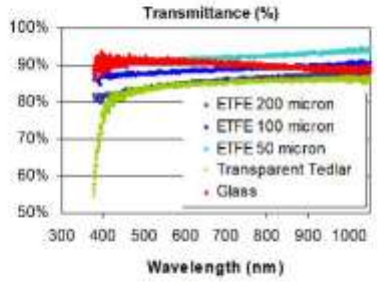


**Figure 2:** Transmittance of different front-sheet materials to be used as a light-weight substitute to glass.

Some of the film weatherability properties are also dependent on the thickness. For this application, however, it is not necessary to ensure 30 years functioning time, this is the reason why the material ETFE of only 50 micron thickness is considered optimum so that the optical efficiency is maximized.

Several one-cell module prototypes were built using different front covers, and the short-circuit current measured before and after lamination. It was observed that almost 3% gain could be obtained using the 50 μm ETFE sheet with respect to the use of extra clear glass.

### 3.2 Back cover selection

A back cover of a multi-wall policarbonate sheet was selected for several reasons: first, weight is only slightly above 1 kg/m$^2$, which implies a dramatic reduction with respect to glass. Thanks to the multi-wall structure the sheet gives mechanical strength to the module with little material consumption. In addition, this type of structure allows air circulation along the channels incorporated in the sheet, lowering the module operating temperature and therefore maximising the output power. The air chamber can alternatively be used as thermal isolation for the pilot inside the car cabin.

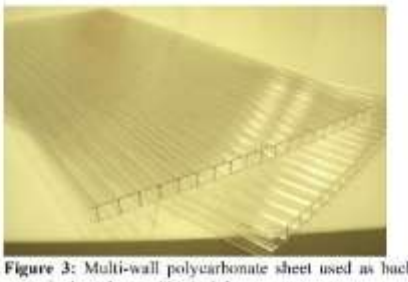

**Figure 3:** Multi-wall polycarbonate sheet used as back cover in the solar car PV modules.

### 3.3 Solar cell design and processing

The solar cells were processed over p-type monocrystalline Si substrates of small size (103x103 mm) in order to facilitate an elongated module shape. The thickness was around 200 μm after texturing. They were fabricated by a standard process consisting of the following steps: alkaline texturing, shallow emitter formation by $POCl_3$ diffusion, plasma edge isolation, $TiO_x$ anti-reflective coating, contacts screen-printing including Al back-surface field, and firing. The maximum efficiency obtained in the batch was 17%, being 16.3% the average value. For additional mismatch reduction all the cells selected for the solar car were re-sorted using specifically designed very narrow sorting classes.

### 3.4 Module prototypes construction

The solar cells were soldered in strings of 16 cells and laminated within the chosen materials. Ethalene-vinyl-acetate (EVA) was used as encapsulant material. The process cycle was slightly modified for the new front and back sheet materials. Adhesion values to the back layer were acceptable, whereas for the front layer adhesion was larger than the material elongation strength.

The substrate size was minimum to reduce the loss of usable area. To save space the string interconnection was performed in the back of the module. Ribbons were extracted to the back through holes habilitated in the substrate, as shown in Figure 4. In this way the white area of the module is kept under 9%, whereas in standard monocrystalline commercial PV modules the white area could reach up to 20% of the glass surface.

## 4 PV MODULE TESTING

### 4.1 Indoor characterization

The IV curves of all the modules were measured giving average efficiencies around 15.5% with respect to the total cell area and around 14% considering the total module area. This efficiency decay from cell to module is very low due to the area loss reduction, the use of an extra-trasmittance front cover, and the optimal cell interconnection with optimized ribbon dimensions and number of soldering points.

**Figure 4:** Ultra-light weight PV module prototype of 32 solar cells 103x103 mm constructed for the solar race car Despertaferro 2.

4.2 Outdoor exposure and temperature monitoring

Several module prototypes of 4x3 solar cells, constructed with the same materials as the solar car modules, were built and subject to an outdoor exposure test. During a period of one month there was no power degradation in the modules, as expected. IV data were selected at temperature and irradiance conditions within 5% of T = 30°C and within 2% of Irrad = 900 W/m$^2$, at the beginning and end of the exposure period. The results are shown in Table I corrected for 30°C and 900 W/m$^2$.

**Table I:** Results from outdoor test of 12-cell module prototypes with the new materials and the standard, showing that there is no significant variation in the IV characteristics. The data selected are corrected to 30°C and 900 W/m$^2$.

| | Date | Isc (A) | Voc (V) | Pm (W) | FF (%) |
|---|---|---|---|---|---|
| New materials | 4/8/06 | 2,86 | 6,65 | 14,4 | 75,7 |
| | 30/8/06 | 2,85 | 6,62 | 14,2 | 75,3 |
| Reference | 4/8/06 | 2,83 | 6,67 | 14,3 | 75,8 |
| | 30/8/06 | 2,80 | 6,66 | 14,1 | 75,6 |

Two modules were built incorporating a PT100 sensor behind one central cell, one module with the materials selected and the other one with standard encapsulation: glass, EVA and Tedlar. The operating temperature during outdoor exposure was monitored, observing no differences (within 3°C) under no wind conditions. The multi-wall polycarbonate module is expected to lower the operating temperature when air is made to circulate along the channels as it happens during the normal car functioning. Further tests will be performed in order to quantify this property.

**Figure 5:** Outdoor test set-up for power degradation check and temperature monitoring of modules with the new design proposed.

4.3 Accelerated degradation tests

One prototype was exposed to thermal cycling and damp-heat tests in a climate chamber according to the specifications of IEC61215, to investigate the durability of the materials. Although durability is not a key issue for solar car applications, this would open the prospect of using the selected materials in other applications.

There was no power degradation during the thermal cycling. After the damp-heat tests both the ETFE and the polycarbonate sheets were in excellent conditions, there was no brittlement or decolouration of the materials and the ETFE film kept the high transmittance values. However, slight delamination of the front layer to the EVA was observed, which should be corrected for long-life applications with the use of adhesion enhancing primers.

## 5 SOLAR CAR ASSEMBLY

The elongated shape of the PV modules facilitates its distribution over the car housing and the final assembly in a glass fiber and poliester structure, specially designed to fit in the previous car structure. The modules are distributed over the car surface in three rows, two rows of 9 modules forming a fixed structure and one set of 6 modules forming the car door, 3 modules at each side of the driver cabin.

Each module was connected to a charge regulator to adapt the tension to 300 V in order to feed in the battery system. The regulators are provided with a maximum power point tracker (MPPT) system to optimise the output power; they stop the charge flow in case of full load of the batteries.

The battery voltage was increased with respect to the previous version of the car, from 192 to 300 V, this improves the energetical performance of the chain battery-driver-engine. The battery system was composed of 25 Pb-acid batteries giving a capacity of 7 Ah.

The engine of the car was not modified with respect to the previous version of Despertaferro. The transmission, however, was redesigned with a gear system in order to make the car able of overcoming large slopes. In addition, the new transmission has a double chain which helps correcting the traction wheels damping. The braking system and the rims and tyres were not modified from the previous system.

A new data control system was constructed with a bus (CAN) that control and manages the data collected by the different sensors (speed, energy consumption, battery voltage, vehicle temperature). These sensors are fully isolated and are fed by an indepent battery system. One of the bus nodes is connected to a wireless router (WI-FI) to communicate the car with a computer laptop.

**Figure 6:** The Despertaferro 2 solar race car with the new PV modules incorporated.

## 6 CONCLUSIONS AND PROSPECTS

A competition solar car has been built from a previous prototype, optimising the system for a high mountain circuit in the Pyrinees. The PV modules constructed are extremely light weight and have incorporated a back cover which allows circulation of air behind the modules, helping to reduce the operating temperature and maximise the power output.

The vehicle constructed will participate in several exhibitions and competitions in the next few months, including the circuit Phebus across the Pyrinees, helping to enhance public awareness of environmentally friendly technologies such as photovoltaics.

The new materials selected for this application have been tested through accelerated degradation giving promising results, with opens the prospects for new applications of the proposed design in other PV niche markets.

## ACKNOWLEDGEMENTS

The authors gratefully acknowledge the large effort and motivation of the production personnel at Isofotón, and thank especially the engineers Daniel Montiel and Ricardo Casasola for many fruitful discussions.

We would like to thank Hilde Rockens from Dupont, for kindly giving technical advice and donating material for the front cover of the PV modules; Enric Feixas from Electronica Feixas, S.C.P for kindly donating the charge regulators; Ficosa International for the software and development material for the control bus; and the Facultat de Nàutica de Barcelona for their help with the frames fabrication.

The collaboration of Michel Pilougine, Juan Miguel Cortés and Mariano Sidrach from the University of Málaga, regarding the module outdoor exposure tests, is gratefully acknowledged.

Finally, we are in debt with the members of the Mediterrani team, who designed and produced the first version of the Despertaferro solar car.

## REFERENCES

[1] "Despertaferro, primer prototipo de coche solar fabricado en España", Era Solar vol. 95 (Jan/Feb 2000).

## D.1.3. Poster divulgativo

5BV.3.46 21st EUPVSEC Dresden 2006

# PHOTOVOLTAIC MODULE DESIGN FOR A SOLAR RACE CAR

P. Sánchez-Friera[1], F. Farré[2], B. Lalaguna[1], C. Vázquez[1], J. Alonso[1], M. Fernández[1], M.A. Vázquez[1], J.A. Montañez[1], R. Bosch[2], R. López[2], D. Casas[2], K. Salguero[2], M. Almazán[2], J. Tarrega[2]
[1]Isofotón SA, Parque Tecnológico de Andalucía, Severo Ochoa 50, Málaga 29590, Spain.
Tel.: +34 951233500, Fax: +34 951233212, E-mail: paula.sanchez@isofoton.com
[2]ETSEIB. Escola Técnica Superior d'Enginyeria Industrial de Barcelona, Universitat Politècnica de Catalunya, Spain

*Ultra-light-weight PV modules have been designed for a special application: a solar race car. A system of 24 modules with a total area of 8 m² was fabricated, with a total weight of less than 40 kg and a nominal peak power of 1,2 kWp. The solar car was assembled and optimized for a high mountain competition across the Pyrinees.*

## Back cover selection

A multi-wall polycarbonate sheet is selected for a sub-strate configuration. The sheet weighs 7 times less than glass, provides mechanical stability to the modules and facilitates ventilation.

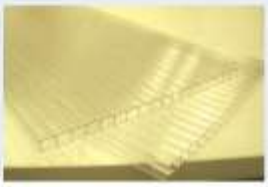

## Front cover selection

Several polymeric front covers were evaluated as a light-weight alternative to glass. ETFE of 50 µm thickness offers the higher transmittance.

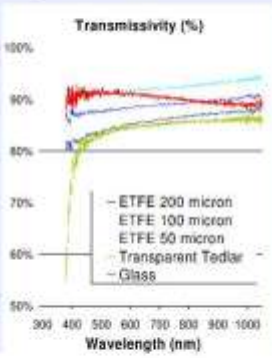


## Module testing

The new materials selected suffered no degradation during thermal cycling/damp-heat.

There was no power decay during 1 month outdoor exposure test.

## Module configuration

Two strings of 16 Si solar cells of 180 µm and 103x103 mm size were interconnected in each module. Cell efficiencies were up to 17%.

The string interconnection was performed in the back of the module, reducing the white area to less than 9%, instead of the typical value of 20%. Efficiency decay was under 1%.

## The DESPERTAFERRO 2 solar race car

The solar car was optimised for frequent tunnels, adverse meteorological conditions and steep slopes. A battery system of 300 V and 7 Ah was used. Each of the 24 modules was independently connected to a charge regulator to feed the battery system.

## D.2. Ciencia en Acción.

### D.2.1. Premio Categoría Sostenibilidad

Estimado concursante:

En primer lugar, queremos agradecerle la participación de su grupo en la séptima edición de ***Ciencia en Acción***, modalidad "*Sostenibilidad*".

El Jurado ha evaluado el trabajo presentado por usted titulado "MEJORAS INTRODUCIDAS EN EL COCHE SOLAR DESPERTAFERRO" y ha decidido que ha sido seleccionado para ser presentado en la final que tendrá lugar en el museo "CosmoCaixa" de Alcobendas (Madrid), los días 29, 30 de septiembre y 1 de octubre.

Permítannos felicitarles por haber sido seleccionados como finalistas entre los numerosos trabajos recibidos y animarles a participar en próximas ediciones. Gracias a todos ustedes, verdaderos protagonistas del concurso, *Ciencia en Acción* se consolida y aumenta su prestigio año tras año. Estamos convencidos de que el número de participantes, la calidad de sus trabajos y los premios que concedamos crecerán en el futuro.

Si desean ustedes consultar el acta del jurado de la presente edición del concurso para conocer los premios concedidos en otras modalidades, obtener imágenes de recuerdo o cualquier otra información, les invitamos a visitar nuestra página web durante los próximos días http://www.fecyt.es/cienciaenaccion.

Agradeciéndoles de nuevo su participación y esperando volver a contar con ustedes en futuras ediciones, reciban un afectuoso saludo de la Organización.

Atentamente,

Rosa M. Ros
Directora de Ciencia en Acción

## D.3. Science on Stage 2

### D.3.1. Exposición permanente.

SCIENCE on Stage

Ciencia en Acción

**Place Robert Schuman Grenoble 3 Avril 2007**

# Despertaferro: Voiture Solaire

Le «Despertaferro» est une voiture solaire construite comme projet de fin d'études par l'Equipe «Mediterrani» composée de neuf étudiants de l'Université Polytechnique de Catalogne dessinée pour concourir dans la course Australienne «Sunrace 2000» entre Sydney et Melbourne, obtenant la « pole position », une sixième place bien méritée ainsi que le prix à l'équipe la plus courageuse. Présentée dans plusieurs foires, elle est aujourd'hui exposée au musée des Sciences de Terrassa.

Présentement l'Equipe «MontSENY», formée de sept étudiants de la même université, élaborent leur projet de fin d'études en préparant cette voiture à concourir dans les courses de montagne comme le « Rallye Phébus » (du 1 juin au 4 juin 2007 entre Gérone et Toulouse au travers des Pyrénées www.raliesolaire.free.fr), où les fortes pentes et l'étape de nuit exigent de repenser le dessin d'une voiture solaire projetée pour les plaines ensoleillées d'Australie. Le concept du système de captage solaire a été redessiné afin d'améliorer l'acquisition d'énergie en augmentant les champs de Photovoltaïque et en les réglant indépendamment, étant donné que la radiation incidente varie pour les différentes inclinaisons de chaque module photovoltaïque établies afin d'obtenir une bonne aérodynamique.

La nouvelle carcasse supérieure a été construite en utilisant des matériaux composés (fibre de verre + polyester) qui évite les problèmes sporadiques de court-circuit de l'antérieure carcasse de fibre de carbone, où se placent les modules dont les canaux permettent la réfrigération des cellule avec air assurant, en outre, l'étanchéité de l'ensemble. L'ensemble des données permettra d'améliorer l'intelligence du comportement du véhicule au moyen de l'acquisition de valeurs recueillies par les témoins et leur stockage pour une analyse postérieure.

CSIC MINISTERIO DE EDUCACIÓN Y CIENCIA FECYT

**Avec la collaboration de l'Université Polytechnique de Catalogne (Espagne)**

## D.3.2. Press Kit

SCIENCE on Stage 2

### THE DESPERTAFERRO SOLAR CAR

Despertaferro is a solar car which was constructed as part of a master's thesis by the Mediterrani Team (made up of nine students). It was designed to compete in the Australian Sunrace 2000, where it achieved a commendable result. This experiment will be presented by the Spanish delegation.

### THE DISCOVERY TRUCK

The RuG Discovery is a fascinating science truck of the Faculty of Mathematics and Natural Sciences of the University Groningen. The project aims to attract more students to science studies and increase the awareness of science among the general public as well. The students carry out small experiments that can be performed within one class hour. More information about the Discovery truck can be found at www.rug.nl/discovery, Theo Jurriëns, T.A.Jurriens@rug.nl.

11

## D.3.3. Training Workshop: THE SOLAR FUEL CELL CAR From theory to practice

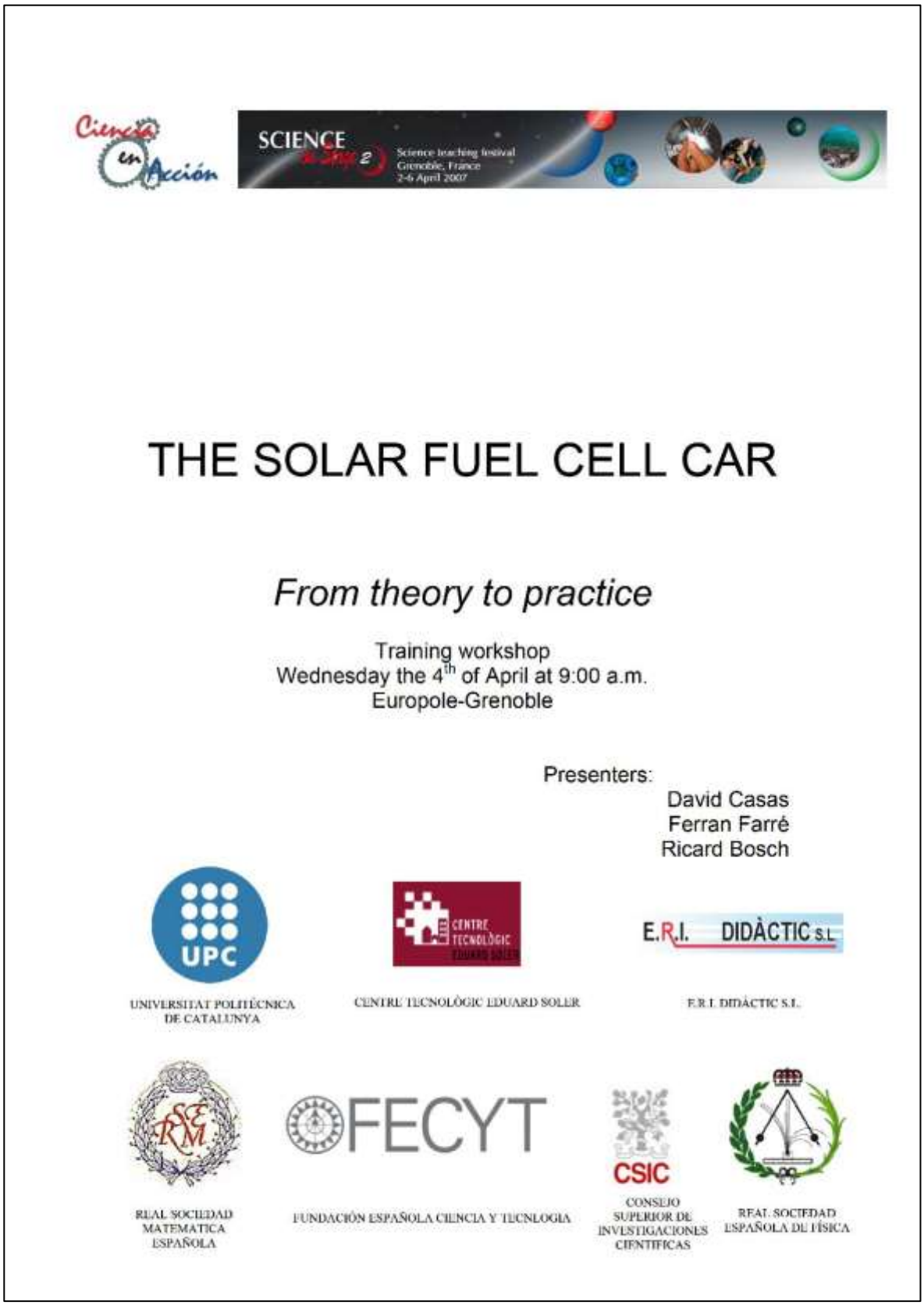

## The solar-fuel cell car: From theory to practice

Dear colleagues,

This presentation sheet will give you some information about the workshop we will participate describing a solar fuel cell car prototype.

We are two students of industrial engineering writing our master thesis linked to the development of improvements introduced in the solar car Despertaferro which was constructed 7 years ago by a group of students called the Mediterrani Team. Now the MontSENY team are preparing the solar car to compete in a mountain race where the specifications become harder than the Australian races.

The solar cars are still far from become a viable alternative to replace cars with internal combustion motor, but they are an excellent test bench to develop the sustainable technologies that will solve the current energetic problem.

These technologies will be built up by the students in the near future so it is time to start introducing them in their school program in such a way they learn basic educational concepts while they became aware of overcame the energetic challenge.

Within the framework of these concepts E.R.I. Didàctic and the Centre Tecnològic Eduard Soler are developing together a solar fuel cell kit with school practices based on its devices.

The workshop will consist on the explanation of the basic operating concepts and the realization of some practices parts, where you will see the educative potential of these experiments in order to teach your students in different subjects, while they learn "playing" with the kit.

See you in Grenoble.

*David Casas Pozuelos*
*MontSENY Team*
*UPC-ETSEIB*
*(Universitat Politécnica de Catalunya)*
*Barcelona-Spain*
*despertaferr@gmail.com*

UPC

REAL SOCIEDAD MATEMATICA ESPAÑOLA

REAL SOCIEDAD ESPAÑOLA DE FÍSICA

FECYT
FUNDACIÓN ESPAÑOLA CIENCIA Y TECNOLOGIA

CSIC
CONSEJO SUPERIOR DE INVESTIGACIONES CIENTIFICAS

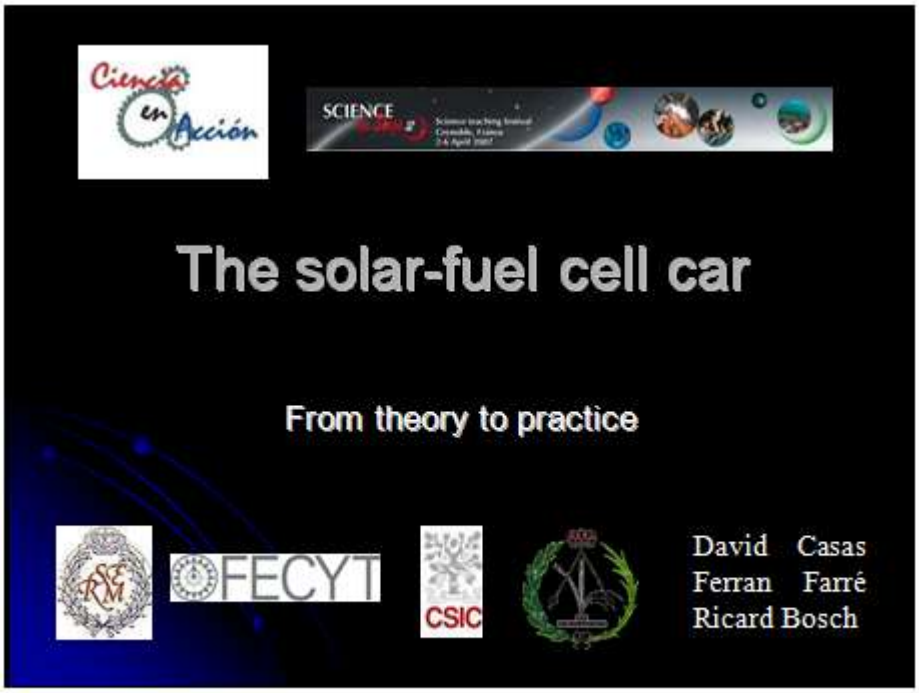
Ciencia en Acción
SCIENCE
The solar-fuel cell car
From theory to practice
FECYT
CSIC
David Casas
Ferran Farré
Ricard Bosch

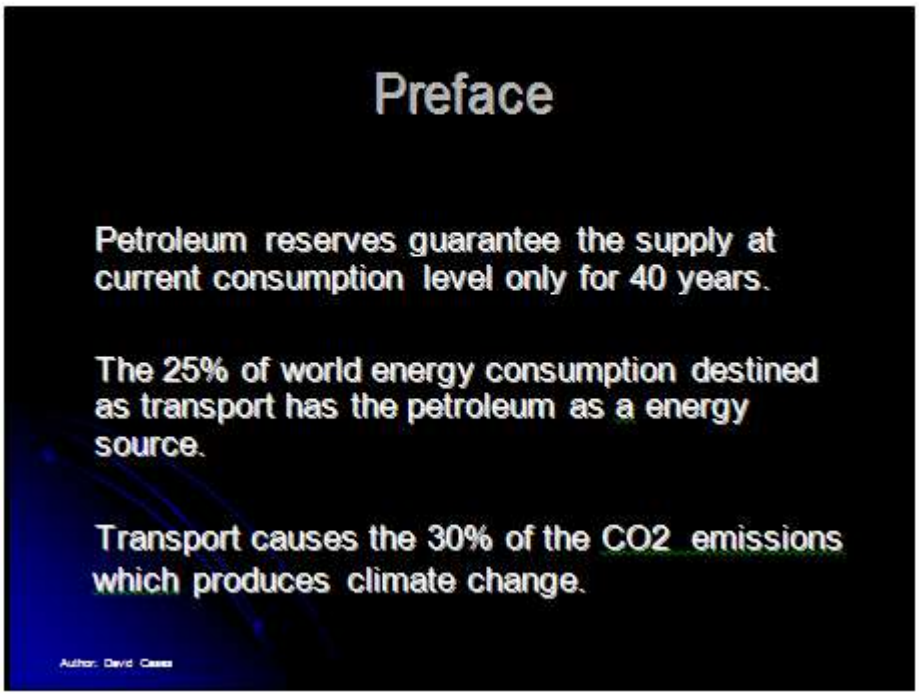
Preface
Petroleum reserves guarantee the supply at current consumption level only for 40 years.
The 25% of world energy consumption destined as transport has the petroleum as a energy source.
Transport causes the 30% of the CO2 emissions which produces climate change.
Author: David Casas

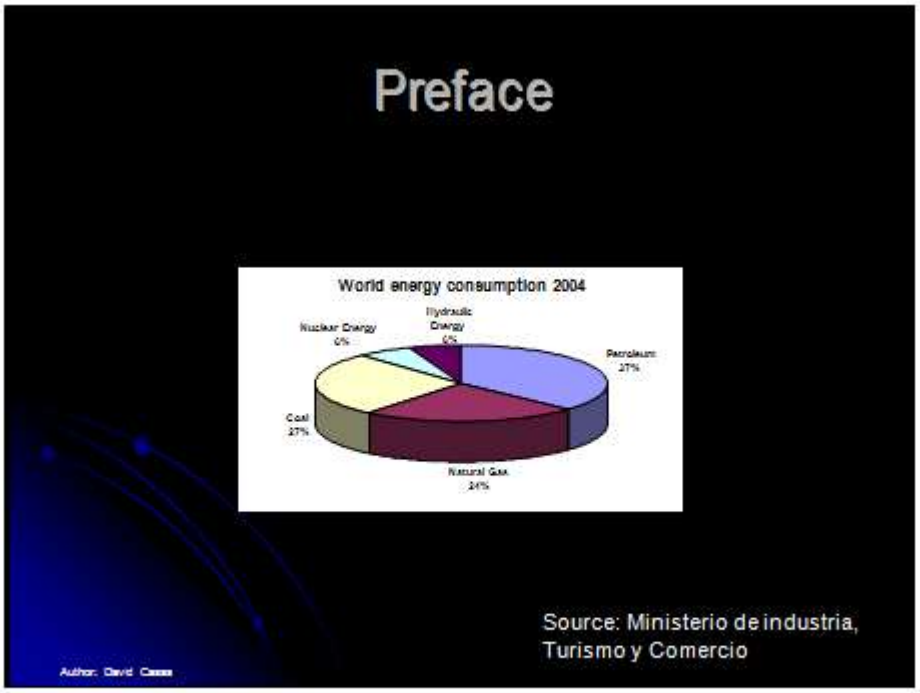
Preface
World energy consumption 2004
Hydraulic Energy 6%
Nuclear Energy 6%
Petroleum 37%
Coal 27%
Natural Gas 24%
Source: Ministerio de industria, Turismo y Comercio
Author: David Casas

Preface
Development of the sustainable technologies for its viability is the key to attenuate the global energy problem.
Hybrid car prototypes are an excellent work camp to extract sustainable technologies from the laboratory to the real world.
Author: David Casas

Preface
Solar car Despertaferro
Author: David Casas

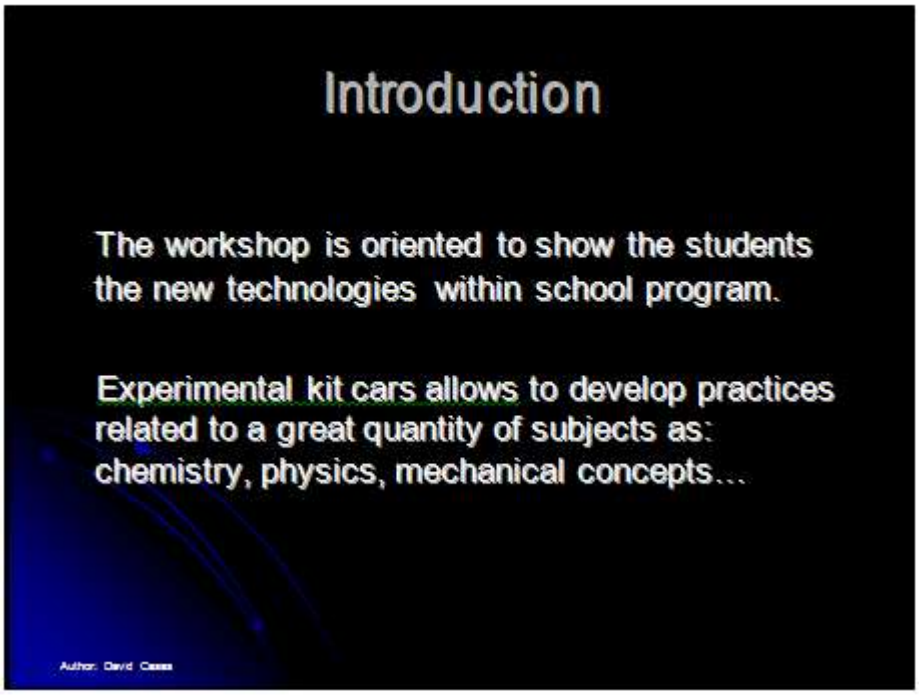
Introduction
The workshop is oriented to show the students the new technologies within school program.
Experimental kit cars allows to develop practices related to a great quantity of subjects as: chemistry, physics, mechanical concepts...
Author: David Casas

# Introduction

Teach the students about the technologies based on renewable energies that they will develop in the future.

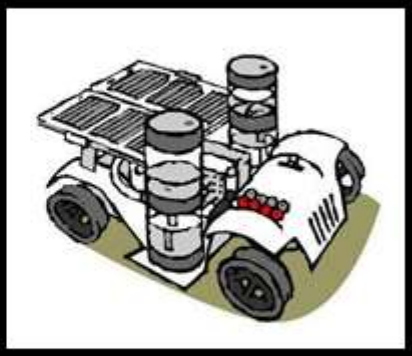

Author: David Casas

# Introduction

Car and briefcase kit is designed by ***Centre Tecnologic Eduard Soler*** *and* ***ERI Didactic*** *together* to carry out a set experiences in High School level. ***www.kithidrogenosolar.com***

***UPC*** (Polytechnic University of Catalonia) is preparing school informative sessions based in this kits.

E.R.I. DIDÀCTIC S.L.

CENTRE TECNOLÒGIC EDUARD SOLER

UPC

Author: David Casas

ETSEIB

## Working basic principles

Photovoltaic cell
Electrolyser
Fuel cell
DC current motor
System operation

Author: David Casas

## Working basic principles
## Photovoltaic cell

The most of the Earth's energy is provided by the sun

Wind is caused by an irregular heating of the Earth's surface.

The petroleum is a mixture of organic compounds subjected to high temperatures and pressures. Basically this compounds are made of plants so they used the solar energy to realize photosynthesis.

Author: David Casas

## Working basic principles
## Photovoltaic cell

The photovoltaic cell transforms the solar radiation into electric energy.

This transformation is based on the photoelectric effect.

Author: David Casas

## Working basic principles
## Photovoltaic cell

The photoelectric effect consists on the electrons emission by a material which is illuminated by a electromagnetic radiation.

The nature of light can be explained under the concept of the wave-particle duality.

Author: David Casas

## Working basic principles Photovoltaic cell

The electrons absorb energy from the photons of the light.

If the energy absorbed is sufficient the electron is freed from the atom nucleus.

It is supposed for each photon absorbed i is freed one electron.

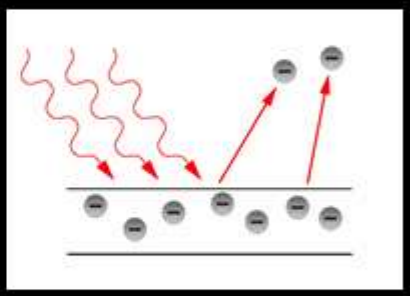

Author: David Casas

## Working basic principles Photovoltaic cell

The energy absorbed kick electron out from the valence band into a higher level-energy: conduction band.

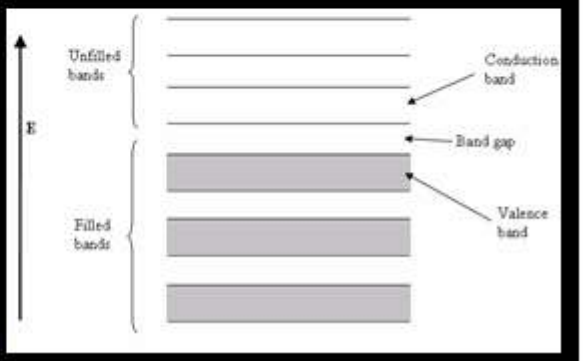


Author: David Casas

## Working basic principles Photovoltaic cell

The electrons of the conduction band are recollected thanks to the p-n junction of the cell .

The p-n junction is a junction of two parts charged positively and negatively. This creates a difference of potential that causes the movement of the freed electrons producing the electric current.

Author: David Casas

## Working basic principles Photovoltaic cell

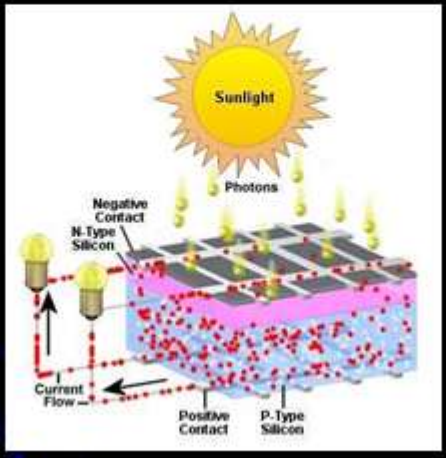


Author: David Casas

## Working basic principles Electrolyser

The electrolyser is a device that separates substances by means of electric current.

The source supply provide electrical energy for the reactions oxidation-reduction happen.

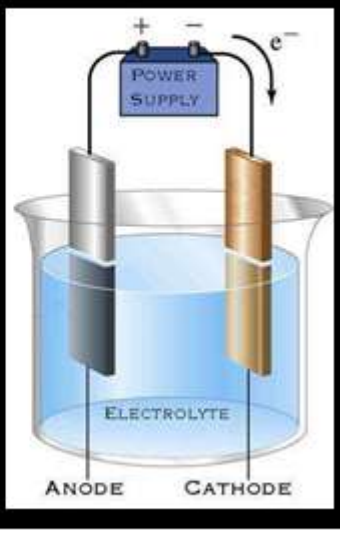


Author: David Casas

## Working basic principles Electrolyser

The technology of the fuel cell is based on the electrolysis of water.

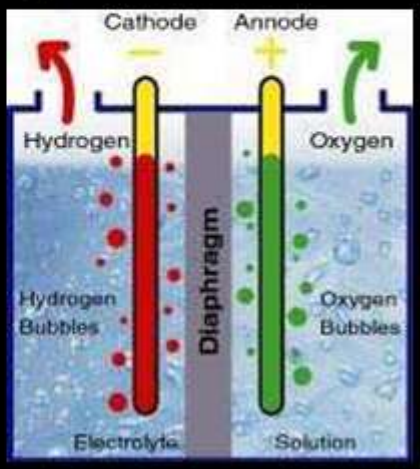


Author: David Casas

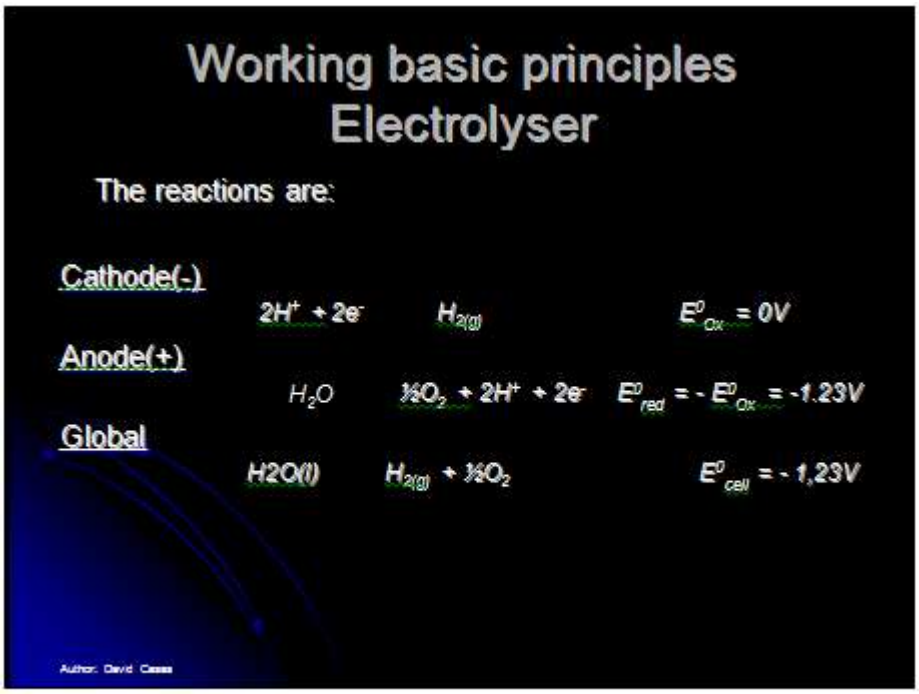
Working basic principles
Electrolyser
The reactions are:
Cathode(-)
$2H^+ + 2e^-$ $H_{2(g)}$ $E^0_{Ox} = 0V$
Anode(+)
$H_2O$ $½O_2 + 2H^+ + 2e^-$ $E^0_{red} = - E^0_{Ox} = -1.23V$
Global
$H2O(l)$ $H_{2(g)} + ½O_2$ $E^0_{cell} = - 1,23V$
Author: David Casas

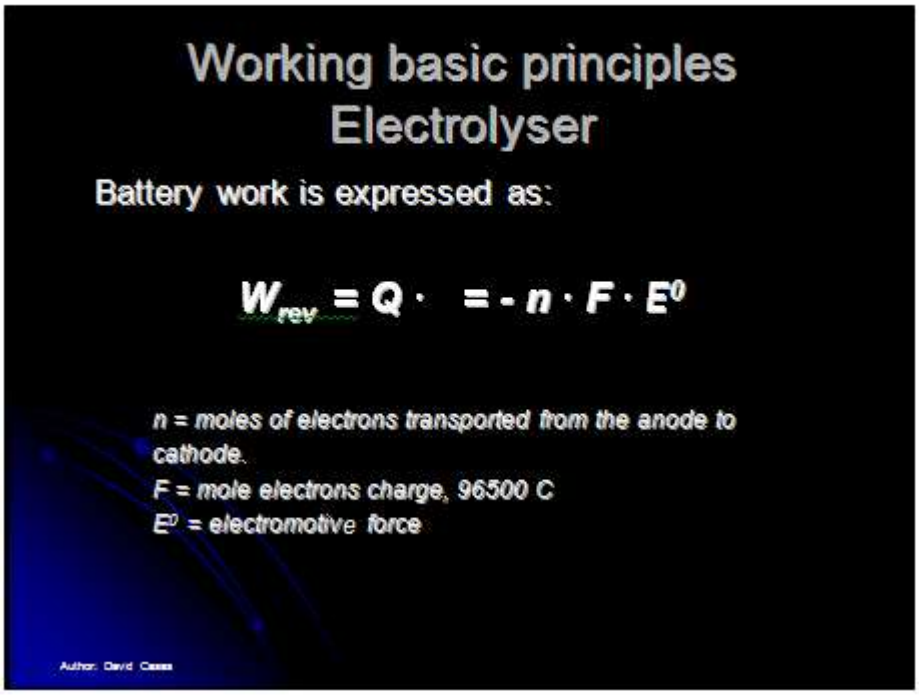
Working basic principles
Electrolyser
Battery work is expressed as:
$W_{rev} = Q \cdot = - n \cdot F \cdot E^0$
n = moles of electrons transported from the anode to cathode.
F = mole electrons charge, 96500 C
$E^0$ = electromotive force
Author: David Casas

## Working basic principles Electrolyser

Variation in **Gibbs free energy** is equal to reversible working minus possible expansion work in a constant temperature and pressure process. In case of a fuel cell there is not the expansion work:

$$W_{rev} = G = -n \cdot F \cdot E^0$$

Author: David Casas

## Working basic principles Electrolyser

The reaction will be spontaneous if **G** is negative, otherwise we need to supply energy for the reactions happen.

The water electrolysis needs a power supply at least with 1.23 volts.

Author: David Casas

## Working basic principles
## Fuel cell

The fuel cell is an electrochemical energy conversion device as a battery with the difference that it is designed for a continuous supplying.

The substances supplied react exchanging electrons which movement produces an electric current.

Author: David Casas

## Working basic principles
## Fuel cell

The hydrogen and the oxygen is supplied in the cathode and the anode respectively in the hydrogen cell technology.

The product of the reaction is water so the factor that determines if it is a clean energy comes from the energy source for produce the hydrogen.

Author: David Casas

## Working basic principles
## Fuel cell

The electrodes are coated with platinum that acts as a catalyser to accelerate the water decomposition.

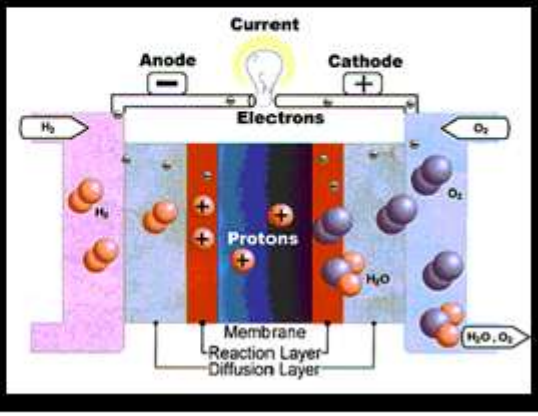


*Detail of a PEM cell operatin where it can be observed how flow the protons through th electrodes and the electron through the exterior circuit.*

Author: David Casas

## Working basic principles
## Fuel cell

The core of a PEM (proton exchange membrane) fuel cell is a semipermeable membrane that acts as a electrolyte.

This membrane is made of special polymer material and it allows the pass of the H+ protons whereas the electrons pass through the exterior circuit producing the electric current.

Author: David Casas

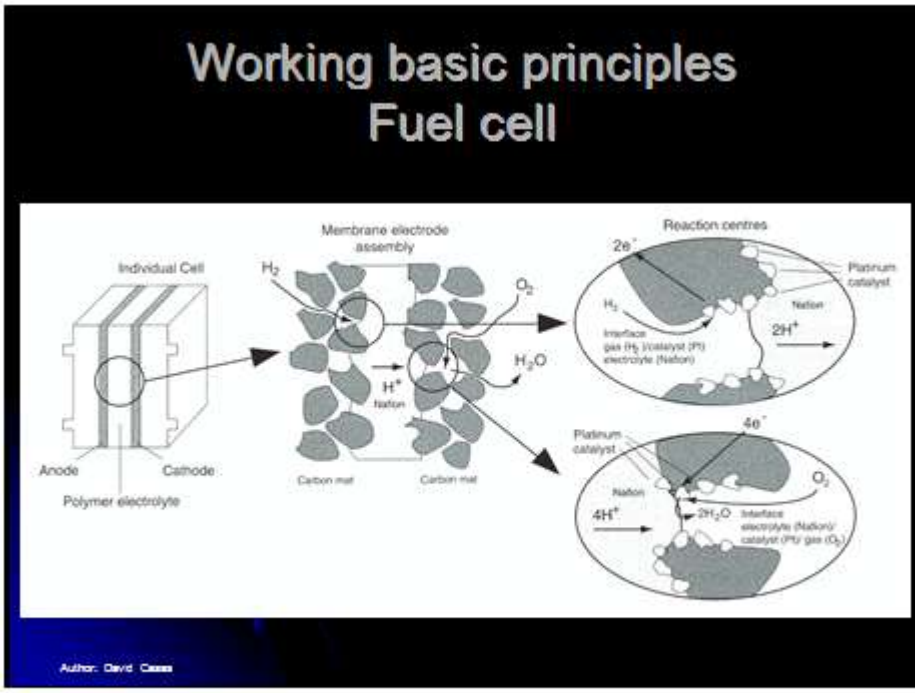
Working basic principles
Fuel cell
Individual Cell
Membrane electrode assembly
Reaction centres
Anode
Cathode
Polymer electrolyte
Carbon mat
Carbon mat
Platinum catalyst
Nafion
Author: David Casas

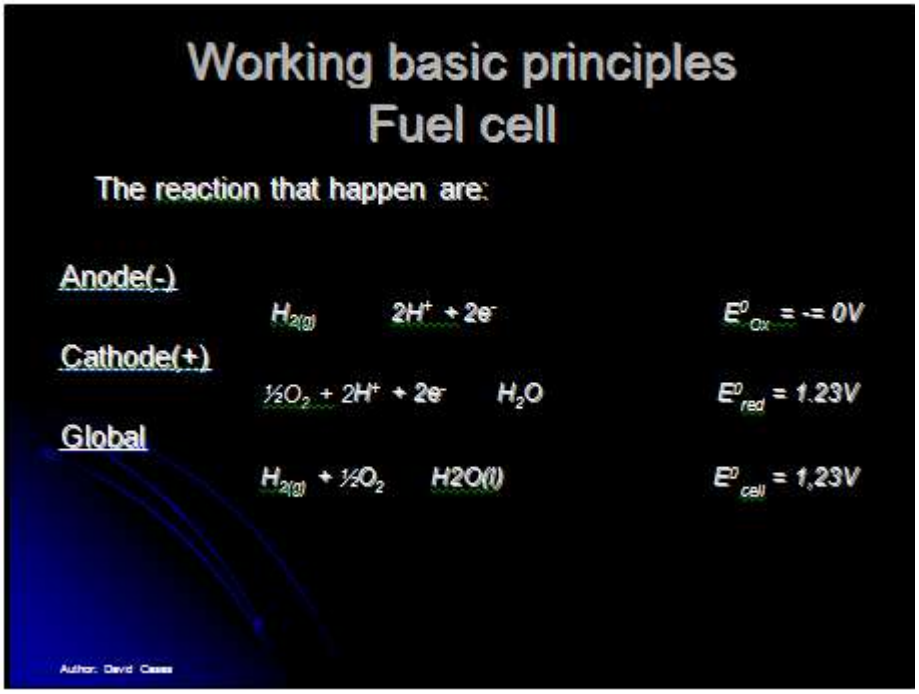
Working basic principles
Fuel cell
The reaction that happen are:
Anode(-)
Cathode(+)
Global
Author: David Casas

## Working basic principles
## Fuel cell

Recombination of hydrogen and oxygen is a spontaneous reaction due to Gibbs free energy is negative in this case:

$$W_{rev} = Q \cdot \quad = - n \cdot F \cdot E^0$$

Operating cell voltage is at the most 1.23 V, but it is always is low due to parasite losses in the internal resistances of electrodes and because some energy is transformed into heat.

Author: David Casas

## Working basic principles
## DC current motor

The electric motor is an electromechanical energy conversion device.

This conversion is based in the production of a magnetic field when there is a variation of an electric current according to Faraday's Law.

Author: David Casas

## Working basic principles DC current motor

The electric motor has a rotary part called the rotor and an static part called the stator.

The movement is produced due to the alignment between the two magnetic fields produced in the rotor and the stator.

Author: David Casas

## Working basic principles DC current motor

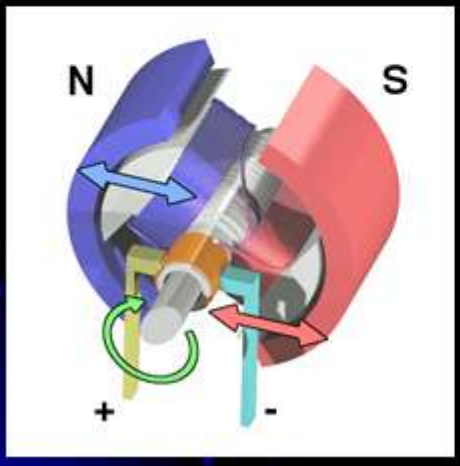


When the coil of the rotor is powered a magnetic field is generated around the armature like a virtual magnet.

Author: David Casas

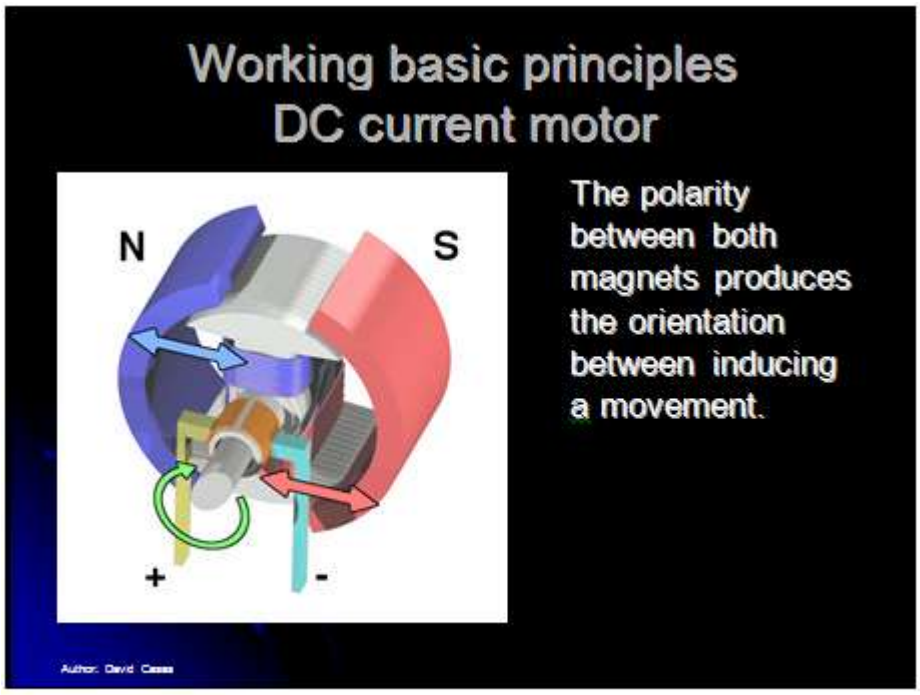
Working basic principles
DC current motor
N
S
+
-
The polarity between both magnets produces the orientation between inducing a movement.
Author: David Casas

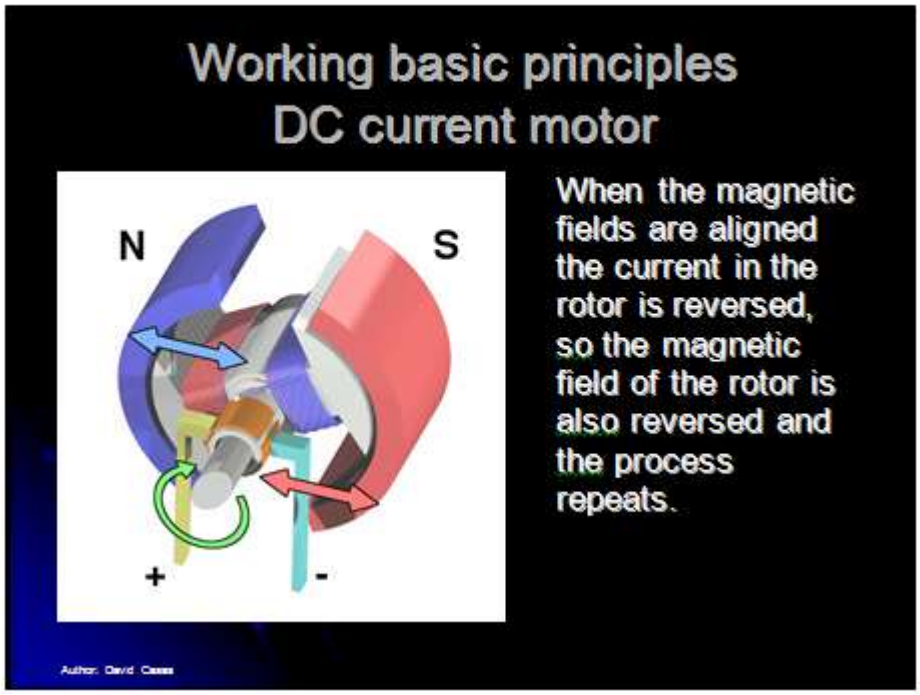
Working basic principles
DC current motor
N
S
+
-
When the magnetic fields are aligned the current in the rotor is reversed, so the magnetic field of the rotor is also reversed and the process repeats.
Author: David Casas

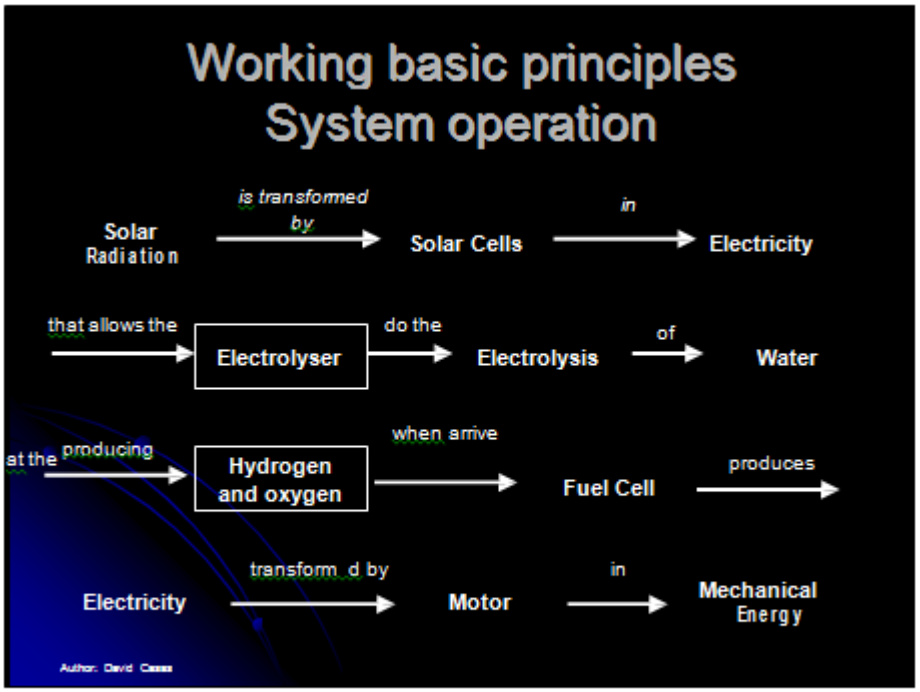
Working basic principles
System operation
Solar Radiation
is transformed by
Solar Cells
in
Electricity
that allows the
Electrolyser
do the
Electrolysis
of
Water
at the
producing
Hydrogen and oxygen
when arrive
Fuel Cell
produces
Electricity
transform d by
Motor
in
Mechanical Energy
Author: David Casas

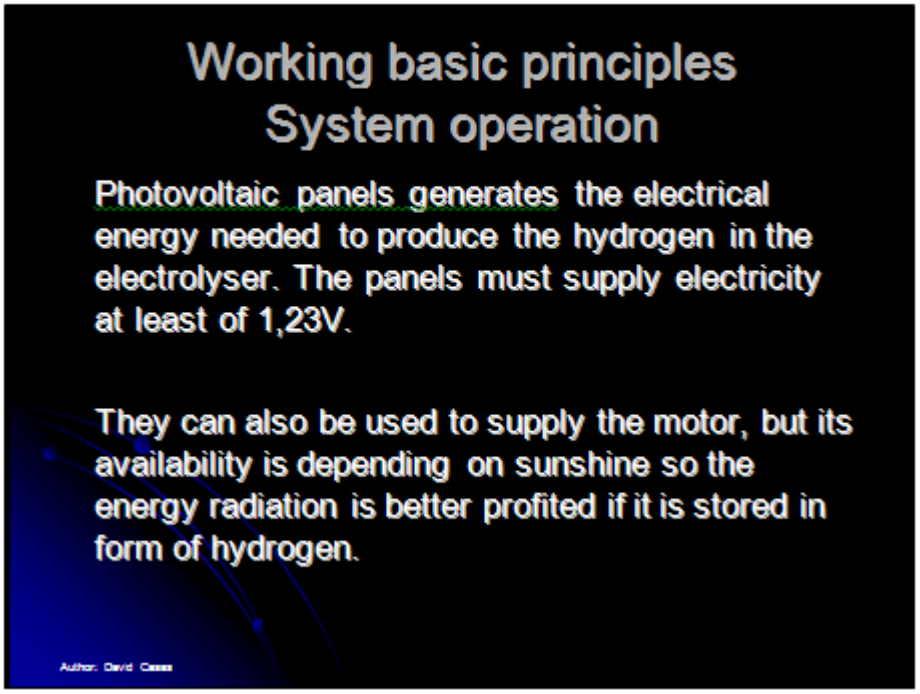
Working basic principles
System operation
Photovoltaic panels generates the electrical energy needed to produce the hydrogen in the electrolyser. The panels must supply electricity at least of 1,23V.
They can also be used to supply the motor, but its availability is depending on sunshine so the energy radiation is better profited if it is stored in form of hydrogen.
Author: David Casas

## Working basic principles
## System operation

Electrolyser production capacity of hydrogen stored in the tank during sunshine time should be higher than fuel cell demand.

Notice the hydrogen produced volume is twice as oxygen produced volume.

Author: David Casas

## Working basic principles
## System operation

The operation voltage of the fuel cell depends on the load for which it has been designed.

As a simple fuel cell has a theoretic 1.23V voltage usually there is assembled some fuel cells in series connection to reach higher voltage values.

Author: David Casas

## Working basic principles
## System operation

Factors like temperature or pressure favour the gases diffusion increasing the fuel cell efficiency.

Author: David Casas

## Elements characterization.
## Physic measurements.

Solar panels

Electrolyser

Fuel cell

Characteristic curve of the DC motor

Author: David Casas

## Elements characterization. Solar panels.

It is observed in this chart the solar panel characteristic curve.

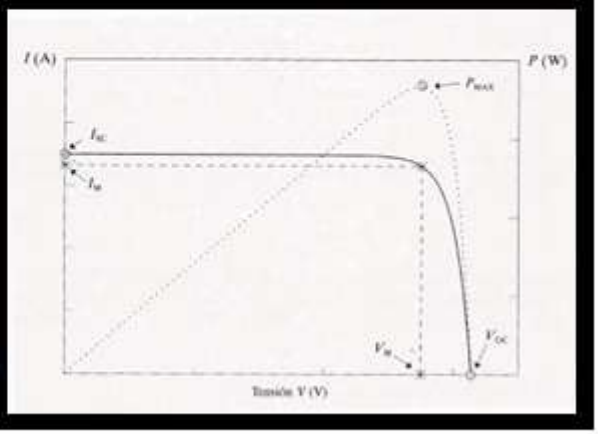


Author: David Casas

## Elements characterization. Solar panels.

This charts show how the characteristic curve changes in function of the:

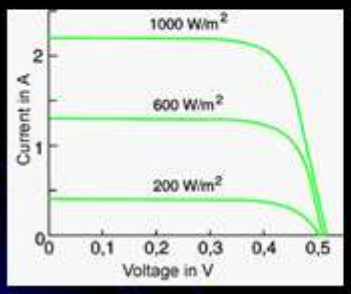


Radiation Intensity

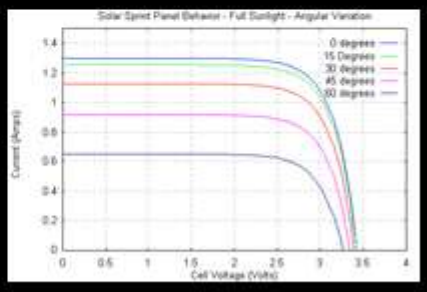


Angle variation

Author: David Casas

ETSEIB

## Elements characterization. Solar panels.

Current generated is proportional to intensity radiation received, although there is a physical limit to the current generation.

A typical photovoltaic cell gives 0,6 V in open circuit and 30mA/cm$^2$ as a short circuit current value.

Author: David Casas

## Elements characterization. Solar panels.

Voltage vary as the load changes, but the current is not affected significantly until it is close to 0.

Therefore the behaviour of a photovoltaic cell is like a current source.

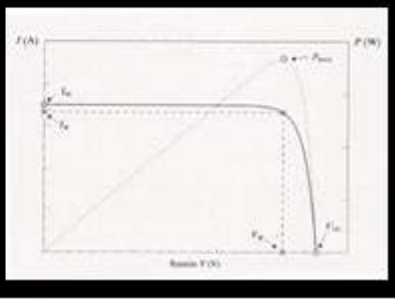

Author: David Casas

## Elements characterization. Solar panels.

The most important factor in a photovoltaic cell is its efficiency due to it is a energy conversion device.

In order to extract the maximum energy available, the load value is adjusted for maximize the power supplied. (Maximum Power Point Tracking)

Author: David Casas

## Elements characterization. Solar panels.

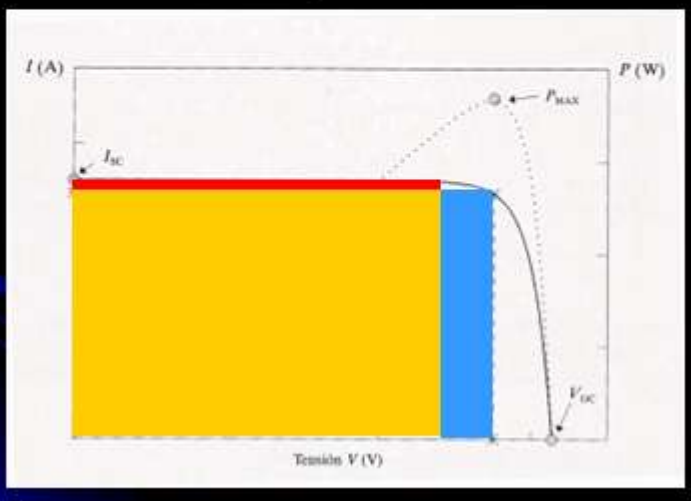


Author: David Casas

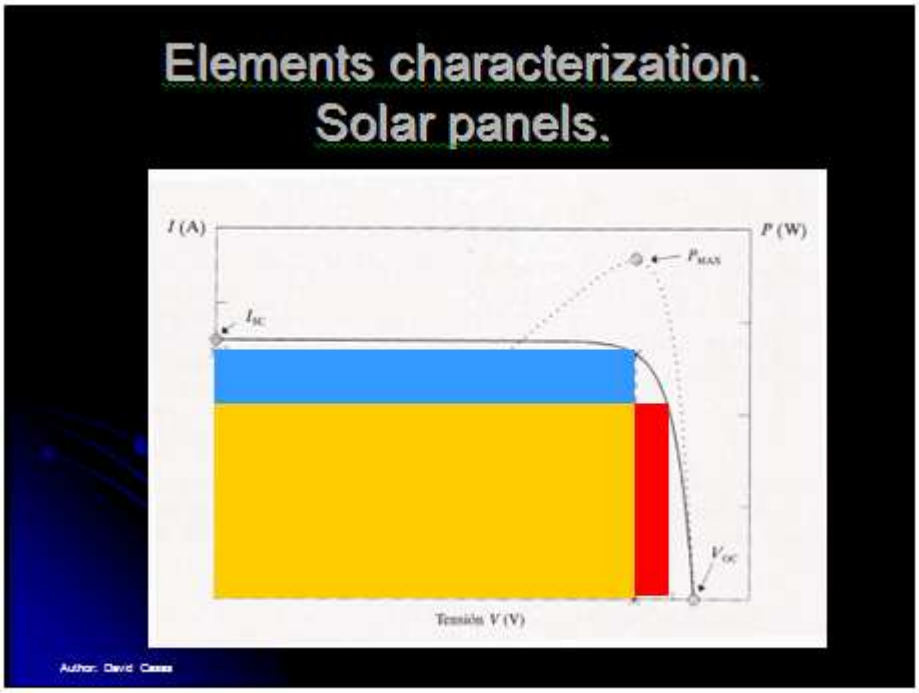
Elements characterization.
Solar panels.
I (A)
P (W)
$P_{MAX}$
$I_{SC}$
$V_{OC}$
Tensión V (V)
Author: David Casas

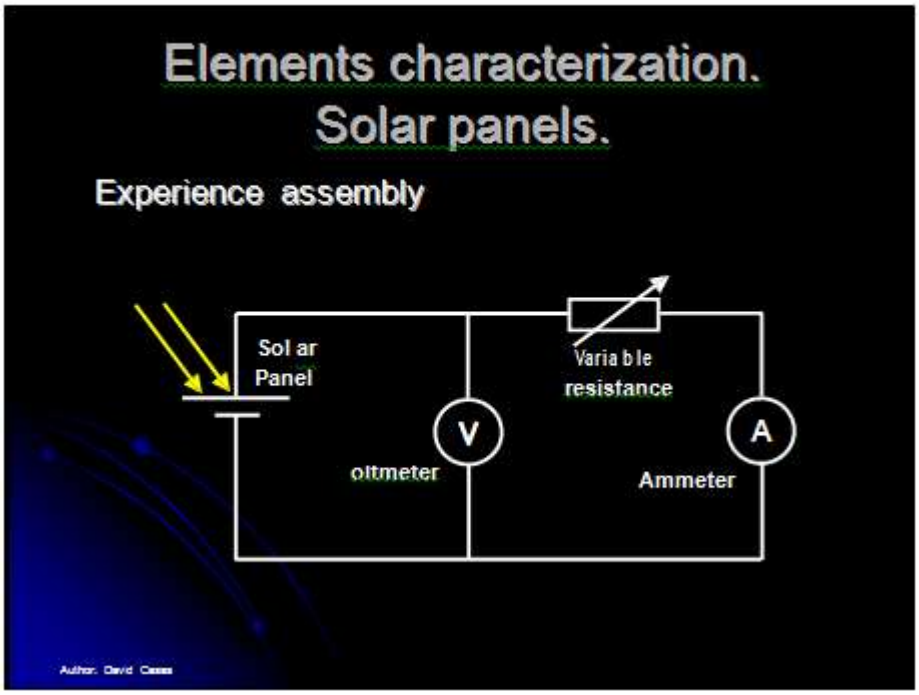
Elements characterization.
Solar panels.
Experience assembly
Sol ar
Panel
Varia b le
resistance
V
oltmeter
A
Ammeter
Author: David Casas

## Elements characterization. Solar panels.

Connect the solar panel by means of wires to the previous assembly according to this photo.

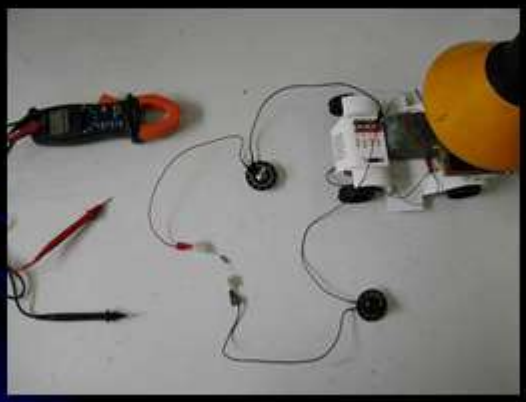

Author: David Casas

## Elements characterization. Solar panels.

Fill the following table with the obtained measurements.

| Resistance (Ω) | Current (mA) | Voltage (V) | Power (W) |
|---|---|---|---|
| 100+1 | | | |
| 30+1 | | | |
| 20+1 | | | |
| 17+1 | | | |
| 14+1 | | | |
| 12+1 | | | |
| 10+1 | | | |
| 1 | | | |

Author: David Casas

# Elements characterization. Solar panels.

Draw the graph of current versus voltage.

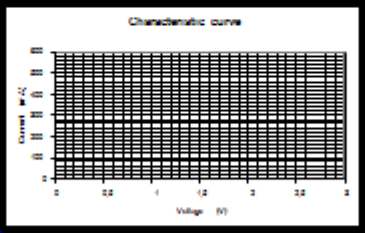


Author: David Casas

# Elements characterization. Solar panels.

Maximum efficiency

*P/S= Max. Power/Suseful*

| Cell panel surface | Total cell panels surface | Generated electric power per surface unit | Solar radiation intensity | Cell efficiency |
|---|---|---|---|---|
| S(cm²) | $S_{useful}$(cm²) | P/S (W/m²) | I (W/m²) | $\frac{P/S(cell)}{Light\ Intensity}$ |
| 17 | 50 | | | |

Author: David Casas

# Elements characterization. Solar panels.

Expected results

| Resistance (Ω) | current (mA) | Voltage (V) | Power (W) |
|---|---|---|---|
| 100+1 | 27 | 2,822 | 0,076 |
| 30+1 | 82 | 2,72 | 0,223 |
| 20+1 | 178 | 2,583 | 0,460 |
| 17+1 | 269 | 2,452 | 0,660 |
| 14+1 | 364 | 2,27 | 0,826 |
| 12+1 | 418 | 1,96 | 0,819 |
| 10+1 | 435 | 0,589 | 0,256 |
| 1 | 436 | 0,6 | 0,262 |

Author: David Casas

# Elements characterization. Solar panels.

Expected results

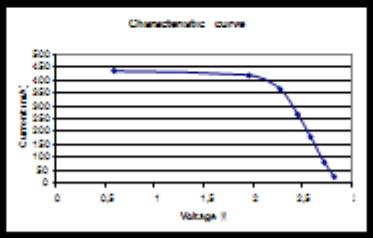


Author: David Casas

# Elements characterization. Solar panels.

**Expected results**

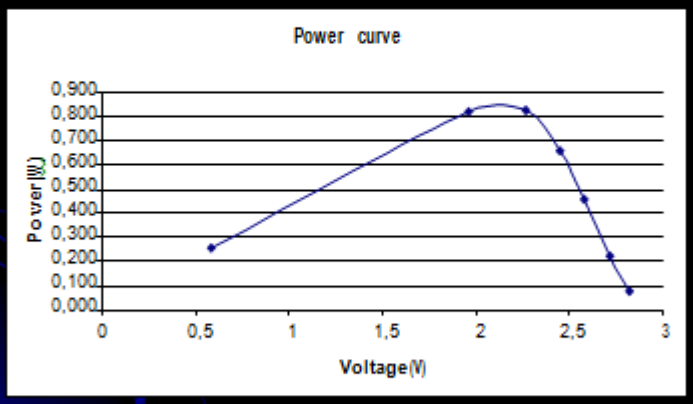


Author: David Casas

# Elements characterization. Solar panels.

**Maximum efficiency**

$P/S$ = Max. Power/Suseful = 0,83 W / 90 · $10^{-4}$ $m^2$ = 92,22

| Cell panel surface | Total cell panels surface | Generated electric power per surface unit | Solar radiation intensity | Cell efficiency |
|---|---|---|---|---|
| S(cm²) | $S_{useful}$(cm²) | P/S (W/m²) | I (W/m²) | $\frac{P/S(cell)}{Light\ Intensity}$ |
| 15 | 90 | 92,22 | 1000 | 9,22 % |

Author: David Casas

## Elements characterization. Solar panels.

This solar panel acts as a current source until voltage is close to 2V. After increasing this voltage value, the current drops-off.

Author: David Casas

## Elements characterization. Electrolyser

Calculate energetic efficiency of the electrolyser.

Water is separated into hydrogen and oxygen with a theoretic voltage of 1,23V, besides if the voltage or the current are not modified, the gases production will be constant and uniform during the time.

Author: David Casas

# Elements characterization. Electrolyser

Electrolyser energetic efficiency depends on its hydrogen production capacity.

$$\eta_{energetic} = \frac{E_{hydrogen}}{E_{electric}} = \frac{V_{H2} \cdot H_0}{V \cdot I \cdot t}$$

Where:

$H_0$ = Combustion enthalpy = 12,745 J/cm³, includes the water condensation according to:

$$H_{2(g)} + \tfrac{1}{2}O_{2(g)} \rightarrow H_2O_{(l)}$$

$VH_2$= hydrogen volume produced in $m^3$

$V$ = voltage in volts

$I$ = current in amperes

$t$ = time in seconds

Author: David Casas

# Elements characterization. Electrolyser

Experience assembly:

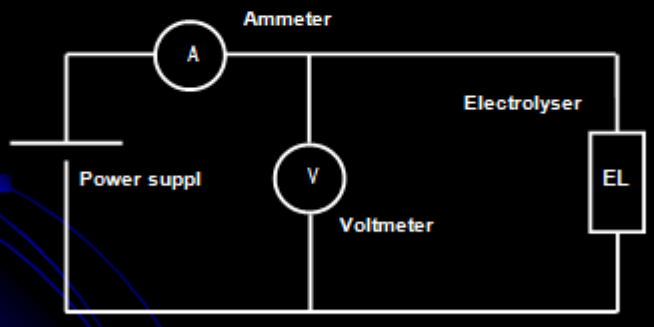


Author: David Casas

## Elements characterization. Electrolyser

Check the output taps of the tanks-electrolyser group to the cell are closed and then connect the electrolyser to the power supply with constant current and voltage.

Author: David Casas

## Elements characterization. Electrolyser

Fill the following table with the obtained measurements.

| Time | Voltage | Current | Power | Volume $H_2$ |
|---|---|---|---|---|
| s | V | A | W | $cm^3$ |
| | | | | |
| | | | | |
| | | | | |
| | | | | |

Author: David Casas

# Elements characterization. Electrolyser

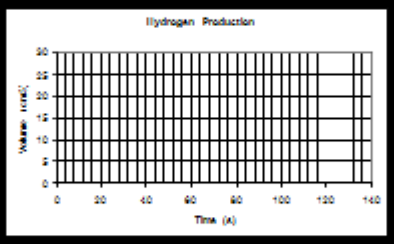


Author: David Casas

# Elements characterization. Electrolyser

## Expected results

| Time | Voltage | Current | Power | Volume $H_2$ |
|---|---|---|---|---|
| s | V | A | W | $cm^3$ |
| 130 | 3,2 | 0,3 | 0,96 | 5 |
| 270 | 3,2 | 0,3 | 0,96 | 10 |
| 402 | 3,2 | 0,3 | 0,96 | 15 |
| 530 | 3,2 | 0,3 | 0,96 | 20 |

Author: David Casas

ETSEIB

# Elements characterization. Electrolyser

## Expected Results

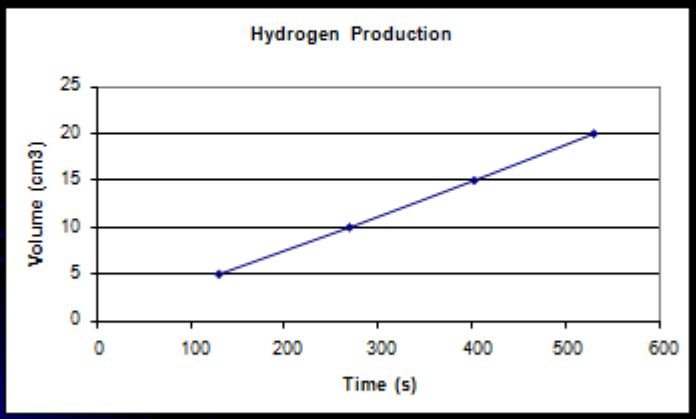


Author: David Casas

# Elements characterization. Electrolyser

## Expected results

| | | | | | |
|---|---|---|---|---|---|
| exergetic | $\frac{E_{hydrogen}}{E_{electric}}$ | $\frac{V_{H2} \cdot H_0}{V \cdot I \cdot t}$ | $\frac{20cm^3 \cdot 12.745 \cdot J/cm^3}{3.2V \cdot 0.3A \cdot 530s}$ | 0.501 | 50.1% |

- The electrolyser efficiency increases when the voltage of the power supply is close to 1,23V. However it must always be superior than 1,23V.

Author: David Casas

ETSEIB

## Elements characterization. Electrolyser

It seems the water is not consumed, but it is. The reason is the water volume necessary is smaller than the hydrogen volume produced.

$$P \cdot V = n \cdot R \cdot T \qquad n_{H_2} = \frac{P \cdot V}{R \cdot T} = \frac{1 atm \cdot 0{,}02 l}{0{,}082 \cdot 298 K} = 8{,}18 \cdot 10^{-4} moles H_2$$

$$1 mole H_2 \quad 1 mole H_2O$$

$$8{,}18 \cdot 10^{-4} moles H_2 \cdot \frac{1 mole H_2O}{1 mole H_2} \cdot \frac{18 g H_2O}{1 mole H_2O} \cdot \frac{1 cm^3 H_2O}{1 g H_2O} = 0{,}015 cm^3 H_2O$$

Author: David Casas

## Elements characterization. Fuel cell

Calculate the fuel cell energetic efficiency.

Theoretical energetic efficiency is described by:

$$_{ideal} = \frac{G}{H} = \frac{H - T \cdot S}{H} = 1 - \frac{T \cdot S}{H} = 1 - \frac{298 K \cdot (-162{,}985 J/(mol \cdot K))}{285840 J/mol}$$

$$_{ideal} = 0.83 = 83\%$$

Author: David Casas

## Elements characterization. Fuel cell

Energy loses are due to the transformation of a fraction of the electric energy into heat.

However the fraction that is transformed into heat is higher in real world.

Author: David Casas

## Elements characterization. Fuel cell

Experience assembly.

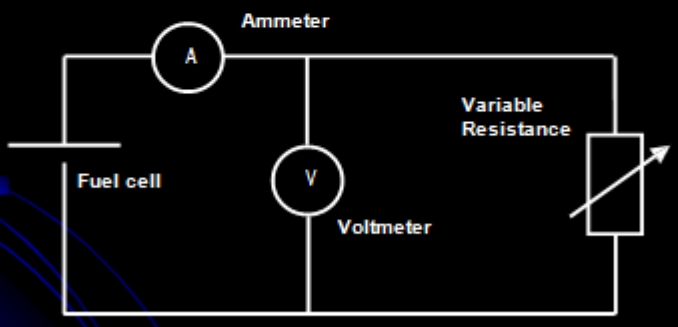


Author: David Casas

## Elements characterization. Fuel cell

Connect the fuel cell to the tanks with hydrogen and oxygen (or directly to the electrolyser)

Connect the variable resistances.

Author: David Casas

## Elements characterization. Fuel cell

Fill the following table with the obtained measurements.

| Resistance (Ω) | Voltage (V) | Current (mA) | Power (W) |
|---|---|---|---|
| 1 | | | |
| 3+1 | | | |
| 6+1 | | | |
| 15+1 | | | |
| 20+1 | | | |
| 40+1 | | | |
| 60+1 | | | |
| 100+1 | | | |

Author: David Casas

# Elements characterization. Fuel cell

Draw the graph of current versus voltage.

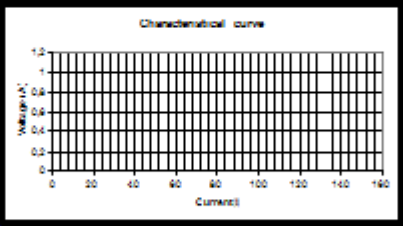


Author: David Casas

# Elements characterization. Fuel cell

Fill the following table with the obtained measurements.

| Resistance (Ω) | Voltage (V) | Current (mA) | Power (W) |
|---|---|---|---|
| 1 | 0,36 | 52 | 0,0187 |
| 3 | 0,4 | 45 | 0,0180 |
| 6 | 0,43 | 38 | 0,0163 |
| 15 | 0,55 | 25 | 0,0139 |
| 20 | 0,62 | 18 | 0,0112 |
| 40 | 0,68 | 12 | 0,0082 |
| 60 | 0,72 | 10 | 0,0072 |
| 100 | 0,78 | 6 | 0,0047 |

Author: David Casas

## Elements characterization. Fuel cell

Draw the graph of current versus voltage.

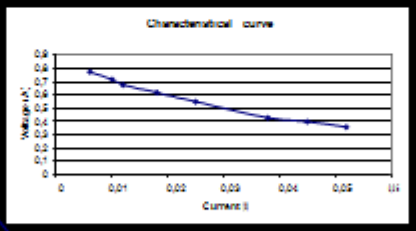


Author: David Casas

## Elements characterization. Fuel cell

Fuel cell acts as a power supply with an electromotive force with EFM E and a internal resistance r.

$$E = V + I \cdot r$$

$$V = E - I \cdot r$$

Author: David Casas

## Elements characterization. Fuel cell

Fuel cell model.

$$E = V + I \cdot r \Rightarrow V = E - I \cdot r$$

$$E = 0{,}8\ V \qquad r = 9\ \Omega$$

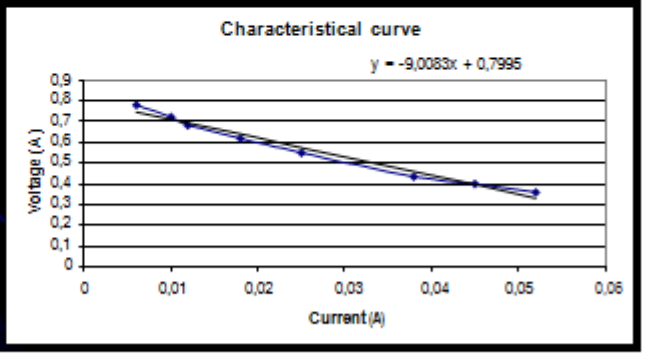


Author: David Casas

## Elements characterization. Fuel cell

If the electrical load is fixed then the hydrogen consumption will be constant during all the time.

The hydrogen consumption level is proportional to the charge movement, in other words, it is proportional to electric current.

Author: David Casas

## Elements characterization. Fuel cell

Hydrogen fuel cell technology will not be viable until the distribution system would be extended.

Generally the hydrogen produced in the generating stations would be far from the consumption point to optimize the efficiency, otherwise the PEM fuel cells are reversible so they can act as autonomous system if there is a electric power supply.

Author: David Casas

## Elements characterization. Characteristic curve of the DC motor

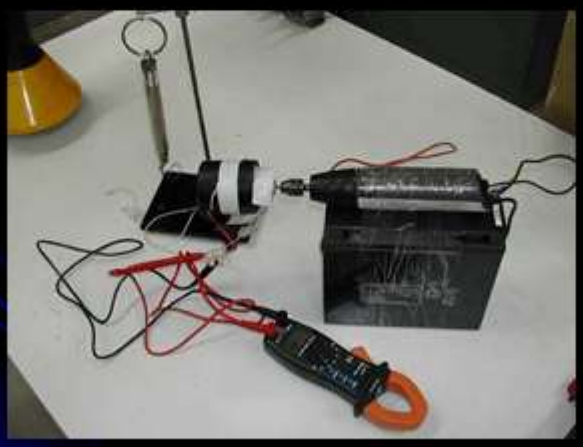

Author: David Casas

## Elements characterization.
### Characteristic curve of the DC motor

Estimate the torque-current curve for this drill (DC motor). As we will see later, this will be useful to obtain the mechanical power that drill supplies.

The characteristic curve of a DC motor is a straight line in the plane torque versus current, so we only need two points to get it.

Author: David Casas

## Elements characterization.
### Characteristic curve of the DC motor

In order to avoid damaging the magnets in the blocked rotor test it is connected in series with the motor a resistance.

As the voltage motor is also proportional to its current we can extrapolate the real current would pass if the motor voltage were the voltage battery.

Author: David Casas

# Elements characterization.
## Characteristic curve of the DC motor

Take a note of these measurements.

| | $I_{drill}$ (A) | W (rad/s) | $V_{drill}$ (V) |
|---|---|---|---|
| Open circuit | | 16000 | – |
| Rotor Blocked | | 0 | |

*Added a fixed resistance for not damage the motor

$$I_{drill}(real) \quad I_{drill}(measured)\ \frac{V_{battery}}{V_{drill}}$$

Author: David Casas

# Elements characterization.
## Characteristic curve of the DC motor

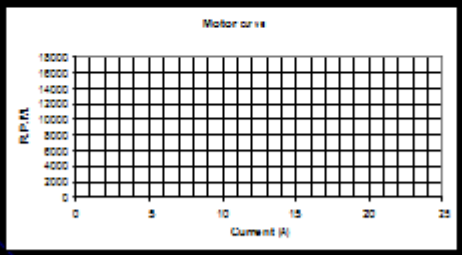


Author: David Casas

## Elements characterization.
## Characteristic curve of the DC motor

### Expected results

| | $I_{drill}$ (A) | W (rad/s) | $V_{drill}$ (V) |
|---|---|---|---|
| Open circuit | 1,9 | 16000 | – |
| Rotor Blocked | 5 | 0 | 2,8 |

$$I_{drill}(real) \quad I_{drill}(measured)\frac{V_{battery}}{V_{drill}} \quad 5\cdot\frac{12,5}{2,8} \quad 22,3A$$

Author: David Casas

## Elements characterization.
## Characteristic curve of the DC motor

### Expected results

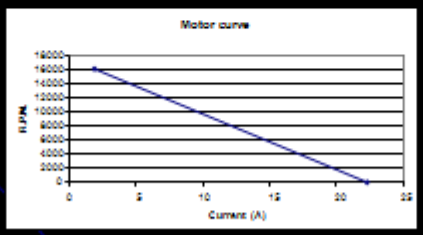


Author: David Casas

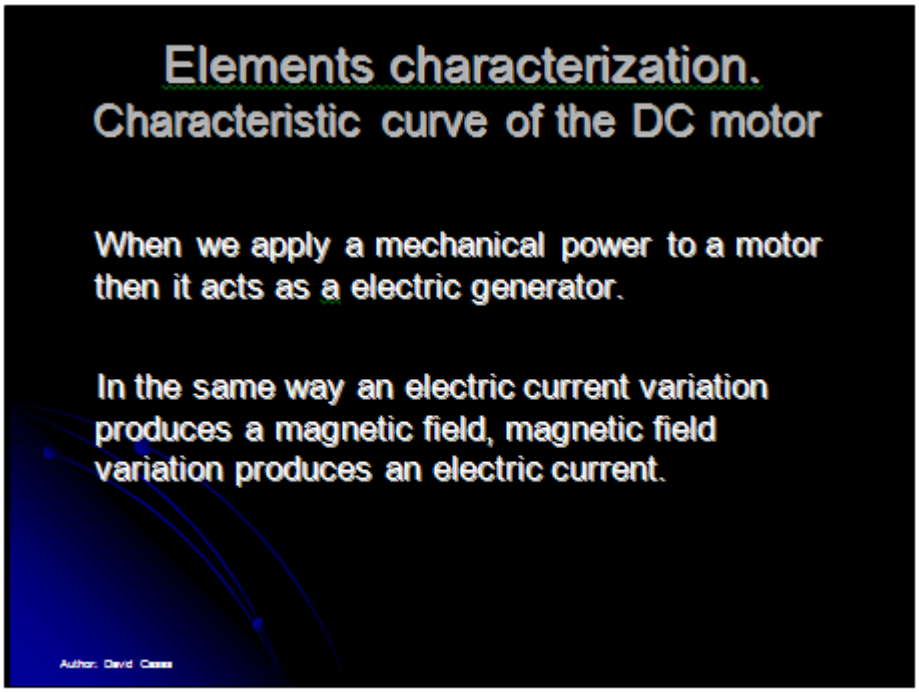
Elements characterization.
Characteristic curve of the DC motor
When we apply a mechanical power to a motor then it acts as a electric generator.
In the same way an electric current variation produces a magnetic field, magnetic field variation produces an electric current.
Author: David Casas

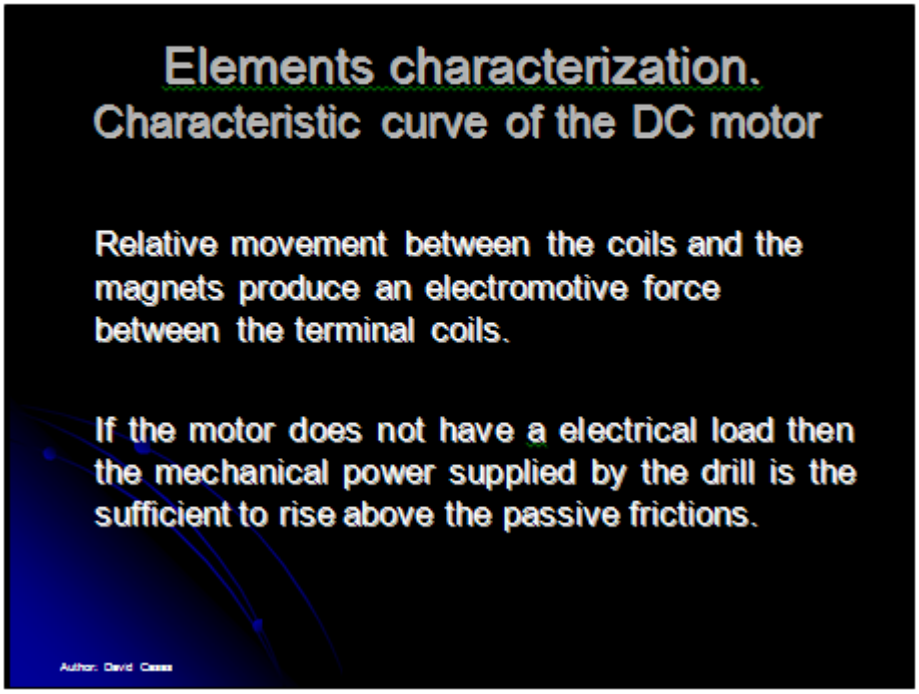
Elements characterization.
Characteristic curve of the DC motor
Relative movement between the coils and the magnets produce an electromotive force between the terminal coils.
If the motor does not have a electrical load then the mechanical power supplied by the drill is the sufficient to rise above the passive frictions.
Author: David Casas

## Elements characterization.
## Characteristic curve of the DC motor

In case of connect to the motor a electrical load then the energy consumed by the load is supplied by the drill, so torque rises until is equal to rotor load torque.

The point where motor torque curve and load torque curve coincide is the operating motor point.

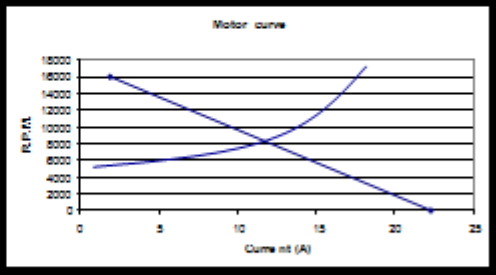


Author: David Casas

## Elements characterization.
## Characteristic curve of the DC motor

Fill the following table

| | I drill (A) | Vdrill (V) | Pele (W) | F (N) | Torque (Nm) | Speed (rpm) | Speed (rad/s) | Pot Mec | Igen (I) | Vgen (V) | Pele (W) |
|---|---|---|---|---|---|---|---|---|---|---|---|
| 100 ohms | | | | | | | | | | | |
| Bulb | | | | | | | | | | | |

$$Speed(\ ad/s) = Speed(rpm) \cdot 2 \cdot \ / 60$$

$$r = 6{,}5mm$$

Author: David Casas

ETSEIB

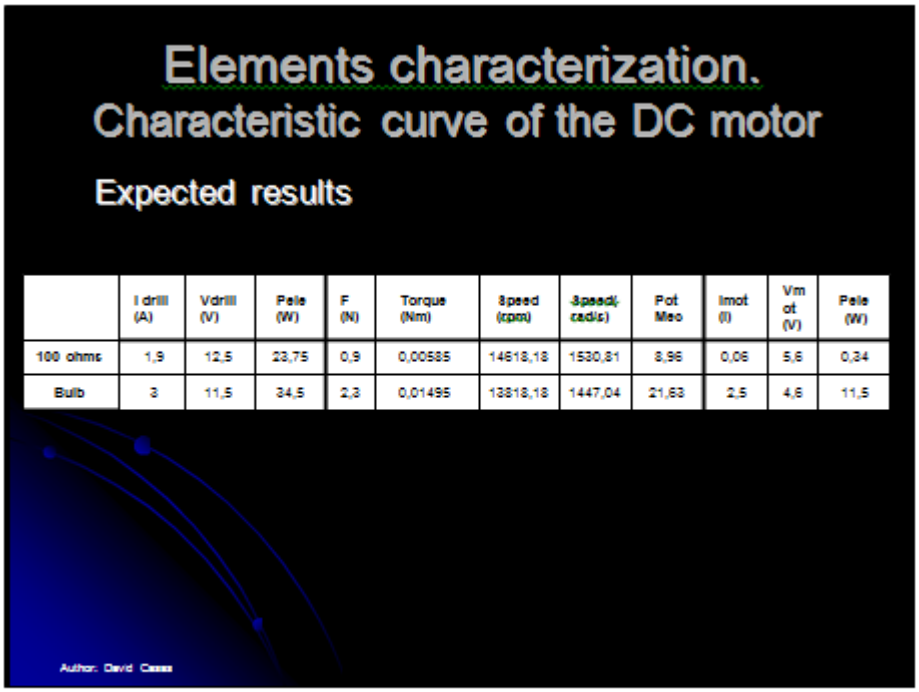


| | I drill (A) | Vdrill (V) | Pele (W) | F (N) | Torque (Nm) | Speed (rpm) | Speed( rad/s) | Pot Mec | Imot (I) | Vm ot (V) | Pele (W) |
|---|---|---|---|---|---|---|---|---|---|---|---|
| 100 ohms | 1,9 | 12,5 | 23,75 | 0,9 | 0,00585 | 14618,18 | 1530,81 | 8,96 | 0,06 | 5,6 | 0,34 |
| Bulb | 3 | 11,5 | 34,5 | 2,3 | 0,01495 | 13818,18 | 1447,04 | 21,63 | 2,5 | 4,6 | 11,5 |

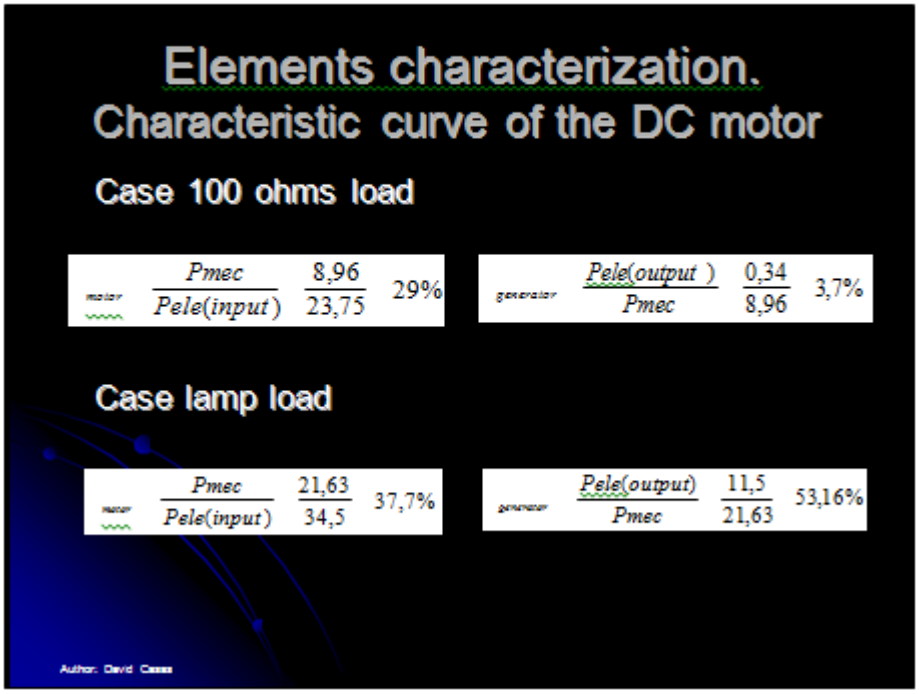

## Global energy balance

Alternative experiment is the global energy balance where the efficiency coefficient of the different devices are evaluated to predict the final energy we can dispose.

Author: David Casas

## Global energy balance

Calculate the system energetic efficiency for a fixed conditions. What could do to increase the system efficiency?

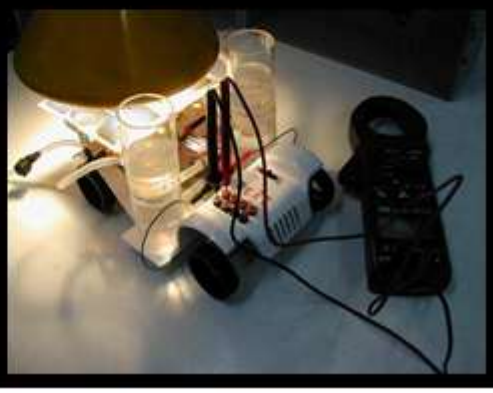

Author: David Casas

## Critical angle

Calculate the critical angle for the car stops moving.

First take a measure of the motor torque with the dynamometer.

Mesaure the mass of the car with the dynamometer too.

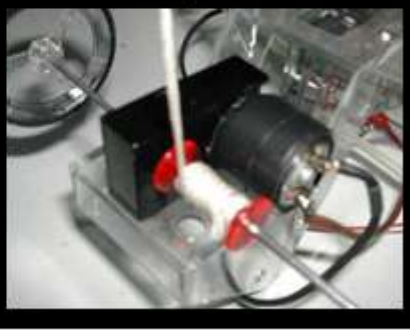

Author: David Casas

## Critical angle

System will be in balance when the weight force is equal to the reaction of the force that does the motor to the ground.

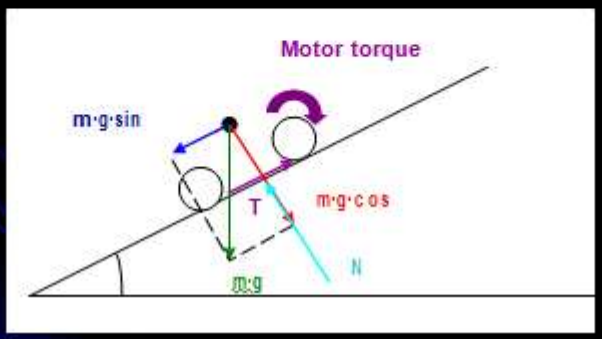


Author: David Casas

## Critical angle

$F_H = m \cdot g \cdot \sin - T = 0 =$
$= m \cdot g \cdot \sin - Torque_{motor} / r_{wheel}$

$F_V = m \cdot g \cdot \cos - N = 0$

Author: David Casas

## Conclusion

We hope you have seen the educative potential of these experiments in order to teach your students in different subjects, while they learn "playing" with the kit.

One day in the near future they may change the world developing sustainable technologies and we should start teaching them now.

Author: David Casas

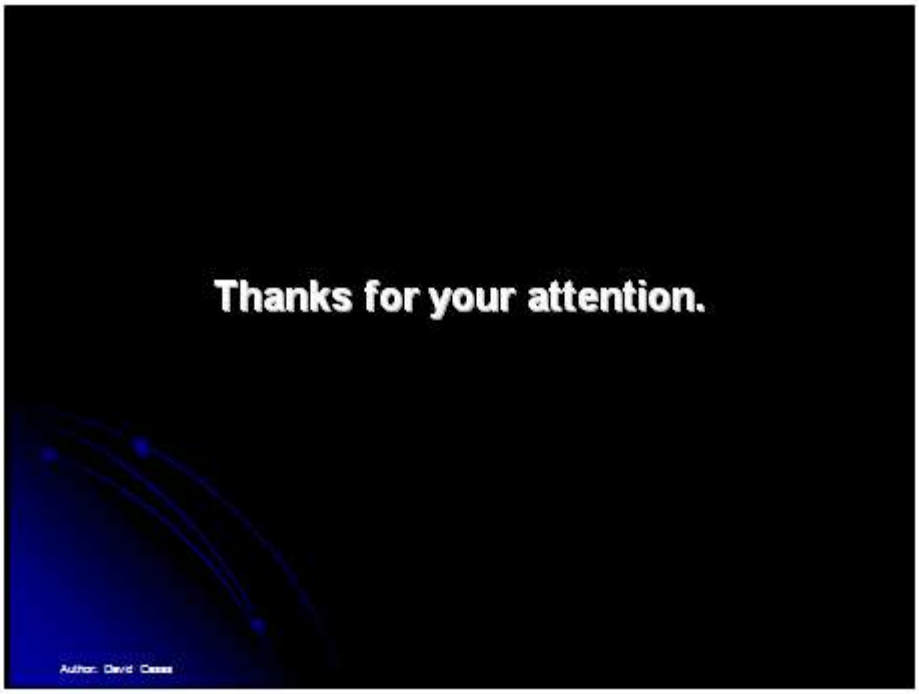
Thanks for your attention.
Author: David Casas

# The solar fuel cell car

*From the theory to the practice*

## Experiences Notepad

### Experience 1: Solar Panels

**Objectives:**

Calculate the maximum solar panel efficiency

**Experience Assembly**

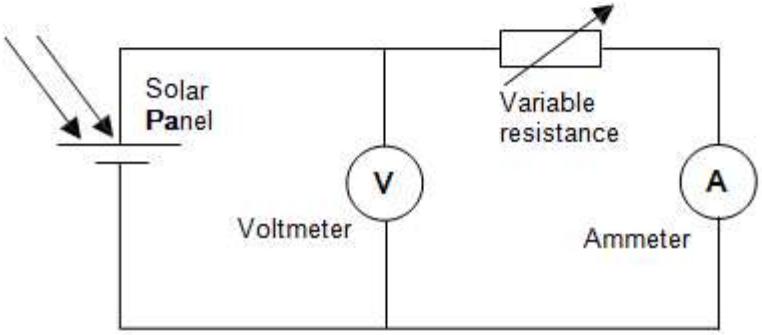


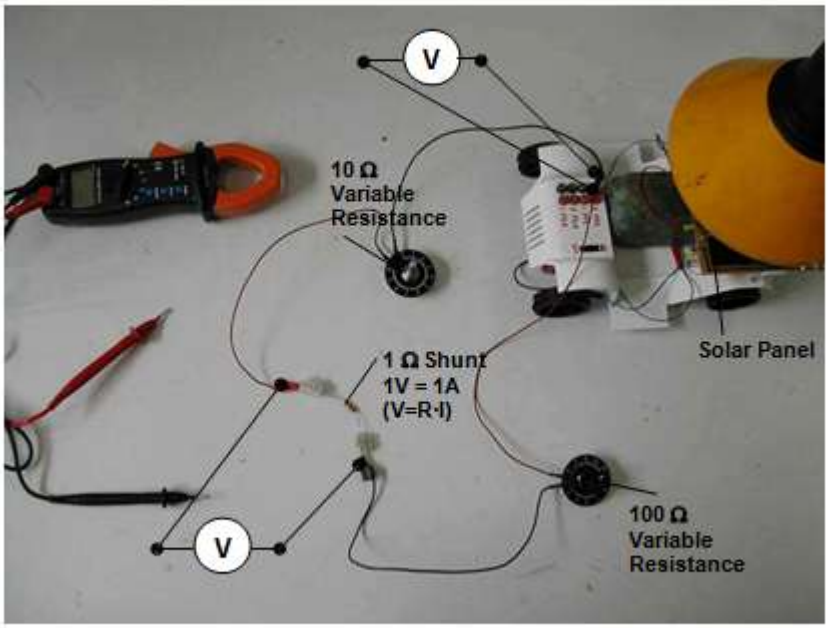

**Procedure**

1. Plug in the lamp and turn it on.
2. Apply a resistance value for the load circuit. For example if the desired resistance value you want to apply is "13+1" ohms then put the 100 potentiometer in 1 (scale 1:10) and the 10 potentiometer in 3 (scale 1:1). The "+1" values is already applied in the circuit as a shunt from wich we can know the circuit current measuring the voltage difference between shunt terminals and converse it directly to Amperes.
   V=R·I V=1·A.
3. Make a note of voltage differences in solar panel terminals and shunt terminals for each resistance described below. Converse directly the difference voltage in the shunt to amperes.

**Fill the following table**

| Resistance (W) | Current (A) = V (R 1Ω) | Solar Panels Voltage (V) | Power (W) |
|---|---|---|---|
| 100+1 | | | |
| 30+1 | | | |
| 20+1 | | | |
| 17+1 | | | |
| 14+1 | | | |
| 12+1 | | | |
| 10+1 | | | |
| 1 | | | |

**Draw the graph of current versus voltage**

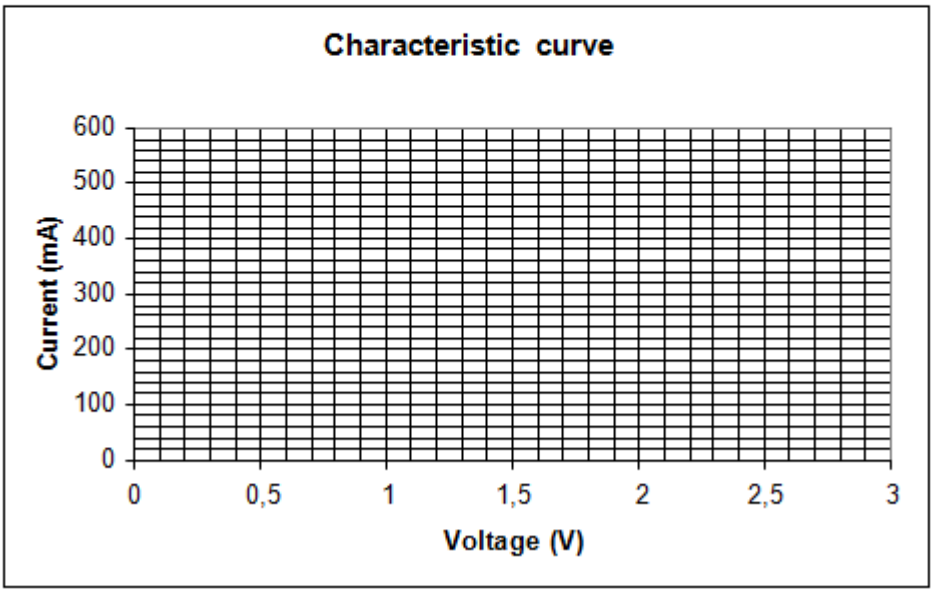

Maximum efficiency

*P/S= Max. Power/Suseful*

| Cell panel surface | Total cell panels surface | Generated electric power per surface unit | Solar radiation intensity | Cell efficiency |
|---|---|---|---|---|
| S(cm2) | Suseful(cm2) | P/S (W/m2) | I (W/m2) | $\frac{P/S(cell)}{Light\ Intensity}$ |
| 12.5 | 75 | | 1000 | |

**Calculus notes**

## Experience 2: Electrolyser

**Objectives:**

Check the hydrogen production is constant.

Calculate the energetic efficiency of the electrolyser

**Experience Assembly**

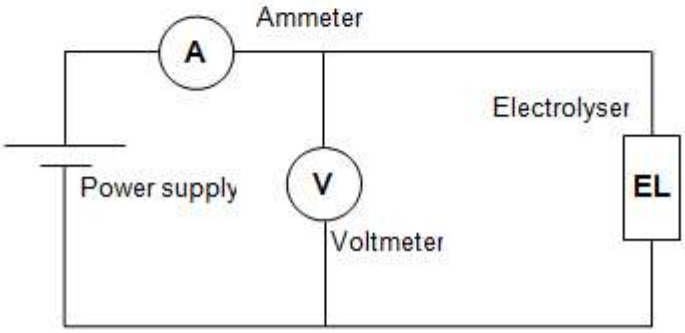


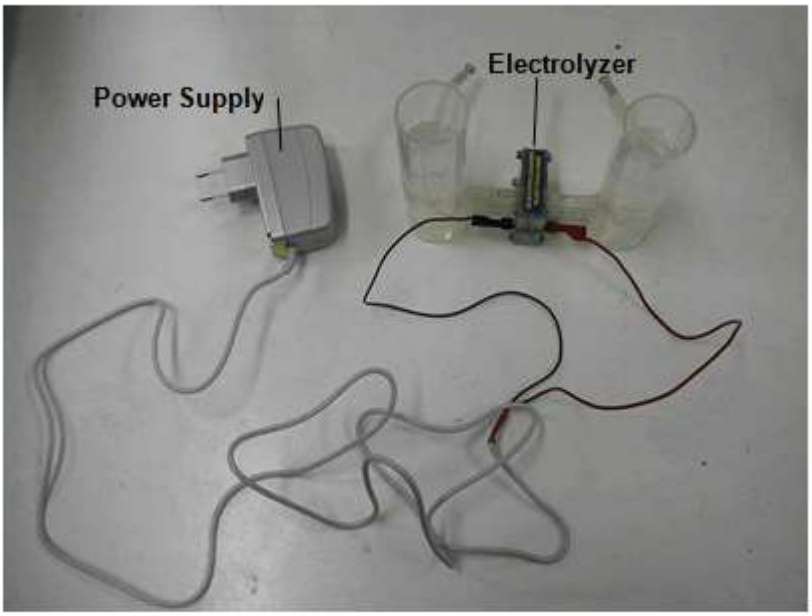

**Procedure**

1. Plug in the power supply.
2. Make a note of the time passed since the power supply was plugged in for each hydrogen volume described below. Note the hydrogen tank is the one connected to the negative part of the electrolyser.

**Fill the following table with the obtained measurements.**

| Produced volume $H^2$ | Time |
|---|---|
| $cm^3$ | s |
| 5 | |
| 10 | |
| 15 | |
| 20 | |

**Draw the volume $H_2$ produced versus time.**

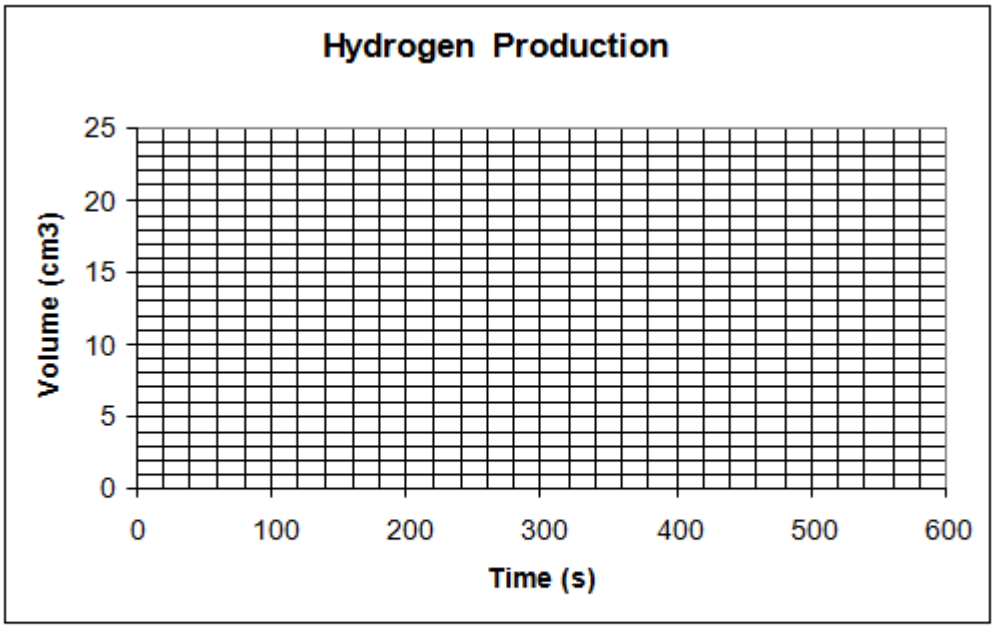

## Calculate electrolyser energetic efficiency

Electrolyser energetic efficiency depends on its hydrogen production capacity.

$$\eta_{energetic} = \frac{E_{hydrogen}}{E_{electric}} = \frac{V_{H2} \cdot H_0}{V \cdot I \cdot t}$$

*Where:*

*H0 = Combustion enthalpy = 12,745 J/cm3, includes the water condensation according to:*

*$H_2(g) + \frac{1}{2}O_2(g) \rightarrow H_2O(l)$*

*VH2= hydrogen volume produced in m3*
*V = voltage in volts*
*I = current in amperes*
*t = time in seconds*

*Power Supply characteristics:*

*V= 3,2 V*
*I = 0,3 A*

## Calculus notes

# Experience 3: Fuel Cell

## Objectives:

Find the maximum power operating point of the fuel cell.
Model of the fuel cell

## Experience Assembly

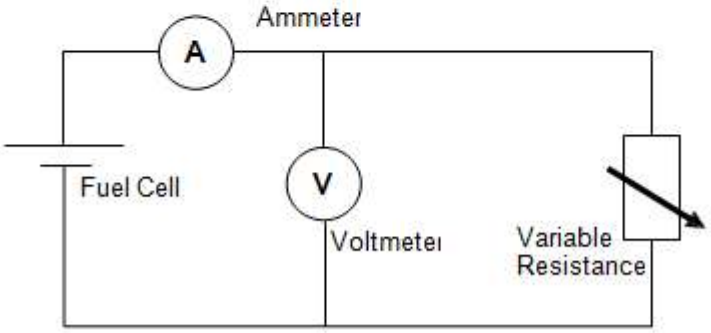


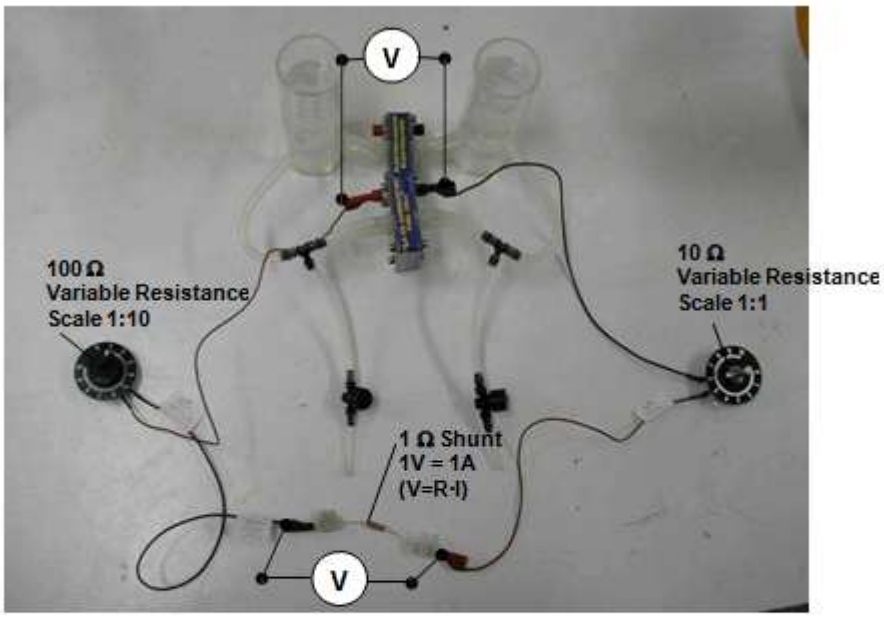

## Procedure

1. Connect the load circuit to the fuel cell.
2. Apply a resistance value for the load circuit. For example if the desired resistance value you want to apply is "13+1" ohms then put the 100 potentiometer in 1 (scale 1:10) and the 10 potentiometer in 3 (scale 1:1). The "+1" values is already applied in the circuit as a shunt from wich we can know the circuit current measuring the voltage difference between shunt terminals and converse it directly to Amperes. V=R·I V=1·A.
3. Make a note of voltage differences in fuel cell terminals and shunt terminals for each resistance described below. Converse directly the difference voltage in the shunt to amperes.

Fill the following table with the obtained measurements.

| Resistance (Ω) | Fuel cell Voltage (V) | Current (mA) = V (R 1Ω) | Power (W) |
|---|---|---|---|
| 1 | | | |
| 3+1 | | | |
| 6+1 | | | |
| 15+1 | | | |
| 20+1 | | | |
| 40+1 | | | |
| 60+1 | | | |
| 100+1 | | | |

Draw the graph of current versus voltage. $V = E - I \cdot r$.

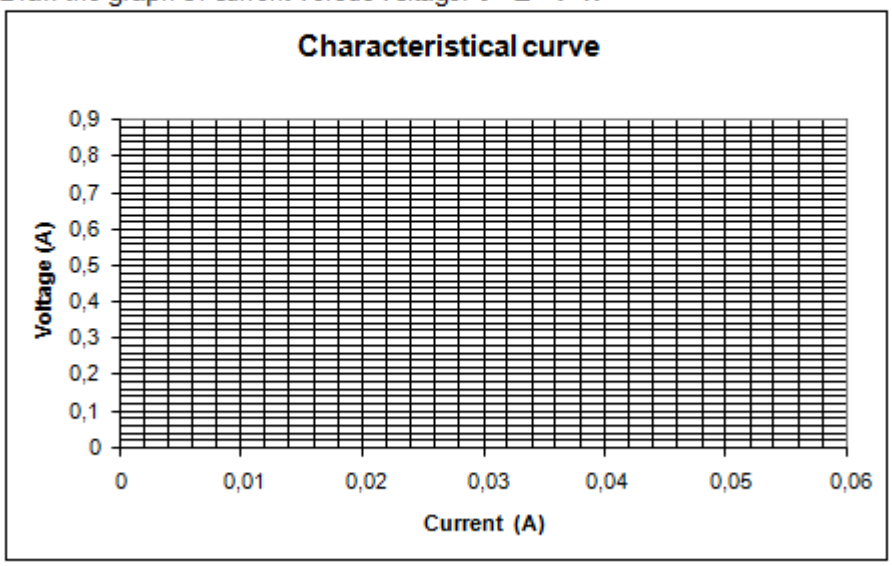

## Experience 4: DC Motor

**Objectives:**

Estimate a DC Motor curve
Regenerative break efficiencies

**Experience Assembly**

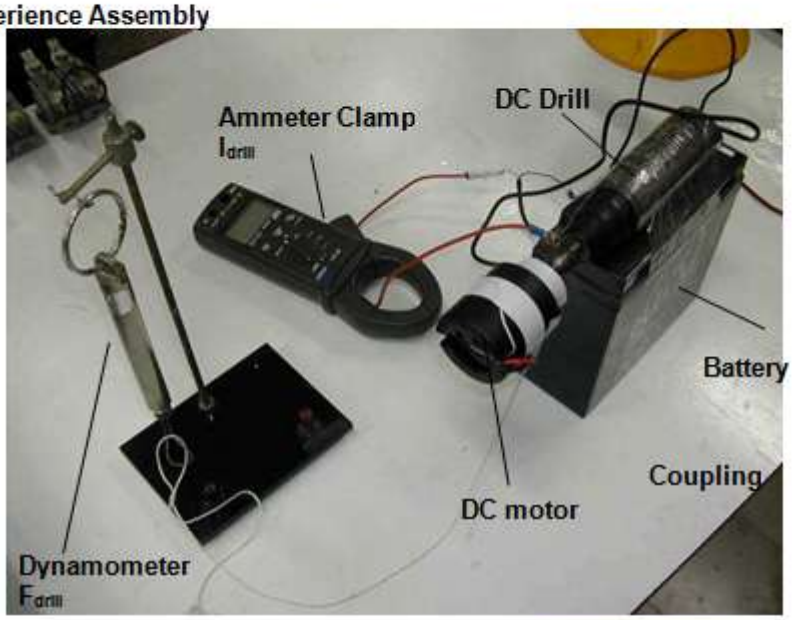


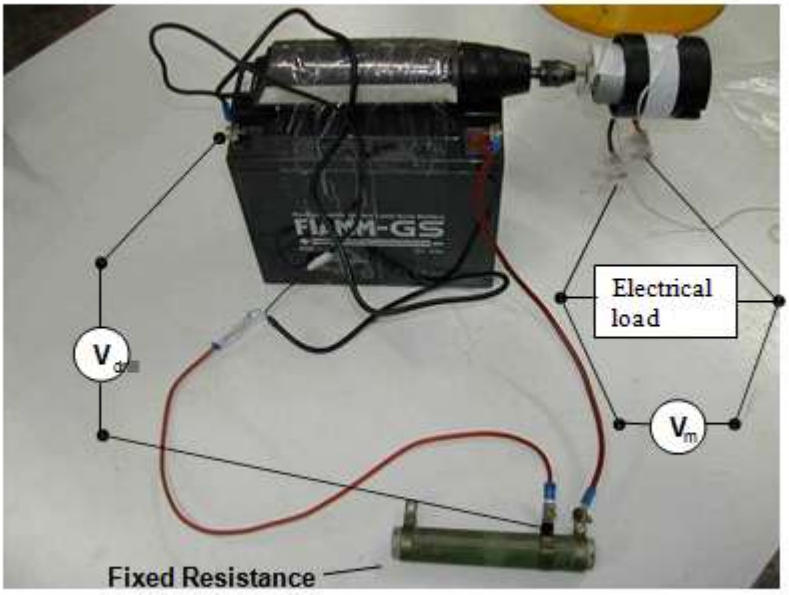

# Workshop:

## The Solar Fuel Cell Car: from theory to practice.

***Additional Information***

Next, there is a manual piece of the solar fuel cell car developed betweer ERI Didàctic and Centre Tècnologic Eduard Soler. This project is not finishec yet, but in this manual piece you can get an idea of the sort of experiments the full version will contain.

The workshop objectives are introduce the sustainable technologies tc the teachers interested in teach them in their classes, so it will only be explained the basic concepts. If you want more information I recommend you tc visit the web: http://www.kithidrogenosolar.com.

Some of the experiences described in the manual can be shown to students without all the kit parts, so if you use your imagination severa experiences can be didactic and spectacular at the same time with a minima cost.

I hope all this information will be useful for you.

Best wishes,

*David Casas Pozuelos*
*MontSENY Team*
*UPC-ETSEIB*
*(Universitat Politécnica de Catalunya)*
*Barcelona-Spain*
*despertaferr@gmail.com*

# E. Trabajos adicionales en el diseño y construcción del Despertaferro II.

## E.1. Maleta de telemetría. Calibración de sensores Ibat y Vbat

La colaboración de Txinto Vaz en el proyecto del Despertaferro II abrió las puertas al patrocinio de FICOSA. Su experiencia profesional, en el campo de la electrónica de la automoción, fue clave para elaborar un proyecto de fin de carrera aplicado en una maqueta cuyos componentes semi-comerciales podían ser instalados en el vehículo.

La maqueta consistía en una serie de PCBs, que colgaban de un bus de comunicaciones CAN, que conmutaban unos relés de potencia que daban tensión sucesivamente a dos motores de un coche de radiocontrol, en función de la órdenes enviadas por el celebro que se encontraba en el nodo puente.

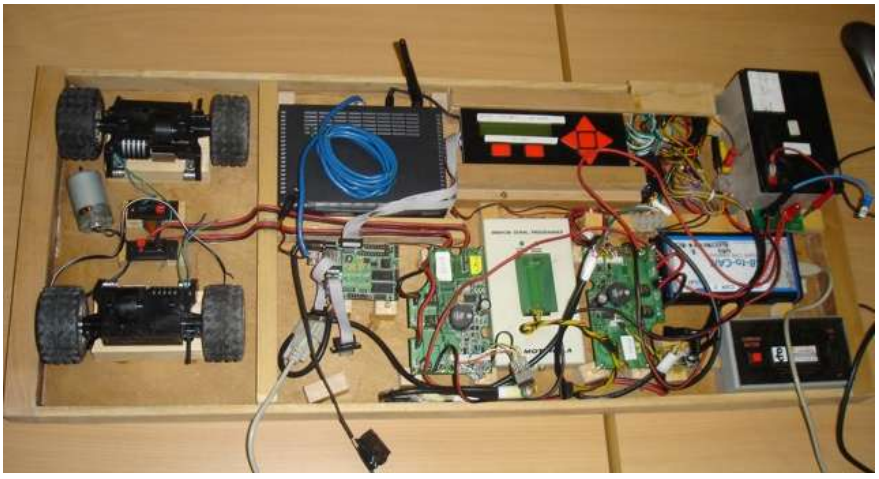

**Figura E.1 - Maqueta del PFC de Txinto Vaz**

El objetivo final del proyecto se trataba de utilizar las PCBs a modo de servo, de forma que a través de la comunicación con el nodo puente mediante protocolo CAN, se pudiera implementar un algoritmo de control cargado en el microprocesador del nodo puente.

En el desarrollo del Despertaferro II, se utilizó a modo de telemetría. Las entradas analógicas en tensión de 0-5V servirían para sensar la tensión de baterías (Vbat) y la corriente a través de ellas (Ibat).

Se integró el conjunto en una maleta para mejorar la transportabilidad y la protección frente a golpes y el polvo. Se recableó la maqueta en el interior de la maleta y se instaló el transformador de tensión como sensor de corriente y se elaboró un pequeño circuito para sensar la tensión de las baterías.

**Figura E.2 - Maleta de telemetría durante la integración de componentes.**

A continuación se calibraron los sensores para obtener la relación entre la señal medida y el valor real, para reprogramar el microprocesador del nodo puente, y poder disponer de los valores de tensión y corriente de las baterías tanto en el display, como en el ordenador de soporte sin necesidad de conversión.

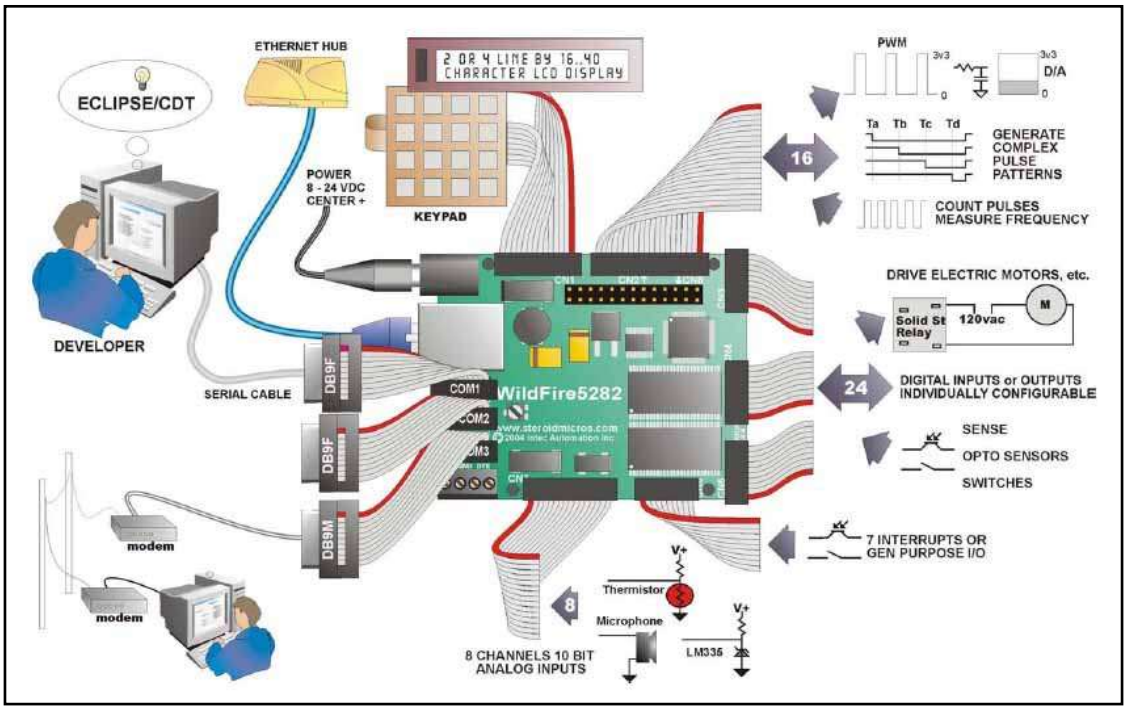


**Figura E.3 - Nodo Puente Wildfire5282**

## E.2. CAD Despertaferro II. Diseño cúpula.

El *equip Mediterrani* diseñó el perfil del vehículo bajo el programa de CAD Catia v5.0, para poder analizar su comportamiento aerodinámico con programas de análisis de dinámica de fluidos, y generar un prototipo a escala, con el que realizar las pruebas de verificación en el túnel de viento. El resto de componentes mecánicos fueron también diseñados y ensamblados con el mismo programa antes de iniciar la construcción del vehículo.

El *equip MontSENY* utilizó la versión educativa de SOLIDWORKS para el diseño de la nueva carcasa superior, portilla y transmisión del Despertaferro II, por parte de la sección mecánica del equipo. La conversión de los archivos dio numerosos problemas, ya que la diferente forma de generar las superficies y los volúmenes entre ambos programas, provocaba pérdida de información. Se consiguió finalmente compatibilizar los archivos, y la sección mecánica pudo trabajar en el diseño de la nueva carcasa superior.

El diseño de la cúpula se realizó con Proengineer, dado la limitación de la versión utilizada de SOLIDWORKS para generar piezas partiendo de una superficie curva. El diseño de la nueva cúpula se basaba en el frontal del modelo instalado en el Despertaferro I, pero más corta por la parte posterior.

Finalmente no se fabricó dado el alto coste que suponía su ejecución, del orden de los 300€ por pieza más unos 1000€ del molde. Se optó por aprovechar la antigua cúpula.

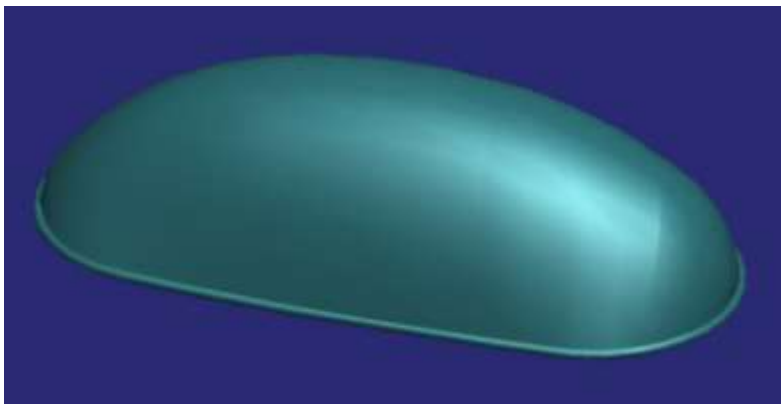

**Diseño cúpula Despertaferro II.**

## E.3. Prueba de carga del sistema de captación.

La prueba de carga del sistema de captación sirvió para verificar el funcionamiento de todos los MPPT conectados a los paneles fotovoltaicos, y ver como evolucionaba la tensión de la bancada de baterías durante la carga.

La secuencia de pasos que se efectuaron para llegar a la prueba de validación del sistema fue la siguiente:

- Carga grupos de menor tensión
- Ecualización de baterías
- Descarga controlada
- Carga sistema captación fotovoltaica

### E.3.1. Carga grupos de menor tensión

Las 24 baterías se subdividían en cuatro grupos. Las baterías que forman el grupo 1 y el grupo 2 habían sido utilizadas previamente para otras pruebas, y algunas de ellas estaban muy descargadas.

Se realizó una carga previa para los grupos con menor tensión, controlando la corriente de carga en todo momento para que no superara los 2A.

**Tabla E.1 - Tensiones durante la carga de los grupos descargados**

| | 0min | 5min | 10min | 20min | 40min | 100min | 160min |
|---|---|---|---|---|---|---|---|
| **1** | 9,29 | 13,19 | 12,47 | 12,2 | 12,35 | 12,78 | 13,19 |
| **2** | 9,14 | 13,36 | 13,36 | 12,23 | 12,36 | 12,77 | 13,16 |
| **3** | 11,24 | 12,52 | 12,57 | 12,23 | 12,37 | 12,79 | 13,23 |
| **4** | 9,18 | 13,28 | 13,28 | 12,25 | 12,37 | 12,79 | 13,19 |
| **5** | 10,35 | 12,72 | 12,72 | 12,23 | 12,38 | 12,81 | 13,23 |
| **6** | 8,77 | 13,43 | 13,43 | 12,18 | 12,27 | 12,67 | 13,09 |
| **7** | 9,42 | 13,16 | 12,58 | 12,27 | 12,35 | 12,69 | 13,00 |
| **8** | 10,31 | 12,69 | 12,23 | 12,11 | 12,23 | 12,63 | 12,93 |
| **9** | 7,96 | 13,59 | 12,54 | 12,18 | 12,21 | 12,54 | 12,84 |
| **10** | 8,89 | 13,53 | 12,55 | 12,29 | 12,35 | 12,72 | 13,00 |
| **11** | 10,24 | 12,55 | 12,12 | 12,1 | 12,26 | 12,66 | 12,97 |
| **12** | 9,71 | 12,96 | 12,36 | 12,15 | 12,23 | 12,61 | 12,93 |

### E.3.2. Ecualización de baterías.

En primer lugar, antes de que se iniciase la descarga parcial de baterías, para poder cargar con el sistema de captación fotovoltaico, se ecualizaron las baterías. Se conectaron todas las baterías en paralelo, de este modo se compensó la carga entre ellas.

Si se decidiese partir de un estado de máxima carga, se debería recurrir a una carga total de cada una de ellas. Para asegurar una carga del 100%, se debe sobrecargar la batería, punto en el que la elevada tensión de carga provoca gasificación en el interior de las baterías, reduciendo su vida útil.

**Tabla E.2 - Ecualización de baterías**

| | V0 | Vf |
|---|---|---|
| 1 | 12,6 | 12,49 |
| 2 | 12,58 | 12,46 |
| 3 | 12,66 | 12,51 |
| 4 | 12,57 | 12,45 |
| 5 | 12,66 | 12,46 |
| 6 | 12,49 | 12,41 |
| 7 | 12,53 | 12,41 |
| 8 | 12,5 | 12,42 |
| 9 | 12,35 | 12,34 |
| 10 | 12,45 | 12,44 |
| 11 | 12,55 | 12,52 |
| 12 | 12,46 | 12,43 |
| 13 | 12,17 | 12,4 |
| 14 | 12,12 | 12,37 |
| 15 | 12,12 | 12,4 |
| 16 | 12,11 | 12,37 |
| 17 | 12,1 | 12,4 |
| 18 | 12,19 | 12,37 |
| 19 | 12,11 | 12,34 |
| 20 | 12,18 | 12,37 |
| 21 | 12,14 | 12,18 |
| 22 | 12,18 | 12,23 |
| 23 | 12,2 | 12,28 |
| 24 | 12,15 | 12,22 |

### E.3.3. Descarga controlada.

Se efectuó una descarga controlada a 1Ah durante dos horas con todas las baterías conectadas en serie con un reóstato de 300 ohms. De forma que el estado de carga de las baterías fuera del 75% antes de la carga mediante los módulos fotovoltaicos.

**Tabla E.3 - Tensiones en bornes de batería durante la descarga controlada a 1A**

| Bateria | 0min | 30min | 45min | 60min | 75min | 90min | 105min | 120min |
|---|---|---|---|---|---|---|---|---|
| **1** | 12,59 | 12,53 | 12,47 | 12,42 | 12,36 | 12,32 | 12,28 | 12,26 |
| **2** | 12,58 | 12,52 | 12,47 | 12,42 | 12,35 | 12,31 | 12,28 | 12,25 |
| **3** | 12,62 | 12,56 | 12,51 | 12,46 | 12,4 | 12,37 | 12,34 | 12,31 |
| **4** | 12,58 | 12,51 | 12,46 | 12,41 | 12,34 | 12,31 | 12,28 | 12,25 |
| **5** | 12,62 | 12,55 | 12,5 | 12,45 | 12,38 | 12,35 | 12,32 | 12,26 |
| **6** | 12,54 | 12,47 | 12,42 | 12,37 | 12,3 | 12,26 | 12,23 | 12,2 |
| **7** | 12,57 | 12,5 | 12,45 | 12,4 | 12,33 | 12,25 | 12,26 | 12,23 |
| **8** | 12,58 | 12,5 | 12,45 | 12,4 | 12,33 | 12,3 | 12,26 | 12,23 |
| **9** | 12,47 | 12,4 | 12,34 | 12,29 | 12,22 | 12,18 | 12,19 | 12,12 |
| **10** | 12,56 | 12,49 | 12,43 | 12,38 | 12,32 | 12,28 | 12,25 | 12,22 |
| **11** | 12,61 | 12,55 | 12,49 | 12,44 | 12,38 | 12,34 | 12,31 | 12,28 |
| **12** | 12,55 | 12,48 | 12,42 | 12,37 | 12,31 | 12,27 | 12,24 | 12,21 |
| **13** | 12,71 | 12,67 | 12,63 | 12,59 | 12,53 | 12,49 | 12,46 | 12,43 |
| **14** | 12,65 | 12,61 | 12,57 | 12,53 | 12,47 | 12,43 | 12,4 | 12,37 |
| **15** | 12,7 | 12,66 | 12,61 | 12,57 | 12,51 | 12,47 | 12,44 | 12,41 |
| **16** | 12,69 | 12,65 | 12,61 | 12,57 | 12,5 | 12,46 | 12,43 | 12,4 |
| **17** | 12,68 | 12,64 | 12,6 | 12,56 | 12,5 | 12,46 | 12,42 | 12,4 |
| **18** | 12,69 | 12,66 | 12,61 | 12,57 | 12,51 | 12,47 | 12,44 | 12,41 |
| **19** | 12,67 | 12,63 | 12,59 | 12,54 | 12,48 | 12,44 | 12,41 | 12,38 |
| **20** | 12,69 | 12,65 | 12,61 | 12,57 | 12,51 | 12,47 | 12,44 | 12,41 |
| **21** | 12,66 | 12,62 | 12,58 | 12,53 | 12,47 | 12,43 | 12,39 | 12,36 |
| **22** | 12,68 | 12,64 | 12,6 | 12,55 | 12,49 | 12,45 | 12,42 | 12,39 |
| **23** | 12,71 | 12,67 | 12,63 | 12,59 | 12,53 | 12,49 | 12,45 | 12,43 |
| **24** | 12,66 | 12,63 | 12,58 | 12,54 | 12,47 | 12,43 | 12,4 | 12,37 |
| **Tensión Total** | 302,8 | 301,5 | 300,6 | 299,2 | 297,8 | 296,7 | 295,8 | 295,3 |

### E.3.4. • Carga sistema captación fotovoltaica

El día que se realizó la prueba, un día del mes de abril por la tarde, la radiación solar era menor de lo que cabía esperar durante el funcionamiento normal del sistema de captación. No obstante serviría para validar el funcionamiento de los reguladores instalados:

- Polaridad de las conexiones.
- No hubiera reguladores MPPT dañados.
- Adaptar la tensión de carga de las baterías en función de la tensión total dela bancada.
- Estimar el rendimiento

**Tabla E.4 - Tensiones y corriente de carga de baterías durante carga mediante módulos FV**

| Batería | 0 min | 5 min | 15 min | 30 min | 60 min |
|---|---|---|---|---|---|
| **1** | 12,47 | 12,54 | 12,54 | 12,56 | 12,59 |
| **2** | 12,47 | 12,55 | 12,55 | 12,57 | 12,6 |
| **3** | 12,53 | 12,6 | 12,61 | 12,64 | 12,67 |
| **4** | 12,46 | 12,52 | 12,53 | 12,56 | 12,59 |
| **5** | 12,49 | 12,55 | 12,57 | 12,59 | 12,62 |
| **6** | 12,42 | 12,48 | 12,5 | 12,52 | 12,56 |
| **7** | 12,42 | 12,48 | 12,49 | 12,51 | 12,54 |
| **8** | 12,42 | 12,48 | 12,5 | 12,53 | 12,56 |
| **9** | 12,32 | 12,39 | 12,42 | 12,45 | 12,49 |
| **10** | 12,42 | 12,48 | 12,51 | 12,53 | 12,57 |
| **11** | 12,48 | 12,55 | 12,57 | 12,6 | 12,64 |
| **12** | 12,4 | 12,46 | 12,48 | 12,5 | 12,54 |
| **13** | 12,26 | 12,3 | 12,31 | 12,33 | 12,35 |
| **14** | 12,23 | 12,26 | 12,27 | 12,29 | 12,32 |
| **15** | 12,26 | 12,29 | 12,31 | 12,32 | 12,35 |
| **16** | 12,24 | 12,27 | 12,29 | 12,3 | 12,33 |
| **17** | 12,25 | 12,29 | 12,3 | 12,32 | 12,35 |
| **18** | 12,26 | 12,29 | 12,3 | 12,32 | 12,34 |
| **19** | 12,21 | 12,24 | 12,26 | 12,27 | 12,3 |
| **20** | 12,25 | 12,28 | 12,3 | 12,32 | 12,34 |
| **21** | 12,18 | 12,21 | 12,23 | 12,25 | 12,37 |
| **22** | 12,23 | 12,26 | 12,27 | 12,29 | 12,32 |
| **23** | 12,26 | 12,29 | 12,31 | 12,33 | 12,36 |
| **24** | 12,2 | 12,23 | 12,24 | 12,26 | 12,29 |
| **Corriente de carga** | 0A | 2,0A | 1,2A | 1,5A | 1,0A |

Durante el ensayo no se tuvo facilidad de acceso a todos los reguladores MPPT para medir los valores de entrada y salida para determinar su eficiencia. Se optó por medir cuatro de los MPPTs, con mejor accesibilidad, y se obtuvieron unos valores medios de:

- $V_{in}$=13,2A
- $I_{in}$= 1,4A

La potencia de extrapolada de generación para el conjunto de los 18 módulos era de 333W. La potencia de carga era de 298,99V·1A=299W, por lo que la eficiencia media del regulador era del orden del 90%, en las condiciones de ensayo.

Dado que se trataba de una prueba, todas las mediciones de corriente se realizaron con pinzas amperimétricas en vez de shunts. Al ser corrientes tan bajas, la precisión del instrumento no fue la adecuada, pero los resultados que se obtuvieron servían para validar el funcionamiento del conjunto.

# F. Datos técnicos.

## F.1. Datos de los módulos fotovoltaicos proporcionados por ISOFOTON.

La tabla Tabla F.1 muestras las pruebas que realizó ISOFOTON a los módulos fotovoltaicos en el banco de caracterización.

**Tabla F.1 - Características nominales de los módulos fotovoltaicos**

| Serial # | Isc(A) | Voc(V) | Imp(A) | Vmp(V) | Pmp(W) | Module eff. | Cell eff. | Fill factor |
|---|---|---|---|---|---|---|---|---|
| **P20** | 3,566 | 19,638 | 3,341 | 16,039 | 53,578 | 14,496 | 16,068 | 76,515 |
| **P15** | 3,532 | 19,590 | 3,330 | 15,890 | 52,919 | 14,318 | 15,871 | 76,492 |
| **P10** | 3,543 | 19,648 | 3,299 | 16,013 | 52,822 | 14,292 | 15,842 | 75,887 |
| **P8** | 3,562 | 19,576 | 3,317 | 15,917 | 52,801 | 14,286 | 15,835 | 75,723 |
| **P11** | 3,552 | 19,579 | 3,282 | 16,040 | 52,646 | 14,244 | 15,789 | 75,690 |
| **P6** | 3,551 | 19,656 | 3,305 | 15,923 | 52,624 | 14,301 | 15,726 | 75,399 |
| **P16B** | 3,545 | 19,589 | 3,293 | 15,969 | 52,581 | 14,226 | 15,769 | 75,720 |
| **P12** | 3,565 | 19,556 | 3,312 | 15,864 | 52,539 | 14,215 | 15,757 | 75,356 |
| **P17** | 3,545 | 19,579 | 3,283 | 15,988 | 52,486 | 14,201 | 15,741 | 75,621 |
| **P16** | 3,531 | 19,551 | 3,284 | 15,962 | 52,420 | 14,183 | 15,721 | 75,935 |
| **P7** | 3,515 | 19,619 | 3,298 | 15,877 | 52,364 | 14,230 | 15,648 | 75,937 |
| **P14** | 3,511 | 19,524 | 3,290 | 15,837 | 52,106 | 14,098 | 15,627 | 76,019 |
| **P7B** | 3,507 | 19,536 | 3,254 | 16,008 | 52,094 | 14,095 | 15,623 | 76,041 |
| **P6B** | 3,521 | 19,559 | 3,263 | 15,937 | 51,996 | 14,068 | 15,594 | 75,515 |
| **P5** | 3,517 | 19,542 | 3,289 | 15,802 | 51,969 | 14,123 | 15,530 | 75,611 |
| **P13** | 3,512 | 19,587 | 3,264 | 15,919 | 51,958 | 14,058 | 15,583 | 75,523 |
| **P18** | 3,471 | 19,497 | 3,263 | 15,854 | 51,733 | 13,997 | 15,515 | 76,439 |

| Serial # | Isc(A) | Voc(V) | Imp(A) | Vmp(V) | Pmp(W) | Module eff. | Cell eff. | Fill factor |
|---|---|---|---|---|---|---|---|---|
| **P14B** | 3,479 | 19,469 | 3,272 | 15,797 | 51,681 | 13,983 | 15,499 | 76,308 |
| **P19** | 3,497 | 19,564 | 3,226 | 16,029 | 51,705 | 13,989 | 15,507 | 75,580 |
| **P1** | 3,512 | 19,532 | 3,267 | 15,801 | 51,617 | 14,027 | 15,425 | 75,245 |
| **P3** | 3,529 | 19,495 | 3,264 | 15,748 | 51,399 | 13,968 | 15,360 | 74,743 |
| **P4** | 3,513 | 19,524 | 3,250 | 15,803 | 51,365 | 13,958 | 15,350 | 74,895 |
| **P9** | 3,334 | 19,568 | 3,050 | 16,673 | 50,845 | 13,757 | 15,249 | 77,940 |
| **P2** | 3,463 | 19,478 | 3,116 | 16,080 | 50,100 | 13,615 | 14,972 | 74,282 |
| **Media** | **3,515** | **19,561** | **3,267** | **15,949** | **52,098** | **14,114** | **15,608** | **75,767** |

## F.2. Curvas características del Motor MA-55

# LABORATORY

### Performance Curves

**Motor Type:** MA55 **Date:** 30/04/2009

| | SYMBOLS | Units | |
|---|---|---|---|
| Stall Torque | Ms | Nm | 31,8 |
| Peak Torque | Mj | Nm | 190,8 |
| EMF Constant | Ke | Vs/rad | 0,6 |
| Torque Constant | Kt | Nm/A | 1 |
| Winding Resistance | R | Ohms | 0,2 |
| Winding Inductance | L | mH | 1,9 |
| Thermal Time Constant | Tth | s | 1500 |
| Thermal Resistance | Rth | °C/W | 0,284 |
| Ambient Temperature | AT | °C | 25 |
| Winding Temperature | WT | °C | 155 |

Ke & Kt units : rms

**Power Supply: AC**

| | Input Power Supply Range | Speed at 0Nm |
|---|---|---|
| +10% | 253 | 3820 |
| Nominal | 230 | 3476 |
| -10% | 207 | 3123 |

| Current Drive Curve (A) | 45 |
|---|---|

| Derating Curve | Stall Torque (Nm) | Ambient Temperature (°C) |
|---|---|---|
| | 31,78 | 24,94 |

**Torque/Speed Datas:**

| | N-m | | RPM |
|---|---|---|---|
| Torque | 31,800 | At Speed of | 0 |
| Torque | 28,709 | At Speed of | 1000 |
| Torque | 25,000 | At Speed of | 2200 |
| Torque | 22,527 | At Speed of | 3000 |
| Torque | 20,982 | At Speed of | 3500 |

**Torque/Speed Curve**

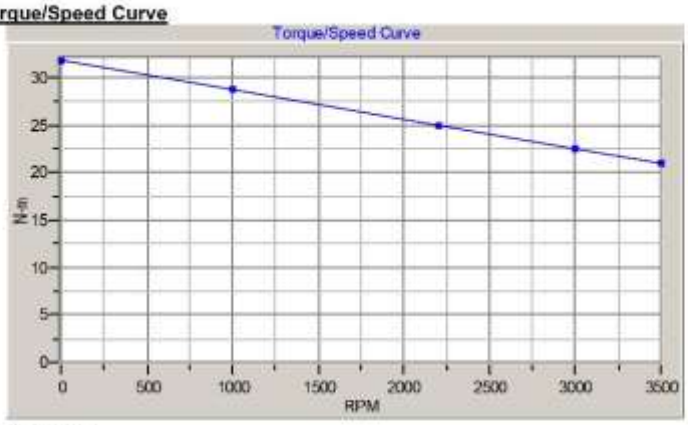


**Limits Curve**

Note: Output Drive voltage : Input Power voltage ±10% & internal lost Drive –5%.

**Derating Curve**

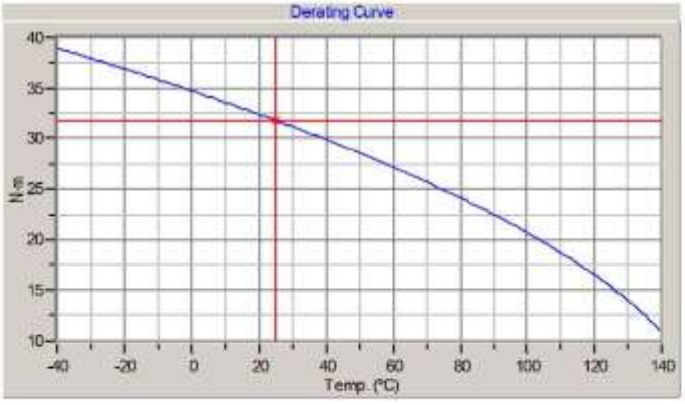

# G. ADVISOR. Bloques principales.

## G.1. Bloque Subsistema Fotovoltaico

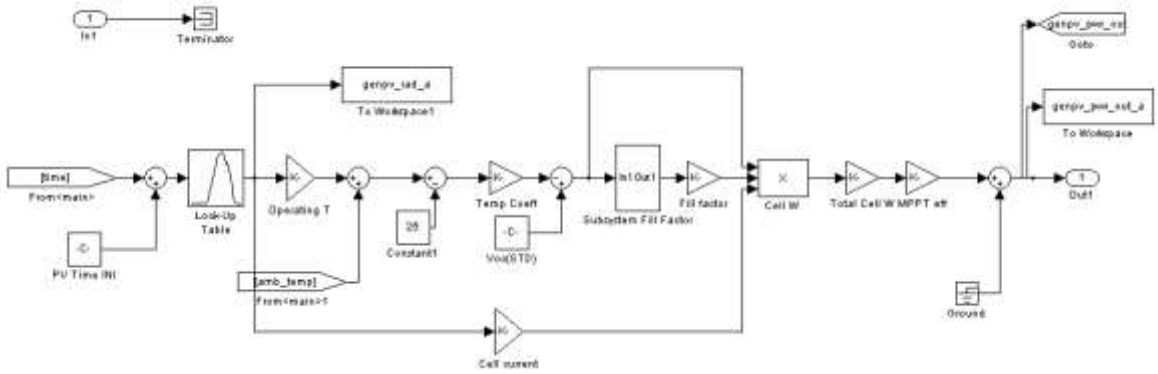

## G.2. Bloque optimización velocidades

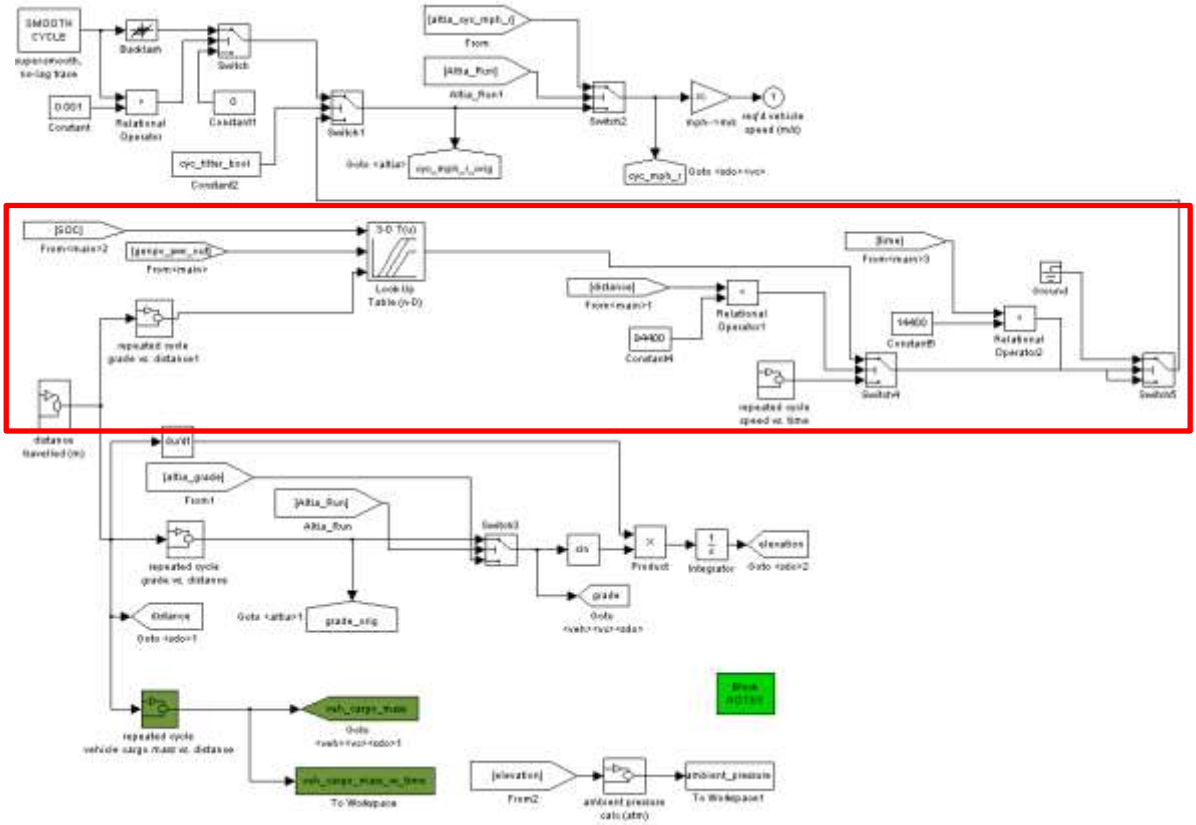

### G.2.1. Tabla de potencias eléctricas en función de la velocidad del vehículo y la pendiente del tramo.

La Tabla G.1 muestra la potencia eléctrica necesaria para mantener una determinada velocidad en una determinada pendiente. Se obtienen los datos simulando con ADVISOR, para el modelo de vehículo con la configuración de 12Ah.

**Tabla G.1 - Tabla de potencias eléctricas en función de la velocidad del vehículo y pendiente del tramo**

| **Pendiente** | **50km/h** | **40km/h** | **30km/h** | **20km/h** | **10km/h** |
|---|---|---|---|---|---|
| **0,5** | 4030W | 3123W | 2280W | 1500W | 740W |
| **0,3** | 2804W | 2143W | 1550W | 1000W | 494W |
| **0,1** | 1580W | 1160W | 812W | 513W | 248W |
| **-0,1** | 347W | 177W | 75W | 22W | 2W |

### G.2.2. Tabla de interpolación de tres dimensiones.

A continuación se muestra el mapa de velocidades, que servirá para evaluar la velocidad óptima de cada tramo. La matriz se indiza:

- en filas en función del SOC [0,0.1,0.3,0.5,0.7,0.9,1]
- en columnas en función de la radiación solar [0,200,400,600,800,1000,1400]
- la tercera dimensión se indiza por la pendiente [-0.5,-0.01,0.01,0.03,0.05,0.5]

```
Pendiente=-0.5
vel_map(:,:,1)=[...
     10     10     10     10     10     10     10
     10     10     10     10     10     10     10
     10     10     10     10     20     20     20
     10     10     20     20     30     30     30
     20     20     30     30     40     40     40
     30     30     40     40     40     40     40
     30     30     40     40     40     40     40
]/1.6093;
```

```
%Pendiente=-0.01
vel_map(:,:,2)=[...
      10      10      10      10      10      10      10
      10      10      10      10      10      10      10
      10      10      10      10      20      20      20
      10      10      20      20      30      30      30
      20      20      30      30      40      40      40
      30      30      40      40      40      40      40
      30      30      40      40      40      40      40
]/1.6093;

%Pendiente=0.01
vel_map(:,:,3)=[...
      10      10      10      10      10      10      10
      10      10      10      10      10      10      10
      10      10      10      10      20      20      20
      10      10      10      20      30      30      30
      10      10      20      20      30      40      40
      20      20      30      30      40      40      40
      20      20      30      30      40      40      40
]/1.6093;

%Pendiente=0.03
vel_map(:,:,4)=[...
      10      10      10      10      10      10      10
      10      10      10      10      10      10      10
      10      10      10      10      10      10      10
      10      10      10      10      10      20      20
      10      10      10      20      20      30      30
      20      20      20      30      30      40      40
      20      20      20      30      30      40      40
]/1.6093;

%Pendiente=0.05
vel_map(:,:,5)=[...
      10      10      10      10      10      10      10
      10      10      10      10      10      10      10
      10      10      10      10      10      10      10
      10      10      10      10      10      10      10
      10      10      10      10      10      20      20
      10      10      10      20      20      30      30
      10      10      10      20      20      30      30
]/1.6093;

%Pendiente=0.3
vel_map(:,:,6)=[...
      10      10      10      10      10      10      10
      10      10      10      10      10      10      10
      10      10      10      10      10      10      10
      10      10      10      10      10      10      10
      10      10      10      10      10      20      20
      10      10      10      20      20      20      20
      10      10      10      20      20      20      20
]/1.6093;
```

## G.3. Caracterísitcas modeladas del motor MA-55 + Driver SMT-BD1/a

Rango del par del motor

mc_map_trq=[-100 -60 -40 -30 -20 -10 0 10 20 30 40 60 100]; (N*m)

Rango de velocidad del motor

mc_map_spd=[0 1000 2200 3000 3500 4000 6000]*(2*pi)/60;(rad·s)

Rango de eficiencia del motor

```
mc_eff_map =[
0.1    0.1    0.1    0.1    0.1    0.1    0.1    0.1    0.1    0.1    0.1    0.1    0.1
0.95   0.95   0.95   0.95   0.95   0.95   0.1    0.95   0.95   0.95   0.95   0.95   0.95
0.95   0.95   0.95   0.95   0.95   0.95   0.1    0.95   0.95   0.95   0.95   0.95   0.95
0.95   0.95   0.95   0.95   0.95   0.95   0.1    0.95   0.95   0.95   0.95   0.95   0.95
0.95   0.95   0.95   0.95   0.95   0.95   0.1    0.95   0.95   0.95   0.95   0.95   0.95
0.95   0.95   0.95   0.95   0.95   0.95   0.1    0.95   0.95   0.95   0.95   0.95   0.95
0.95   0.95   0.95   0.95   0.95   0.95   0.1    0.95   0.95   0.95   0.95   0.95   0.95
]
```

Curva de par máximo como motor indexado por velocidad

mc_max_trq=[31.8 28.709 25 22.257 20.982 15 0.0]; (N*m)

Curva de par máximo como generador indexado por velocidad

mc_max_gen_trq=-0.05*[31.8 28.709 25 22.257 20.982 15 0.0]; (N*m)

# H. Presupuesto Detallado.

## H.1. Materiales de fabricación

| Subgrupo | Concepto | Origen | Cantidad | Unidad | Precio Total | Precio Unitario | Subtotal | Coste asumido |
|---|---|---|---|---|---|---|---|---|
| Baterías | Baterias NP7-12, de Pb-acido, 12V y 7Ah | Yuasa | 25 | unidad | 391,50 € | 15,66 € | | 1 |
| Baterías | Cable 4mm2 azul | Ferreteria | 11,8 | m | 11,80 € | 1,00 € | | 1 |
| Baterías | Terminales hembra FASTON 4mm | Onda Radio | 50 | unidad | 4,44 € | 0,09 € | | 1 |
| Baterias | Tela Ex. Fuerte | Erosky | 2 | m | 11,99 € | 6,00 € | | 1 |
| Baterias | Maderas | Bauhaus | 2 | m2 | 10,00 € | 5,00 € | | 1 |
| Baterias | Cola de impacto | Bauhaus | 3 | tubo | 17,55 € | 5,85 € | | 1 |
| Baterías | Plancha de metracrilato de 5mm | Gran Supefície | 0,5 | m2 | 7,50 € | 15,00 € | | 1 |
| | | | | | | | 454,78 € | |
| Carcasa y portilla | Resina Poliester Palatal 5kg | Servicecat S.L. | 11 | bote | 252,09 € | 22,92 € | | 1 |
| Carcasa y portilla | Peroxido de Mek 100g | Servicecat S.L. | 8 | bote | 28,34 € | 3,54 € | | 1 |
| Carcasa y portilla | Paletina | Servicecat S.L. | 10 | unidad | 22,36 € | 2,24 € | | 1 |
| Carcasa y portilla | Roving 200g | Jordi Sagristà | 29 | m | 218,30 € | 7,53 € | | 1 |
| Carcasa y portilla | Roving 500g | Servicecat S.L. | 7,5 | m | 31,67 € | 4,22 € | | 1 |
| Carcasa y portilla | MAT 300g | Servicecat S.L. | 23 | m | 326,65 € | 14,20 € | | 1 |
| Carcasa y portilla | Roving 500g | FAR | 14 | m | 59,12 € | 4,22 € | | 0 |
| Carcasa y portilla | MAT 300g | FAR | 25 | m | 355,05 € | 14,20 € | | 0 |
| Carcasa y portilla | Acetona 5 lts | Servicecat S.L. | 4 | bote | 51,41 € | 12,85 € | | 1 |
| Carcasa y portilla | Cera | Servicecat S.L. | 1 | bote | 12,85 € | 12,85 € | | 1 |
| Carcasa y portilla | Gelcoat parafinado | Servicecat S.L. | 5 | bote | 72,82 € | 14,56 € | | 1 |
| Carcasa y portilla | Teflón | Serv. Estación | 4 | láminas | 110,80 € | 27,70 € | | 1 |
| Carcasa y portilla | Tablas aglomerado acabado melamina cortadas a medida | Bauhaus | 5 | Tablas | 47,25 € | 9,45 € | | 1 |
| Carcasa y portilla | Masilla | Leroy M. | 4 | bote | 48,08 € | 12,02 € | | 1 |
| Carcasa y portilla | Sílice | Servicecat | 1 | bote | 13,90 € | 13,90 € | | 1 |
| Carcasa y portilla | Porexpan | Bauhaus | 3 | placas | 15,60 € | 5,20 € | | 1 |
| Carcasa y portilla | Poliuretano | Jordi Sagristà | 4 | planchas | 217,40 € | 54,35 € | | 1 |
| Carcasa y portilla | Perfiles Aluminio | Serv. Estación | 4 | unidad | 28,76 € | 7,19 € | | 1 |
| Carcasa y portilla | Barra F/Poliester | Servei Estació | 3 | unidad | 4,50 € | 1,50 € | | 1 |
| Carcasa y portilla | Reparador de fibra | Bric-Cat, S.L. | 1 | bote | 5,58 € | 5,58 € | | 1 |
| Carcasa y portilla | Celo | Papelerias Namar | 6 | paquetes | 15,60 € | 2,60 € | | 1 |
| Carcasa y portilla | Precinto Blanco | Leroy Merlin | 1 | unidad | 1,78 € | 1,78 € | | 1 |
| Carcasa y portilla | Cinta Americana | Armengol | 4 | unidad | 39,00 € | 9,75 € | | 1 |
| | | | | | | | 1.978,91 € | |
| Conexiones | Terminales hembra FASTON 4mm | Diotronic, S.A. | 50 | unidad | 4,44 € | 0,09 € | | 1 |
| Conexiones | Cable bicolor 2x1,5mm | Diotronic, S.A. | 12,5 | m | 13,73 € | 1,10 € | | 1 |
| Conexiones | Terminales hembra FASTON 6mm | Diotronic, S.A. | 50 | unidad | 5,27 € | 0,11 € | | 1 |
| Conexiones | Cable 1,5mm2 rojo | Ferreteria | 78 | m | 39,00 € | 0,50 € | | 1 |
| Conexiones | Cable 2mm2 negro | Ferreteria | 11 | m | 7,70 € | 0,70 € | | 1 |
| Conexiones | Conectores | Diotronic, S.A. | 1 | lot | 17,48 € | 17,48 € | | 1 |
| | | | | | | | 87,62 € | |
| Control y medida | Sensor de intensidad | RS | 2 | unidad | 37,92 € | 18,96 € | | 1 |
| Control y medida | Sensor de tensión | RS | 1 | unidad | 50,29 € | 50,29 € | | 1 |
| Control y medida | PCB de desarrollo(ECUs) | Ficosa | 3 | unidad | 120,00 € | 40,00 € | | 0 |
| Control y medida | Wildfire3252 Nodo Punte | Steroid Micros | 1 | unidad | 263,15 € | 263,15 € | | 1 |
| Control y medida | Display con pantalla LCD | Texas Inst. | 1 | unidad | 20,00 € | 20,00 € | | 1 |

| Subgrupo | Concepto | Origen | Cantidad | Unidad | Precio Total | Precio Unitario | Subtotal | Coste asumido |
|---|---|---|---|---|---|---|---|---|
| Control y medida | Cable apantallado de 6 polos | Diotronic, S.A. | 5 | m | 10,00 € | 2,00 € | | 1 |
| Control y medida | Juego de connector de 6 canals | Diotronic, S.A. | 7 | unidad | 3,50 € | 0,50 € | | 1 |
| Control y medida | Potenciometro | Diotronic | 2 | unidad | 12,00 € | 6,00 € | | 1 |
| Control y medida | Cab. USB a Serie | Personal Computer Green S.L. | 1 | unidad | 18,44 € | 18,44 € | | 1 |
| Control y medida | PC | ETSEIB | 1 | unidad | 500,00 € | 500,00 € | | 0 |
| | | | | | | | 1.035,30 € | |
| Cuadro general | Plancha de metracrilato de 5mm | Gran Supefície | 0,5 | m2 | 7,50 € | 15,00 € | | 1 |
| Cuadro general | Guia de perfil DIN | Ferreteria | 1 | m | 2,00 € | 2,00 € | | 1 |
| Cuadro general | Magnetotérmicos bipolares de 5, 10, 30 i 40A | Merlin Gerin | 4 | unidad | 80,00 € | 20,00 € | | 1 |
| Cuadro general | Juego de bridas transparentes | Ferreteria | 0,5 | paquet | 1,00 € | 2,00 € | | 1 |
| Cuadro general | Cable 6mm2 | Diotronic, S.A. | 6 | m | 6,05 € | 1,01 € | | 1 |
| | | | | | | | 96,55 € | |
| Módulos FV | Plancha policarbonato alveolar de 8mm cortada a medida | Servei Estació | 9 | planchas | 229,41 € | 25,49 € | | 0 |
| Módulos FV | Células fotovoltaicas | Isofotón | 800 | célula | 5.600,00 € | 7,00 € | | 0 |
| Módulos FV | Cinta estañada de 2mm | Isofotón | 165 | m | 9,90 € | 0,06 € | | 0 |
| Módulos FV | Cinta estañada de 6mm | Isofotón | 10 | m | 1,00 € | 0,10 € | | 0 |
| Módulos FV | Lámina de EVA | Isofotón | 30 | m2 | 105,00 € | 3,50 € | | 0 |
| Módulos FV | Lamina de ETFE | Isofotón | 10 | m2 | 100,00 € | 10,00 € | | 0 |
| Módulos FV | Lamina de Tedlar blanco | Isofotón | 10 | m2 | 70,00 € | 7,00 € | | 0 |
| Módulos FV | Poliester | gran superficie | 1 | L | 20,00 € | 20,00 € | | 0 |
| Módulos FV | Termoretractil 6mm | Ferreteria | 1 | m | 1,00 € | 1,00 € | | 1 |
| Módulos FV | Silicona | Ferreteria | 1 | tubo | 5,00 € | 5,00 € | | 1 |
| | | | | | | | 6.141,31 € | |
| MPPT | PCB de dos caras | Electrònica Feixas, S.L. | 25 | unidad | 200,00 € | 8,00 € | | 0 |
| MPPT | Transistores MOSFET | Electrònica Feixas, S.L. | 50 | unidad | 150,00 € | 3,00 € | | 0 |
| MPPT | Transformadores a medida | Electrònica Feixas, S.L. | 50 | unidad | 250,00 € | 5,00 € | | 0 |
| MPPT | Resto components de los reguladores MPPT | Electrònica Feixas, S.L. | 25 | pack | 500,00 € | 20,00 € | | 0 |
| MPPT | Envolvente estanca Rohs ABS | Electrònica Feixas, S.L. | 25 | unidad | 174,75 € | 6,99 € | | 0 |
| MPPT | Juego de bridas negras | Ferreteria | 0,5 | paquet | 1,00 € | 2,00 € | | 1 |
| | | | | | | | 1.275,75 € | |
| Patrocionio y divulgación | Trípticos | WORKcenter | 100 | unidad | 150,65 € | 1,51 € | | 1 |
| Patrocionio y divulgación | Dosier Informativo | Fotocopias Diagonal | 10 | unidad | 46,91 € | 4,69 € | | 1 |
| Patrocionio y divulgación | Fotocopias | CPDA | 18 | unidad | 0,54 € | 0,03 € | | 1 |
| Patrocionio y divulgación | Copies Plotter | Papereria Técnica d'Arquitectura | 10 | unidad | 38,00 € | 3,80 € | | 0 |
| | | | | | | | 236,10 € | |
| Varios Auxiliares | Baterias de Pb-àcido, 12V i 14Ah | Diotronic, S.A. | 2 | unidad | 50,00 € | 25,00 € | | 1 |
| Varios Electronica | Material electrónico diverso | Diotronic, S.A. | 1 | lot | 78,43 € | 78,43 € | | 1 |

| Subgrupo | Concepto | Origen | Cantidad | Unidad | Precio Total | Precio Unitario | Subtotal | Coste asumido |
|---|---|---|---|---|---|---|---|---|
| Varios Electronica | Resistencias 1W | Diotronic, S.A. | 1 | lot | 3,93 € | 3,93 € | | 1 |
| Varios Electronica | Terminales Aislados | Diotronic, S.A. | 1 | lot | 18,21 € | 18,21 € | | 1 |
| Varios Mantenimiento | Líquido de Frenos | Autorecanvis BAEZA S.L. | 1 | litro | 13,22 € | 13,22 € | | 1 |
| Varios Mantenimiento | Bombillas 12V | Ferreteria Ramos | 3 | unidad | 3,90 € | 1,30 € | | 1 |
| Pruebas refrigeración | Lámpara halógena dicroica 50W | Philips | 2 | unidad | 10,36 € | 5,18 € | | 1 |
| Pruebas refrigeración | Perfiles aluminio | AKI | 2 | unidad | 4,38 € | 2,19 € | | 1 |
| | | | | | | | 182,43 € | |
| Transmision | Plato 20 dientes | Bike House-Tomas Domingo S.L. | 1 | unidad | 12,00 € | 12,00 € | | 1 |
| Transmision | Cadena bicicleta | Raider's | 2 | unidad | 8,75 € | 8,75 € | | 1 |
| Transmision | Tronchacadenas | Raider's | 1 | unidad | 6,80 € | 6,80 € | | 1 |
| Transmision | Corona 102 dientes | Centro CIM | 2 | unidad | 300,00 € | 150,00 € | | 0 |
| Transmision | Acoplamiento plato 20 dientes | Centro CIM | 1 | unidad | 75,00 € | 75,00 € | | 0 |
| | | | | | | | 402,55 € | |
| **Total** | | | | | | | **11891,3** | |

## H.2. Herramientas y accesorios

| Subgrupo | Concepto | Origen | Cantidad | Unidad | Euros | Precio Unitario | Subtotal | Coste asumido |
|---|---|---|---|---|---|---|---|---|
| Baterias | Varivolt | Dept. eng. El | 1 | unidad | 100,00 € | 100,00 € | | 0 |
| Baterias | Grupo electrógeno Honda Invert | Honda | 1 | unidad | 1.800,00 € | 1.800,00 € | | 0 |
| | | | | | | | 1.900,00 € | |
| CAD | PC | | 1 | unidad | 800,00 € | 800,00 € | | 0 |
| CAD | Licencia Solid Works Estudiante | | 2 | unidad | 0,00 € | 0,00 € | | 0 |
| | | | | | | | 800,00 € | |
| Carcasa y portilla | Compresor portatil 5bar | ABAC | 1 | unidad | 150,00 € | 150,00 € | | 0 |
| Carcasa y portilla | Taladro neumático Recto | Larwid | 1 | unidad | 84,00 € | 84,00 € | | 0 |
| Carcasa y portilla | Escobillas | ALABALL | 2 | juegos | 5,92 € | 5,92 € | | 1 |
| Carcasa y portilla | Tornilleria M6 | Leroy Merlin | 2 | paquete | 4,50 € | 4,50 € | | 1 |
| Carcasa y portilla | Tornillo apriete | Bric-Cat, S.L. | 1 | unidad | 11,01 € | 11,01 € | | 1 |
| Carcasa y portilla | Correa lijadora | Maquinària F | 1 | paquete | 4,23 € | 4,23 € | | 1 |
| Carcasa y portilla | Discos lijadora | Bauhaus | 1 | paquete | 12,90 € | 12,90 € | | 1 |
| Carcasa y portilla | Muela cónica | Serv. Estació | 1 | unidad | 3,25 € | 3,25 € | | 1 |
| Carcasa y portilla | Aro Fijo | Sum. Elec. Vi | 1 | unidad | 9,16 € | 9,16 € | | 1 |
| Carcasa y portilla | Cutter | Leroy M. | 1 | unidad | 7,40 € | 7,40 € | | 1 |
| Carcasa y portilla | Mascarilla con Valvula 3M | Servicecat S. | 3 | unidad | 6,7068 | 2,2356 | | 1 |
| Carcasa y portilla | Rodillos | Servicecat S. | 7 | unidad | 31,92 | 4,56 | | 1 |
| Carcasa y portilla | Guantes | Servicecat | 5 | cajas | 43,5 | 8,7 | | 1 |
| Carcasa y portilla | Lijas Grano 60 | Bauhaus | 8 | hojas | 16,81 | 2,10125 | | 1 |
| Carcasa y portilla | Recipiente | Serv. Estació | 1 | unidad | 8,48 | 8,48 | | 1 |
| | | | | | | | 399,79 € | |
| Conexiones | Alicates de prensar terminales | Diotronic, S. | 1 | unidad | 5,38 € | 5,38 € | | 1 |
| Conexiones | Soldadores | | 2 | unidad | 40,00 € | 20,00 € | | 1 |
| | | | | | | | 45,38 € | |
| Control y medida | PC portàtil amb WI-FI | | 1 | unidad | 600,00 € | 600,00 € | | 0 |
| Control y medida | Adaptador mechero cotxe (pel PC) | | 1 | unidad | 30,00 € | 30,00 € | | 0 |
| Control y medida | Multímetres | | 2 | unidad | 80,00 € | 40,00 € | | 1 |
| Control y medida | Pinzas amperimétricas | | 2 | unidad | 80,00 € | 40,00 € | | 1 |
| Control y medida | Multímetro de precisión | | 1 | unidad | 200,00 € | 200,00 € | | 1 |
| | | | | | | | 990,00 € | |
| Módulos FV | Pistola de calor | STEINEL | 1 | unidad | 45,00 € | 45,00 € | | 1 |
| | | | | | | | 45,00 € | |
| Patrocionio y divulga | Bateria de Pb-acido, 12V y 7Ah | Yuasa | 1 | unidad | 15,66 € | 15,66 € | | 0 |
| Patrocionio y divulga | Taladro 12V | Diotronic | 2 | unidad | 20,00 € | 20,00 € | | 0 |
| Patrocionio y divulga | Potenciometro | Diotronic | 5 | unidad | 30,00 € | 6,00 € | | 1 |
| Patrocionio y divulga | Pinza multimétrica AC/DC | PCE. Iberica | 1 | unidad | 150,00 € | 150,00 € | | 1 |
| | | | | | | | 215,66 € | |
| Varios | Caja de herramientas electro-mecánicas | | 1 | caja | 411,70 € | 411,70 € | | 1 |
| Varios | Alargador 50m | | 1 | unidad | 100,00 € | 100,00 € | | 1 |
| Varios | Llaves | Serv. Estació | 2 | lotes | 13,20 € | 6,60 € | | 1 |
| Pruebas refrigeració | Horno de laboratorio | JP Selecta | 4 | horas | 32,00 € | 8,00 € | | 0 |
| Pruebas refrigeració | Registrador de tensión y temper | Yokogawa | 4 | horas | 24,00 € | 6,00 € | | 0 |
| | | | | | | | 580,90 € | |
| Local | Alquiler de local de 100m2 | E.T.S.E.I.B. | 14 | mes | 7.000,00 € | 500,00 € | | 0 |
| | | | | | | | 7.000,00 € | |
| Transmisión | Llave de gancho | Gran superfí | 1 | unidad | 11,00 € | 11,00 € | | 1 |
| | | | | | | | 11,00 € | |
| | | | | | | | 11.987,73 € | |

## H.3. Recursos Humanos

| Subgrupo | Concepto | Origen | Cantidad | Unidad | Euros | Precio Unitario | Subtotal | Coste asumido |
|---|---|---|---|---|---|---|---|---|
| Baterías | Connexionado de baterias | Becario | 6 | hora | 36,00 € | 6,00 € | | 0 |
| Baterías | Fabricación cajas de protección de baterias | Becario | 10 | hora | 60,00 € | 6,00 € | | 0 |
| | | | | | | | 96,00 € | |
| CAD | Conversión archivos CATIA - SOLIDWORKS | Becario | 16 | hora | 96,00 € | 6,00 € | | 0 |
| CAD | Diseño carcasa superior | Becario | 120 | hora | 720,00 € | 6,00 € | | 0 |
| CAD | Diseño portilla | Becario | 80 | hora | 480,00 € | 6,00 € | | 0 |
| CAD | Diseño transmisión | Becario | 40 | hora | 240,00 € | 6,00 € | | 0 |
| CAD | Diseño corona 102 dientes | Becario | 24 | hora | 144,00 € | 6,00 € | | 0 |
| CAD | Diseño acoplamiento piñon 20 dientes | Becario | 20 | hora | 120,00 € | 6,00 € | | 0 |
| CAD | Diseño cúpula | Becario | 24 | hora | 144,00 € | 6,00 € | | 0 |
| | | | | | | | 1.944,00 € | |
| Carcasa y portilla | Curso fibra de vidrio en el FAR | Personal Cualificado | 18 | hora | 540,00 € | 30,00 € | | 0 |
| Carcasa y portilla | Fabricación moldes base de módulos | Becario | 40 | hora | 216,00 € | 6,00 € | | 0 |
| Carcasa y portilla | Laminado bases de módulos | Becario | 240 | hora | 1.440,00 € | 6,00 € | | 0 |
| Carcasa y portilla | Lijado bases de módulos | Becario | 56 | hora | 336,00 € | 6,00 € | | 0 |
| Carcasa y portilla | Fabricación costillas vehículo | Becario | 40 | hora | 240,00 € | 6,00 € | | 0 |
| Carcasa y portilla | Unión base de módulos carcasa | Becario | 36 | hora | 216,00 € | 6,00 € | | 0 |
| Carcasa y portilla | Lijado bases de módulos carcasa | Becario | 24 | hora | 144,00 € | 6,00 € | | 0 |
| Carcasa y portilla | Reforzamiento costillas transversales carcasa | Becario | 36 | hora | 216,00 € | 6,00 € | | 0 |
| Carcasa y portilla | Fijación base carcasa | Becario | 32 | hora | 192,00 € | 6,00 € | | 0 |
| Carcasa y portilla | Laminado lateral base carcasa | Becario | 86 | hora | 516,00 € | 6,00 € | | 0 |
| Carcasa y portilla | Lijado Carcasa | Becario | 60 | hora | 360,00 € | 6,00 € | | 0 |
| Carcasa y portilla | Eliminar porosidades en juntas | Becario | 40 | hora | 240,00 € | 6,00 € | | 0 |
| Carcasa y portilla | Fabricación molde portilla | Becario | 80 | hora | 480,00 € | 6,00 € | | 0 |
| Carcasa y portilla | Unión bases módulos portilla | Becario | 24 | hora | 144,00 € | 6,00 € | | 0 |
| Carcasa y portilla | Fijación base portilla | Becario | 20 | hora | 120,00 € | 6,00 € | | 0 |
| Carcasa y portilla | Laminado lateral portilla. | Becario | 50 | hora | 300,00 € | 6,00 € | | 0 |
| Carcasa y portilla | Lijado portilla | Becario | 40 | hora | 240,00 € | 6,00 € | | 0 |
| Carcasa y portilla | Capa final Gelcoat | Becario | 56 | hora | 336,00 € | 6,00 € | | 0 |
| | | | | | | | 6.276,00 € | |
| Conexiones | Cableado mòduls-reguladors | Becario | 12 | hora | 72,00 € | 6,00 € | | 0 |
| Conexiones | Cableado reguladores-baterias | Becario | 12 | hora | 72,00 € | 6,00 € | | 0 |
| | | | | | | | 144,00 € | |
| Control y medida | Instalación 3 sensores | Becario | 8 | hora | 48,00 € | 6,00 € | | 0 |
| Control y medida | Instalación accelerador | Becario | 6 | hora | 36,00 € | 6,00 € | | 0 |
| Control y medida | Programar bus CAN | Ingeniero especializado | 10 | hora | 600,00 € | 60,00 € | | 0 |
| Control y medida | Disseny del programa de visualització | Personal Cualificado | 16 | hora | 480,00 € | 30,00 € | | 0 |
| Control y medida | Instalación bus CAN en vehiculo | Becario | 12 | hora | 72,00 € | 6,00 € | | 0 |
| Control y medida | Montaje maleta de telemetría | Becario | 6 | hora | 36,00 € | 6,00 € | | 0 |
| Control y medida | Calibración de sensores | Becario | 8 | hora | 48,00 € | 6,00 € | | 0 |
| Control y medida | Pruebas Telemetría | Becario | 12 | hora | 72,00 € | 6,00 € | | 0 |
| | | | | | | | 1.392,00 € | |
| Cuadro general | Montaje cuadro de control | Becario | 6 | hora | 36,00 € | 6,00 € | | 0 |
| Cuadro general | Dimensionado cableado | Becario | 2 | hora | 12,00 € | 6,00 € | | 0 |
| | | | | | | | 48,00 € | |
| Módulos FV | Internconexión células fv mediante soldadura | Personal Cualificado | 24 | hora | 720,00 € | 30,00 € | | 0 |
| Módulos FV | encapsular módulos | Personal Cualificado | 36 | hora | 1.080,00 € | 30,00 € | | 0 |
| Módulos FV | Soldadura connexiones inferiores | Personal Cualificado | 12 | hora | 360,00 € | 30,00 € | | 0 |
| Módulos FV | Recortar material sobrante y ajuste a carcasa | Becario | 60 | hora | 360,00 € | 6,00 € | | 0 |
| Módulos FV | Termosellado del perímetro del módulo | Becario | 12 | hora | 72,00 € | 6,00 € | | 0 |
| Módulos FV | Protecció de conexiones del módulo | Becario | 24 | hora | 144,00 € | 6,00 € | | 0 |
| Módulos FV | Diseño módulos fotovoltaicos | Ingeniero especializado | 16 | hora | 960,00 € | 60,00 € | | 0 |
| Módulos FV | Pruebas módulos | Becario | 40 | hora | 240,00 € | 6,00 € | | 0 |
| | | | | | | | 3.936,00 € | |
| MPPT | Diseño del regulador MPPT | Ingeniero especializado | 15 | hora | 900,00 € | 60,00 € | | 0 |
| MPPT | Fabricación reguladores | Personal Cualificado | 48 | hora | 1.440,00 € | 30,00 € | | 0 |
| MPPT | Instalar reguladores | Becario | 12 | hora | 72,00 € | 6,00 € | | 0 |
| | | | | | | | 2.412,00 € | |
| Patrocionio y divulgació | Col·laboració Llibre CAEIC | Becario | 12 | hora | 72,00 € | 6,00 € | | 0 |
| Patrocionio y divulgació | Elaboración PPT COSMOCAIXA | Becario | 6 | hora | 36,00 € | 6,00 € | | 0 |
| Patrocionio y divulgació | Elaboración PPT Fires | Becario | 4 | hora | 24,00 € | 6,00 € | | 0 |
| Patrocionio y divulgació | Elaboración PPT Patrocinadores Potenciales | Becario | 6 | hora | 36,00 € | 6,00 € | | 0 |
| Patrocionio y divulgació | Elaboración Workshop Science on Stage | Becario | 60 | hora | 360,00 € | 6,00 € | | 0 |
| Patrocionio y divulgació | Gestión traslado Workshop Science on Stage | Becario | 12 | hora | 72,00 € | 6,00 € | | 0 |
| | | | | | | | 600,00 € | |
| Varios | Trabajos varios | Becario | 60 | hora | 360,00 € | 6,00 € | | 0 |
| | | | | | | | 360,00 € | |
| Transmisión | Instalación corona 102 dientes | Becario | 4 | hora | 24,00 € | 6,00 € | | 0 |
| Transmisión | Corrección tensor | Becario | 10 | hora | 60,00 € | 6,00 € | | 0 |
| Transmisión | Instalación pieza acoplamiento | Becario | 2 | hora | 12,00 € | 6,00 € | | 0 |
| Transmisión | Cambio circuito de frenado | Becario | 8 | hora | 48,00 € | 6,00 € | | 0 |
| Transmisión | Ajuste amortiguador | Becario | 4 | hora | 24,00 € | 6,00 € | | 0 |
| | | | | | | | 168,00 € | |
| **Total** | | | | | | | **17.376,00 €** | |

## H.4. Logística

| Subgrupo | Concepto | Origen | Cantidad | Unidad | Euros | Precio Unitario | Subtotal | Coste asumido |
|---|---|---|---|---|---|---|---|---|
| Desplazamientos | taxis aeroport | Taxi | 4 | trayecto | 118,20 € | 29,55 € | | 1 |
| Desplazamientos | Billete avión BCN-Màlaga | Vueling | 2 | trayecto | 101,00 € | 50,50 € | | 1 |
| Desplazamientos | Taxi Màlaga | Taxi | 2 | trayecto | 41,00 € | 20,50 € | | 1 |
| Desplazamientos | Billete tren Màlaga-BCN | Renfe | 2 | trayecto | 95,40 € | 47,70 € | | 1 |
| Desplazamientos | Desplazamientos a Terrassa | Coche | 180 | km | 27,00 € | 0,15 € | | 0 |
| Desplazamientos | desplaçament a Olesa M. | Coche | 240 | km | 36,00 € | 0,15 € | | 0 |
| Desplazamientos | Desplaçament a Alcobendas | Coche Ricard | 1200 | km | 180,00 € | 0,15 € | | 1 |
| Desplazamientos | Desplaçament a Grenoble | Coche Ricard | 1300 | km | 195,00 € | 0,15 € | | 1 |
| Desplazamientos compra material | Becario | Varios | 40 | hora | 240,00 € | 6,00 € | | 0 |
| | | | | | | | 1.033,60 € | |
| Envíos | Envio de soportes de policarbonato | MRW | 3 | bultos | 45,00 € | 15,00 € | | 1 |
| Envíos | Carta Museo | MovilPack | 1 | envío | 46,89 € | 46,89 € | | 1 |
| | | | | | | | 91,89 € | |
| Transporte vehículo | Transporte vehícle Museu-ETSEIB | Sertrans | 1 | trayecto | 104,72 € | 104,72 € | | 1 |
| Transporte vehículo | Remolque a medida, P.M.A. 750kg | Taller de Barbens, S.L. | 1 | unitat | 2.552,00 € | 2.552,00 € | | 1 |
| Transporte vehículo | Toldo a medida | Sra. Tous | 1 | unitat | 100,00 € | 60,00 € | | 0 |
| Transporte vehículo | Porexpan | Bauhaus | 5 | placas | 24,75 € | 4,95 | | 1 |
| Transporte vehículo | Blister | Bauhaus | 1 | rollo | 46,25 | 46,25 | | 1 |
| Transporte vehículo | Solicitud de Datos del Registro del Vehículo | Dirección General de Tráfico | | | 7,20 € | 7,20 € | | 1 |
| | | | | | | | 2.834,92 € | |
| Total | | | | | | | 3.960,41 € | |